New Mexico Geological Society

Downloaded from: https://nmgs.nmt.edu/publications/guidebooks/45



First-day road log: From Socorro to Magdalena, Datil, western Crosby Mountains, Sawtooth Mountains, Pie Town, Qemado, Quemado Lake

Richard M. Chamberlin, Steven M. Cather, William C. McIntosh, Orin J. Anderson, and James C. Ratte

1994, pp. 1-45. https://doi.org/10.56577/FFC-45.1

in:

Mogollon Slope (West-Central New Mexico and East-Central Arizona), Chamberlin, R. M.; Kues, B. S.; Cather, S. M.; Barker, J. M.; McIntosh, W. C.; [eds.], New Mexico Geological Society 45th Annual Fall Field Conference Guidebook, 335 p. https://doi.org/10.56577/FFC-45

This is one of many related papers that were included in the 1994 NMGS Fall Field Conference Guidebook.

Annual NMGS Fall Field Conference Guidebooks

Every fall since 1950, the New Mexico Geological Society (NMGS) has held an annual Fall Field Conference that explores some region of New Mexico (or surrounding states). Always well attended, these conferences provide a guidebook to participants. Besides detailed road logs, the guidebooks contain many well written, edited, and peer-reviewed geoscience papers. These books have set the national standard for geologic guidebooks and are an essential geologic reference for anyone working in or around New Mexico.

Free Downloads

NMGS has decided to make peer-reviewed papers from our Fall Field Conference guidebooks available for free download. This is in keeping with our mission of promoting interest, research, and cooperation regarding geology in New Mexico. However, guidebook sales represent a significant proportion of our operating budget. Therefore, only *research papers* are available for download. *Road logs*, *mini-papers*, and other selected content are available only in print for recent guidebooks.

Copyright Information

Publications of the New Mexico Geological Society, printed and electronic, are protected by the copyright laws of the United States. No material from the NMGS website, or printed and electronic publications, may be reprinted or redistributed without NMGS permission. Contact us for permission to reprint portions of any of our publications.

One printed copy of any materials from the NMGS website or our print and electronic publications may be made for individual use without our permission. Teachers and students may make unlimited copies for educational use. Any other use of these materials requires explicit permission.

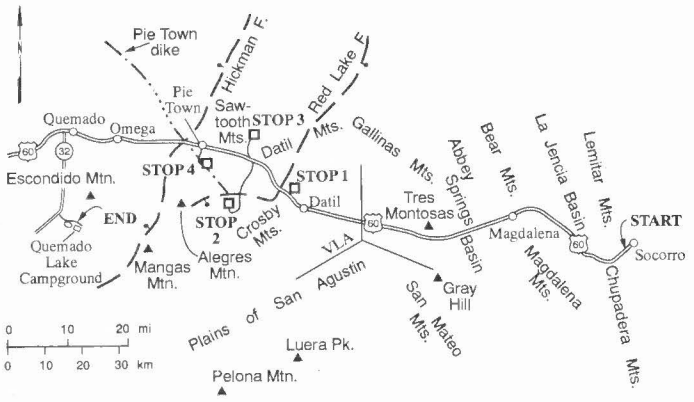
This page is intentionally left blank to maintain order of facing pages.

FIRST-DAY ROAD LOG FROM SOCORRO TO MAGDALENA, DATIL, WESTERN CROSBY MOUNTAINS, SAWTOOTH MOUNTAINS, PIE TOWN, QUEMADO AND QUEMADO LAKE

RICHARD M. CHAMBERLIN, STEVEN M. CATHER, WILLIAM C. MCINTOSH, ORIN J. ANDERSON, and JAMES C. RATTÉ

THURSDAY, SEPTEMBER 29, 1994

Assembly point: Frontage road next to New Mexico State Forestry Division office approximately 1 mile southwest of Socorro on US-60.
Departure time: 7:45 a.m.
Distance: 161.6 mi.
Stops: 4



SUMMARY

The First Day tour emphasizes the Cenozoic stratigraphy and structure of the Mogollon slope in northeastern Catron County. Gently south-dipping Eocene and Oligocene orogenic to volcanogenic strata as much as 1.3 mi thick mark the downwarped (loaded) southeastern margin of the stable Colorado Plateau microplate, referred to here as the Mogollon slope. US-60 west from Socorro generally follows strongly to moderately extended topographically lower terrain of the San Agustin arm of the Rio Grande rift until it crosses onto the Mogollon slope at the Red Lake fault zone west of Datil. The San Agustin arm marks a complex transition zone from rift to plateau; thus US-60 crosses several north-trending extensional basins and distended horsts between Socorro and Datil.

Stop 1 west of Datil provides an overlook of the Red Lake fault zone, a narrow NNE- trending belt of Neogene extension that locally cuts across the Mogollon slope. This mildly distended belt was probably guided by weak lithosphere below a zone of earlier Laramide transpression. The massive south-sloping core of the Datil Mountains visible to the west of Stop 1 locally defines an edge of the gently depressed Mogollon slope.

Stop 2 permits a hands-on look at upper Eocene ignimbrites of the Datil Group and intercalated volcaniclastic sedimentary apron deposits of the middle Spears Group that are well exposed on the west flank of the Crosby Mountains. Both epiclastic braided-stream deposits and syneruptive tuffaceous sandstones deposited by an overloaded stream system are locally well exposed here at Saulsberry Ranch.

Today's third and lunch stop is near Monument Rock in the eastern Sawtooth Mountains. Bold cliffs to the northeast of Monument Rock provide spectacular views of intense soft sediment deformation within the upper Eocene Dog Springs Formation. Intensely folded andesitic sandstones and upturned andesitic debris-flow deposits visible in these cliffs may reflect a seismically triggered regional liquefaction event of late Eocene age.

Stop 4 is along the late Oligocene Pie Town dike, where it forms a large wall-like outcrop at Bright Lake south of Pie Town. Country rocks of Eocene andesitic sandstone and the chilled margin of this basaltic-andesite dike are well exposed here. This great dike, approximately 45 mi long, indicates regional extension in late Oligocene time was to the WSW.

From Pie Town the route follows US-60 west to Quemado and then south along NM-32 to the Apache National Forest and the Quemado Lake Recreation Area. Following a catered barbecue we will camp out below the tall ponderosa pines at the old Quemado Lake campground in the valley southeast of the reservoir.

The first 43.8 mi of this road log is modified and updated after the road log of Chapin et al. (1978), which emphasized then-newly-discovered calderas and their relationship to well-known mining districts in the Mogollon-Datil volcanic field. This log and following road logs adopt the Tertiary stratigraphic nomenclature proposed by Cather et al. in this guidebook. Road logs also use 33.4 Ma as the Eocene-Oligocene boundary following the lead of McIntosh et al. (1992); this boundary was previously placed at 36.6 Ma (Palmer, 1983). Ages of Tertiary ignimbrites and other volcanogenic units are from McIntosh et al. (1991, 1992) and papers in this guidebook unless otherwise specified.

Mileage

0.0 Stop sign at US-60 and road from the Dicaperl perlite mine. **Turn right, and head west on US-60. 0.2**

0.2 Bridge over Socorro flood-control channel. Remnants of the Pliocene basalt of Socorro Canyon (Osburn and Chapin, 1983) cap ridge from 1:00 to 2:00. Pale red piedmont-slope conglomerates and buff axial-river sands of the Sierra Ladrones Formation (upper Santa Fe Group) are conformably overlain by this basalt flow near the white water tank at the east point of the ridge. **0.2**

0.4 Milepost 136. Thick cauldron-facies Hells Mesa Tuff is exposed in low rounded peaks of the central Chupadera Mountains at 12:30. This structurally high, resurgent-like block lies near the eastern center of the Socorro cauldron, from which the Hells Mesa Tuff was erupted at 32.06 Ma (Osburn and Chapin, 1983; McIntosh et al., 1991). **0.3**

0.7 Approaching fault scarp on right that displaces inset terrace gravels of late Pleistocene age (~ 0.1 Ma) as much as 10 ft. Note gravel pile, from trench across fault scarp, near the fence line. This is the recurrent Socorro Canyon fault, which may have moved as recently as the early Holocene (Machette and McGimsey, 1982; Machette, 1982). At 9:00 the middle Pleistocene piedmont slope and remnants of a 3-ft-thick laminar calcrete are offset 100 ft by the Socorro Canyon fault. Pliocene to lower Pleistocene strata of the Sierra Ladrones Formation may be as much as 1150 ft thick on the downthrown eastern side of the Socorro Canyon fault (Chamberlin, 1981a). Based on gravity data, Sanford (1978) estimated that the total structural relief along the west side of the Socorro Basin is as much as 2.2 mi. From 9:15 to 12:15 a thin veneer of middle Pleistocene piedmont gravels unconformably overlies discontinuously and poorly exposed strata of the upper Popotosa Formation (lower Santa Fe Group). Where better exposed in the next canyon to the south these upper Miocene Popotosa beds dip 30° to the east. **0.2**

0.9 At 2:30, bulldozer cuts of the Dicaperl perlite mine expose red mudstones of the upper Popotosa Formation overlapping light gray hills of perlite that define the buried crest of a 7.85-Ma, high-silica, rhyolite lava dome (Chamberlin et al., 1994a). Chemical weathering (hydration) of this small, 0.02 mi^3, glassy lava dome has produced a world-class perlite deposit (see following minipaper). **0.4**

GEOLOGY AND MINING OF THE SOCORRO PERLITE DEPOSIT

James M. Barker[1], Timothy L. Hall[2], and Richard M. Chamberlin[1]

[1]New Mexico Bureau of Mines & Mineral Resources, Socorro, NM 87801;
[2]Dicaperl, Socorro, NM, 87801

The Socorro perlite deposit, mined by Dicaperl (a unit of Grefco), is about 4 mi southwest of Socorro in central New Mexico. The Dicaperl Socorro mine and processing plant is in sec. 27 T3S R1W and occupies 70 to 90 acres on patented claims. The mine is adjacent to the plant and employs about 35 people. Socorro was one of the first perlite mines in the United States when it opened in 1949. Closed from 1959 to 1975, large reserves and high quality have led to continual operation since then.

The small volume, high-yield Socorro perlite deposit lies along a Quaternary fault-line escarpment that defines the eastern flank of the west-tilted Socorro Peak uplift (Weber, 1963, Chamberlin, 1980; Bobrow et al 1983). The Socorro perlite deposit is a zone of weathering (hydration) on a small glassy lava dome of high-silica rhyolite with an $^{40}Ar/^{39}Ar$ age of 7.85 ± 0.04 Ma, from sanidine phenocrysts (Chamberlin et al., 1994), that agrees with an earlier K-Ar whole-rock age of 7.4 ± 0.4 Ma (Chamberlin, 1980).

The following geology is largely from Chamberlin, Barker and Jenkins (1994). The lava dome has a maximum lateral extent of 2800 ft, and is exposed over a topographic interval of 450 ft. The partially buried crest of the dome is flat over a distance of 1200 ft. The high-silica rhyolite lava (76-77% SiO_2, anhydrous), was strongly enriched in lithophile trace elements Rb, Mn, Nb, Ta, Pb, Th, U and heavy rare earths and is relatively depleted in Sr and Ba (Bobrow et al., 1983). The steep flanks of the original dome are largely buried by younger sandstone and mudstone of the lower Santa Fe Group. The southeast margin of the dome is a fault contact; another fault bisects the main perlite outcrop into east and west halves. The bisecting fault is down-to-the-east normal with an approximate throw of 200 ft. Topographic relief in the western block and recent drilling at the south end of the eastern block both require a minimum thickness of 300 ft for the original unfaulted lava dome.

An early phase of cogenetic lithic-rich ash-flow tuff and bedded tuff, as much as 60 ft thick, is discontinuously exposed around the flanks of the lava dome. Large mudstone clasts (>2 ft), in an ash flow cropping out about 0.5 mi north of the dome, indicate proximity to the source vent. Greater than 95% of the exposed lava dome consists of glassy, microvesicular, flow-banded rhyolite. Sparse (<1%), fine-grained phenocrysts of oligoclase, sanidine, quartz and rare biotite are evenly distributed throughout the dome. A large lens of crystalline felsite (approximately 200 ft x 600 ft) at the northeast margin of the dome is interpreted as a syneruptive "crystalline mush." Flow-banding is dominantly defined by flattened microvesicles and locally by stringers of syneruptive felsite. Open tension fractures in the felsite bands pinch out in adjacent glass, thereby demonstrating a ductility contrast. Flow banding is generally steep, irregular and is roughly concentric within the dome. Density and microvesicularity are inversely proportional; density increases downward. Small lenses of dense nonvesicular perlite locally occur near the center of the dome. Some samples of perlite from the core area contain microscopic nodules of obsidian that range in diameter from 0.0125 to 0.025 in.

The eruptive history (Chamberlin et al., 1994) began at about 7.85 Ma with throat-clearing, small-volume, ash-flow tuffs followed by ash falls. A highly viscous, high-silica magma rose slowly in the open conduit. Chilling of the magma cap, at or near the vent walls (at moderate vapor pressure?), locally formed a granophyric crystallite mush that was part of the initial surface extrusion. Finally, a viscous, foamy, high-silica melt was very slowly extruded through a confined(?) orifice, forming a small, circular, steep-sided and flat-topped dome with a volume of about 0.02 mi^3. Cooling by gas expansion (vesiculation) and by gas escape (dehydration), extreme viscosity, and relatively large ratio of surface area to thermal mass, allowed this small body to cool quickly so that the crystalline core, commonly observed in other rhyolite lava domes, did not form here. Flow fractures, cooling cracks, microfractures and flattened microvesicles created a highly permeable obsidian that facilitated relatively complete and homogeneous alteration (hydration) by meteoric waters to form a commercial perlite.

The mining and milling of Socorro perlite described below are largely from Austin and Barker (1994). A mining crew of three works half a shift to replenish the surge pile and then finishes with development and reclamation work. Perlite is ripped with a D9 Caterpillar, and a scraper (Caterpillar 631D with a screw auger) moves it to the 14 in. grizzly over the primary jaw crusher (-2 in.). A 0.25-mi covered belt conveys the perlite to a seven-day surge pile. A vibratory feeder moves ore into the plant where it is screened to -3/8 in. The +3/8 in. is recycled to a vertical

impact crusher. The crushed perlite is dried in a 400°F rotary dryer fired with recycled crankcase oil, to 0.25% free moisture at a discharged temperature of about 250°F. The dry -3/8 in. perlite is rescreened over one of two banks of screens and stored as eight grades, in 12 storage tanks, for blending to customer specifications.

About 150,000 st of crude perlite of all sizes were sold in 1993. Addition of regrind circuits has added capability to better match surges in demand for a particular grade. The capacity of the plant is 45 stph, dropping to 35 stph if intense regrind is underway (maximum of 650 short tons per day [stpd] of crushed and sized perlite). A Santa Fe Railroad spur extends about 3.5 mi from the center of Socorro to the Dicaperl mill.

About 95% of processed perlite is shipped in 100 st bottom-dump railcars or in pressure differential railcars for pneumatic unloading of finer sizes. A Dresser 510 frontend loader switches railcars and moves product around the plant. About 5% of crude perlite is trucked to customers perlite in 1 yd^3 supersacks. Dicaperl expansion plants in Lafayette, LA, and Jackson, MS, take about 10-15% of the total Socorro production. About 10% of production is exported, principally to Canada, with small amounts to Mexico. About 60% of production goes into ceiling tile with most of the remainder used in horticulture. A minor amount goes into filter aids, wallboard, and pipe insulation.

1.3 Road to site of old Great Lakes Carbon perlite mill on right. At 3:30 through small saddle is a view of northerly aligned necks and vent on "M" Mountain, all part of the upper Miocene Socorro Peak Rhyolite (Osburn and Chapin, 1983). **0.3**

1.6 At 3:00 in middle slope, reddish brown craggy outcrops of densely-welded upper Lemitar Tuff (28.0 Ma) define a west-tilted fault block that is unconformably overlain by east-dipping beds of lower and upper Popotosa Formation. High mesa at 3:00 is formed by a flat-topped dacite lava flow of late Miocene age. Vertical columnar jointing visible on west flank of the dacite flow is perpendicular to the flat upper cooling surface. Black Mountain (Mesa) at 2:00 is capped by a 4.1-Ma basalt flow, (Bachman and Mehnert, 1979) designated by Osburn and Chapin (1983) as the basalt of Socorro Canyon. On Black Mountain the basalt of Socorro Canyon unconformably overlies gypsiferous playa deposits of the upper Popotosa Formation. Quaternary landslide blocks of basalt, sliding on incompetent claystones, form the hummocky slope below the mesa. A high-velocity test-track facility of New Mexico Tech (EMRTC) is visible at the east end of the mesa. **1.0**

2.6 Gully at 9:00 exposes varved Popotosa mudstones and siltstones unconformably overlain by middle Pleistocene piedmont gravels. Red Popotosa claystones and siltstones are locally well exposed at 2:45 on north bank of Socorro Canyon. Bowie and McLemore (1987) reported that these gypsiferous claystones consist predominantly of sodium smectite. For the next 0.9 mi, road cuts on the left provide discontinuous exposures of colluvial gravels and underlying red mudstones of the upper Popotosa Formation. **0.9**

3.5 Crossing range-bounding fault on the northeast flank of the Chupadera Mountains. Roadcuts expose west-tilted red andesite porphyry lava and light gray rhyolitic ash beds collectively assigned to the Luis Lopez Formation, that represent the locally erupted post-collapse fill of the Socorro cauldron. The rhyolitic ash beds have been zeolitically altered and contain potassic clinoptilolite (G.S. Austin, oral commun., 1993). A thin ignimbrite below a rhyolite lava just south of this cut has yielded a K-Ar age of 28.6 ± 1.1 Ma from biotite phenocrysts (Chamberlin, 1980). This rhyolite lava member caps the Luis Lopez Formation and is presumably only slightly older than the 28.85 Ma La Jencia Tuff that overlies the Luis Lopez Formation in the southern Chupadera Mountains (Eggleston et al., 1983; McIntosh et al., 1991). The Oligocene andesite porphyry lava is potassium metasomatized; coarse-grained plagioclase phenocrysts are replaced by a chalky white mixture of adularia, clay minerals and quartz (see Dunbar et al., this volume). Preliminary $^{40}Ar/^{39}Ar$ ages of metasomatic adularia in the Socorro region (7.4 and 8.9 Ma) suggest a long period of metasomatism, contemporaneous with playa sedimentation (ca. 15-7 Ma) in the early rift Popotosa basin. Widespread potassium metasomatism in the Socorro-Magdalena region has been attributed to deep circulation of alkaline saline brines associated with playa deposits of the Popotosa basin (Chapin and Lindley, 1986). **0.1**

3.6 Entering north-trending strike valley cut in soft claystones of the upper Popotosa Formation that are downfaulted between resistant rocks of the underlying Luis Lopez Formation. **0.2**

3.8 Roadcut on left in thin basalt flow interbedded in red and green claystones of the upper Popotosa Formation. This thin flow is locally folded into an open northwest-trending syncline apparently sympathetic to a local zone of northeast-trending scissors faults that separate west-tilted Luis Lopez strata on the north from east-tilted Luis Lopez strata on the south. This zone of scissors faults crosses the north end of the Chupadera Mountains about 1.2 mi south of US-60, and is presumably part of the Socorro accommodation zone (SAZ), described in detail by Chapin (1989). The SAZ is a regional domain boundary that trends west-southwest from Socorro and separates strongly extended domains of imbricate fault blocks. Imbricate, domino-style, fault blocks and half grabens north of the SAZ are predominantly tilted to the west, compared to strongly east-tilted domino blocks south of the SAZ. Accommodation zones and transfer faults (strike-slip boundaries of extended domains) are common features in the Basin and Range extensional orogen (Wernicke, 1992) and in the Rio Grande rift (Chapin and Cather, in press). **0.4**

4.2 Cliffs of Luis Lopez Formation tuffs and lavas define the footwall of a fault-line scarp from 9:30 to 1:00; Popotosa claystones are locally exposed on the downthrown block just east of the scarp. **0.2**

4.4 Bridge over Box Canyon; recent attempts to mine placer gold from gravels on the floor of Box Canyon have been unsuccessful. **0.1**

4.5 Large road cuts on right and left expose locally erupted lithic-rich ignimbrites, andesite lavas and a feeder dike collectively assigned to the Luis Lopez Formation. Bouldery red debris flows and pebbly conglomerates of the lower Popotosa Formation disconformably overlie the Luis Lopez ignimbrite and andesite dike toward the west end of the cut. All of the

Luis Lopez members and the lower Popotosa beds are potassium metasomatized.

The light gray, poorly welded, pumiceous, lithic-rich ignimbrite is locally 900 ft thick and characterized by large rounded to angular clasts of densely welded Hells Mesa Tuff and less common clasts of andesitic lavas (Chamberlin, 1980). Another poorly welded, pumiceous, lithic-rich ignimbrite near the base of the Luis Lopez Formation contains mostly andesitic lithic fragments.

The lower Luis Lopez ignimbrite is about 200 ft thick where well exposed about 1.2 mi southeast of here in Black Canyon. Sanidine from the potassium metasomatized lower Luis Lopez ignimbrite at Black Canyon has yielded a relatively low precision $^{40}Ar/^{39}Ar$ age of 29.85 ± 0.31 Ma (M. Heizler, written commun., 1993); approximately 2 Ma younger than the underlying Hells Mesa Tuff. However, potassium metasomatism may have slightly reset this sanidine age. If the apparent 2 Ma hiatus in volcanism is real, then the Luis Lopez Formation may represent a series of small precursor eruptions that culminated in eruption of the large-volume La Jencia Tuff (28.8 Ma) from the Sawmill-Magdalena cauldron (Osburn and Chapin, 1983). The Sawmill-Magdalena cauldron is nested within the older Socorro cauldron. The eastern margin of the Sawmill Canyon depression is locally well defined south of Box Canyon, where the 28.0-Ma Lemitar Tuff laps unconformably onto Luis Lopez Formation at the topographic rim of the caldera. **0.2**

4.7 Road to Luis Lopez manganese district on left. Vent of small andesitic volcano in Luis Lopez Formation is defined by sheeted andesite plug at 2:30, across Socorro Canyon. **0.1**

4.8 Red and green upper Popotosa claystones unconformably overlie red fanglomerates of the lower Popotosa Formation in small pit at 10:00. Bowie and McLemore (1987) summarized published and unpublished clay mineralogy data for this pit. Illite is the dominant clay mineral in the lower Popotosa fanglomerates, and the illite content of the upper Popotosa claystones decreases upward from the unconformity until dioctehedral sodium smectite becomes the dominant species several feet above the contact. They attributed this trend to illitization of smectite by downward percolating potassium metasomatizing fluids. **0.1**

4.9 Road cuts on right and left in Luis Lopez lithic-rich tuff and andesite dikes, unconformably overlain by lower Popotosa fanglomerates. Route crosses buried northeast margin of Sawmill-Magdalena cauldron just west of this road cut. **0.2**

5.1 Road to telephone cable relay station on right. Vent area for the late Miocene (7.1 ± 0.2 Ma; C. E. Chapin, unpubl. data) basalt of Sedillo Hill at 12:30. The upper Miocene basalt of Sedillo Hill was erroneously correlated with the Pliocene basalt that caps Black Mountain at 2:30 (Chamberlin, 1980). Both of these basalt flows overlie claystones of the uppermost Popotosa Formation and are in turn overlain by piedmont-slope gravels of the Sierra Ladrones Formation. **0.3**

5.4 Milepost 131. Range crest west of Socorro Peak, from 3:00 to 1:00, is underlain by thick rhyolite flows and domes of late Miocene age. Below the cliff-forming rhyolite lavas is a hummocky Quaternary landslide terrane consisting of lava blocks that have slid downslope on upper Popotosa claystones. The claystones are only locally exposed in deeper ravines that cut across the landslide terrane. **0.9**

6.3 Road cuts on right in red claystones of the upper Popotosa Formation, largely masked by Quaternary colluvial gravels. Beginning of steep grade up Sedillo Hill. **0.5**

6.8 Break in slope at 2:30 defines poorly exposed contact of upper Santa Fe Group piedmont-slope deposits (Sierra Ladrones Formation) disconformably overlying playa claystones of the lower Santa Fe Group (upper Popotosa Formation). Map patterns at Sedillo Hill (Chamberlin, 1980) suggest that the Sierra Ladrones piedmont gravels locally fill an east-trending paleovalley cut through the basalt of Sedillo Hill and about 200 ft down into the underlying Popotosa claystones. The piedmont gravels thin abruptly to the north, to less than 100 ft, where they overlap the basalt of Sedillo Hill at the apparent north rim of the paleovalley. Pale red, poorly-indurated, conglomeratic sandstones and gravels near the bottom of the paleovalley are locally well exposed in the arroyo wall at 9:00. These beds dip 4° to the west. The thickness of Sierra Ladrones piedmont gravel west of Sedillo Hill is at least 800 ft (Chamberlin, 1980) and may be as much as 1475 ft (C. E. Chapin, unpubl. drill hole log). **1.2**

8.0 Curve right at top of Sedillo Hill. Road cut on left exposes red paleargid soil of early middle Pleistocene age (McGrath and Hawley, 1987). Colorado Plateau (Lucero uplift) is on the distant horizon from 12:00 to 12:30. Hells Mesa, the small butte at 11:50, is capped by gently southwest-dipping Oligocene ignimbrites and marks the northeast end of the Mogollon slope.

Apatite fission-track data from the Ladron Mountains at 12:30 indicate that this triangular west-tilted block, bound by faults on three sides, was rapidly uplifted during the period from 14 to 9 Ma (Kelley et al., 1992). Wernicke and Axen (1988) interpreted the Sierra Ladrones as the isostatically uplifted footwall of a low-angle (25°), east-dipping detachment fault, previously mapped by Black (1964) as the Jeter fault. Fission track data also indicate that temperatures in the Ladron block did not exceed 240°C (Kelley et al., 1992), well below the minimum 300°C required for ductile deformation of quartz as observed in Cordilleran metamorphic core complexes below detachment faults (Wernicke, 1992). **0.4**

8.4 Milepost 128. For the next 11.7 miles, US-60 traverses the western margin of the La Jencia Basin (11:00 to 1:00), a late Miocene to Recent half graben of the central Rio Grande rift (Cather et al., in press). The late Pleistocene to early Holocene scarp of the La Jencia fault (Machette, 1982, 1988), which cuts across the piedmont slope of the Magdalena range from 9:00 to 11:30, delineates the western edge of the La Jencia half graben. The Lemitar Mountains, from 1:30 to 2:00, and Socorro Peak at 3:30, mark the upturned eastern flank of the west-tilted La Jencia half graben. An active fault zone along the west side of the Socorro Basin, the Socorro Canyon-Loma Pelada fault zone (Machette,

1982) bounds the east side of the Lemitar Mountains and presumably interacts with the structurally lower La Jencia fault to facilitate block rotation and spreading within the active domain. A mid-crustal, sill-like, magma body first defined by microearthquake seismograms (Sanford et al., 1977) and later corroborated as a mid-crustal seismic reflection bright spot (Brown et al., 1980) underlies the active domain of extension from Socorro northward to Bernardo. Recently, Lipman (1992) suggested that the Socorro mid-crustal bright spot may represent hydrothermal fluids concentrated along the brittle-ductile transition zone or at the solidification interface of a tabular granitic intrusion. Lipman's interpretation implies that the combined La Jencia and Socorro Canyon-Loma Pelada fault systems may represent an active domain of detachment faulting balanced above a rising or expanding mid-crustal granitic intrusion or hydrothermally softened zone. In this sense, the La Jencia fault would represent a breakaway fault, structurally lower than all other active faults in the domain (Wernicke, 1992). **1.0**

9.4 Milepost 127. Crest of the South Canyon alluvial fan. From 1:45 to 2:30 west-tilted hogbacks of Oligocene ignimbrites in the Lemitar Mountains are the most obvious expression of a late Oligocene episode of domino-style crustal extension (Chamberlin, 1983). High precision $^{40}Ar/^{39}Ar$ ages of Oligocene ignimbrites and of Miocene ash-beds within the middle to upper Popotosa Formation have been combined with stratal tilt data to demonstrate two episodes of relatively rapid extension and block rotation in the Lemitar Mountains, from 28.6 to 27.4 Ma and from 16 to 10 Ma (Cather et al., in press). In the northern Lemitar Mountains a stack of thin basaltic andesite lava flows, each about 23-33 ft thick, forms a wedge-shaped prism as much as 1675 ft thick between the 28.6-Ma Vicks Peak Tuff and the 27.4-Ma South Canyon Tuff. If this lava wedge represents 51 to 73 flows erupted over a span of 1.2 Ma, then on average a basaltic lava flow was erupted every 16,000 to 24,000 yrs during this period. The middle to late Miocene episode of relatively rapid extension began with eruption of the Silver Creek basaltic andesite at 16.2 ± 1.5 Ma (Cather et al., in press). This middle Miocene basaltic andesite is now tilted about 35° to the west. The overlying main body of Popotosa beds, ~2000 ft thick, and intercalated ash beds show a fan-shaped array with dips decreasing to about 10-20° in 12-Ma beds. Total late Cenozoic crustal extension in the Lemitar Mountains is estimated to be about 175% (Chamberlin, 1983). **1.0**

10.4 Milepost 126. **0.9**

11.3 Water Canyon Lodge on right. Route crosses buried northern margin of 32.1-Ma Socorro cauldron and the nested 28.8-Ma Sawmill-Magdalena cauldron near here (Osburn and Chapin, 1983). These volcanic collapse structures locally merge to the southwest where they pass beneath Water Canyon Mesa at 9:00. Cliff-forming debris flows of the lower Popotosa Formation, at canyon mouth on left side, unconformably buried these cauldron margins in Miocene time. Farther south, the cauldron subsidence faults separate and then swing west over the crest of the Magdalena range. An exposure of white, partially welded Hells Mesa Tuff onlaps the northern topographic rim of the Socorro cauldron near North Baldy at 10:00. Palinspastically restored cross sections and elongation of the Socorro cauldron, now 15 mi N-S by 23 mi E-W, indicate an average of 50% crustal extension across the Socorro-Magdalena caldera complex (Chamberlin and Osburn, 1986; Chapin, 1989). **1.6**

12.9 Road to Water Canyon on left. The south-central portion of La Jencia Basin is hydrographically closed and drains into the small playa at 1:00, in middle distance below Ladron Peak. Aggradation and northeastward progradation of the upper Pleistocene Water Canyon alluvial fan, which dominates the southern third of the basin, may have been a factor in the formation of this playa. **0.5**

13.4 Milepost 123. Good view of the crest of the northern Bear Mountains at 11:45 and Hells Mesa at 12:00. The southern Bear Mountains on the lower horizon, at 11:30-11:45, include west-tilted, imbricate fault blocks that represent 25% of west-southwest directed extension (Chamberlin and Osburn, 1986) in comparison to about 5% extension in the northern Bear Mountains (Massingill, 1979). A northeast-trending oblique-slip fault separates the weakly extended northern domain, (part of the Mogollon slope), from the more strongly extended southern domain, which is assigned to the San Agustin arm of the Rio Grande rift (Chapin, 1971). This oblique-slip fault, or transfer fault (Wernicke, 1992), locally marks the southeast margin of the Mogollon slope as defined in the following minipaper by Chamberlin and Cather. **0.9**

DEFINITION OF THE MOGOLLON SLOPE, WEST-CENTRAL NEW MEXICO

Richard M. Chamberlin and Steven M. Cather
New Mexico Bureau of Mines and Mineral Resources, Socorro, NM 87801

Although previously mentioned by Kelley (1957), the Mogollon slope was first defined by Fitzsimmons (1959, p. 114):

> "The Mogollon slope is the southern part of the Colorado Plateau and, in many ways, is a rather nondescript structural unit. In general, the sedimentary rocks in this unit dip gently to the south. The slope is dotted by accumulations of volcanic rocks of many types. Along the south end only volcanic rocks, or sedimentary deposits derived from them, are to be found. At the north end, older sedimentary rocks may be observed in places and the volcanic rocks form local ranges or individual mountains. The precise southern boundary of this unit is not easy to delineate everywhere. Along the Mogollon Rim, where faulting has produced a prominent escarpment the margin is drawn closely. But in much of New Mexico the volcanic accumulations are so thick that, although faults are present, a sharp line cannot be perceived."

The purpose of this minipaper is to present a more explicit definition of the Mogollon slope and to delineate its boundaries relative to other more recently recognized tectonic elements of western New Mexico and eastern Arizona. A generalized tectonic map (Fig. 1.1) shows a first approximation of Cenozoic extensional strain relative to the Mogollon slope and the New Mexico area. Regional topographic trends (Godson, 1981) and physiographic patterns (NMGS, 1982, physiographic map) are used as a guide, but known or inferred extensional strain is the ultimate criteria (e.g., Wernicke, 1992). For example, positive topographic elements such as the Magdalena Mountains and eastern San Mateo Mountains that show strong domino-style crustal extension (e.g.,

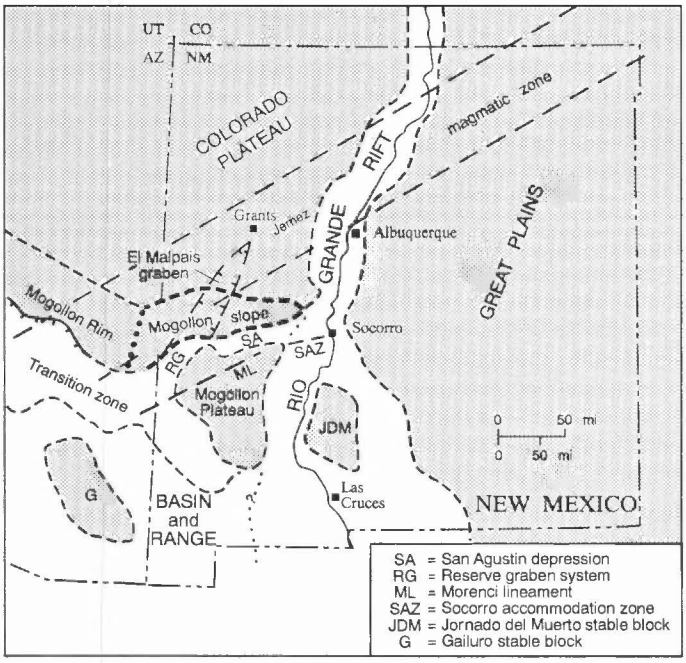


FIGURE 1.1. Generalized tectonic map of New Mexico and eastern Arizona showing the relationship of the Mogollon slope to regional structural elements. Provinces and domains of moderate to strong Cenozoic crustal extension are shown in white. Crustal provinces and blocks that have generally resisted Cenozoic extension are shaded gray. Compiled from Aldrich and Laughlin (1984), Chapin (1971, 1989), Godson (1981), Pierce (1985), Ratté (1989) and Wernicke (1992).

Ferguson, 1991) are mapped as part of the Rio Grande rift. More commonly the rift is defined by the distribution of deep Neogene half grabens. Areas of moderate to strong extension in the Rio Grande rift, Basin and Range, and Arizona transition zone have been lengthened (generally to the west) by about 10 to 100% or more (Wernicke, 1992). Belts of weak extension show about 1 to 10% lengthening in east-west cross sections.

The Mogollon slope is primarily defined by gently south-dipping (2–10°) Eocene to Oligocene orogenic and volcanogenic strata approximately 1.3 to 2.1 km thick that generally parallel the classic (physiographic) southeastern margin of the Colorado Plateau. Eocene continental red-bed deposits were derived from Laramide transpressional welts along the Morenci lineament (Chapin and Cather, 1981; Garmezy, 1990). Overlying volcanic-apron deposits were derived from andesitic volcanoes that buried these welts (Elston et al., 1976) and from subsequent rhyolitic caldera complexes (McIntosh et al., 1991) that developed within the andesitic terrane to form the batholithic nucleus of the Mogollon Plateau. Thick piles of upper Oligocene basaltic andesite lavas that erupted contemporaneously with early strong extension along the axis of the Rio Grande rift locally cap highlands of the Mogollon slope. From east to west, landmarks formed by middle Tertiary volcanic strata along the Mogollon slope include: northern Bear Mountains, Gallinas Mountains, Datil Mountains, Crosby Mountains, Alegres Mountain, Mangas Mountains, Escondido Mountain, Gallo Mountains, Fox Mountain and Escudilla Mountain. The latter is located in eastern Arizona, where the south-dipping Mogollon slope grades into north-dipping strata on the Mogollon Rim.

The northern margin of the Mogollon slope generally parallels and lies a few kilometers north of the outcrop belt of the Eocene Baca Formation (Cather and Johnson, 1984). Here, the underlying Upper Cretaceous strata typically flatten out to a gentle north-northeast dip that is common throughout the Colorado Plateau. The southern margin of the Mogollon slope is defined by moderate to strongly extended domains along the San Agustin arm of the Rio Grande rift (Chapin, 1971). This weaker arm of the rift forms a regional west-southwest-trending topographic low (Godson, 1981) referred to here as the San Agustin depression. North-northeast-trending zones of weak extension along the Puerticito, Red Lake and Hickman faults locally cut across the Mogollon slope and southern margin of the Colorado Plateau (Cather, 1989; Chamberlin and Anderson, 1989b). For simplicity, only the El Malpais graben that parallels the Hickman fault zone is shown here (Fig. 1.1).

The Mogollon Rim section of the southwestern Colorado Plateau margin (between the Mogollon escarpment and the Little Colorado River) probably formed in Neogene time by isostatic uplift during extensional unloading of its footwall in the Arizona transition zone (Pierce, 1985). The northwest-trending extensional structures of the Arizona transition zone appear to give way to the northeast-trending structures of the San Agustin arm of the rift near Alma, New Mexico (Houser, this volume). A narrow, topographically low, distended zone west of Horse Springs (Godson, 1981; Ratté et al., 1991) appears to link the Reserve graben extended domain with the western San Agustin depression (see Third-Day road log). The en echelon pattern of the Reserve graben system and San Agustin depression may be attributed to sinistral transtension associated with Neogene clockwise rotation of the Colorado Plateau as it pulled away from the batholithically rooted Mogollon Plateau block (Chapin and Cather, in press; Fig. 1.1).

The Mogollon slope most likely represents downwarping of the southeastern margin of the cratonic Colorado Plateau microplate as it was loaded by as much as 2.1 km of orogenic and volcanogenic strata in Eocene to Oligocene time. Middle to upper Miocene Fence Lake Formation conglomerate derived from these south-tilted volcanic highlands near Quemado and Mangas show gentle primary dips to the northwest. Thus, the southerly tilt is pre-middle Miocene in the Quemado-Mangas region of the Mogollon slope.

Middle Miocene to Quaternary extension along the El Malpais graben was apparently penecontemporaneous with volcanism along the Jemez magmatic zone, or Jemez lineament of Aldrich and Laughlin (1984). The El Malpais graben is a narrow finger of weak crustal extension that penetrates deeply into the Colorado Plateau as it follows a pre-existing zone of Laramide strike-slip deformation (e.g. Hickman fault zone; Cather, 1989; Chamberlin and Anderson, 1989a). This should not be surprising, since the axis of the Rio Grande rift follows a major dextral strike-slip zone with as much as 120 km of lateral displacement in Laramide time (Chapin, 1983).

14.3 US-60 bends to left near milepost 122. The northern Magdalena Range from 9:00 to 11:30 is formed by a west-tilted hogback of Mississipian Kelly Limestone unconformably overlying a variety of Proterozoic metamorphic rocks and plutonic rocks. Late Oligocene monzonitic stocks and dikes that intrude the Proterozoic rocks in this structurally high block, north of the Socorro cauldron, may be regarded as an expression of the plutonic roots of the caldera complex. **4.6**

18.9 At 10:00, the La Jencia fault scarp displaces a middle Pleistocene fan surface as much as 23 ft (Machette, 1982, 1988). Total structural relief, presumably Neogene, in the La Jencia Basin is about 1.85 mi (Sanford, 1978). As much as half of this displacement may occur on the La Jencia fault. A southeast-trending seismic reflection profile across the La Jencia basin (COCORP line 3, Brown et al, 1980) shows several buried faults below Santa Fe Group basin fill, which is as much as 4500 ft thick. Seismic refraction data of Roberts et al. (this volume) also support the presence of a thick low-velocity basin fill in the La Jencia basin. **1.0**

19.9 Highway climbs over the La Jencia fault scarp. For the next 20 mi, from Magdalena to Tres Montosas, US-60 traverses a strongly extended domain that was stretched rapidly in late Oligocene time (Chapin and Seager, 1975; Ferguson, 1991), moderately extended in early Miocene time (Abbey Springs basin, Chapin and Cather, in press) and apparently inactive since middle Miocene time (Chamberlin and Osburn, 1986). East-northeast-trending transfer faults separate this domain from gently dipping Oligocene ignimbrites farther north on the Mogollon slope (Fig. 1.1). **0.2**

20.1 Knobby peak at 2:30 is capped by 34.17-Ma Rock House Canyon Tuff dipping about 35° to the west. The Rock House overlies and is interbedded with volcaniclastic sandstone and conglomerate of the Spears Group (see Cather et al., this volume). The Rock House Canyon Tuff has been assigned to the redefined Datil Group of Cather et al. (this volume). **0.3**

20.4 Milepost 116. **0.1**

20.5 Highway curves to left. Microwave tower at 1:00 is on crest of Granite Mountain, where 600 ft of granitic-looking, hornfelsed, crystal-rich Hells Mesa Tuff (32.1 Ma) is well exposed as a resistant west-dipping hogback. Volcanclastic sedimentary units of the lower Spears Group and intercalated Datil Group tuffs and lavas occupy the mid-slope. The basal Spears Group here rests in angular unconformity on the Permian San Andres Formation, exposed in the low hill at the east foot of Granite Mountain. This early Tertiary unconformity indicates that the west-tilted domino block of Granite Mountain is superimposed on the north flank of an east-northeast-trending Laramide uplift named the Morenci uplift by Cather and Johnson (1984). Similar exposures of the basal Tertiary unconformity delineate remnants of Laramide uplifts in the Lemitar Mountains, southern Chupadera Mountains, northern Magdalena Mountains, southern San Mateo Mountains, southern Gallinas Mountains near Tres Montosas, and on the southeast flank of Horse Mountain. These are also areas of strong crustal extension related to the Rio Grande rift. Thus it appears that domains of Neogene crustal extension and subsidence are superimposed on the same weak lithosphere that was shortened and uplifted during the Laramide orogeny. Correspondence of Neogene extended domains with Mesozoic and early Tertiary contractional domains is widely recognized in the Basin and Range (Wernicke, 1992) and the Rio Grande rift (Chapin and Cather, in press). **2.2**

22.7 At 3:00 is good view to north-northwest along the structural axis of the Bear Mountains. Northward decrease in west tilt marks southern margin of Mogollon slope within this range. **0.1**

22.8 Road sign on right proclaims Magdalena as the "Trails end". From 1885 to 1971 hundreds of thousands of cattle and sheep were driven eastward from Springerville, AZ and Horse Springs, NM to the rail head at Magdalena, making Magdalena the "trails end" for cows and cowboys. The tracks of the AT & SF Magdalena spur were pulled up in 1973, leaving trucking as the only alternative method for shipping livestock out of west-central New Mexico. The Magdalena spur was originally built in 1884 to haul lead-silver ores from the Kelly Mining district, south of Magdalena, to the Billing smelter in Socorro (Eveleth, 1983). **0.2**

23.0 Beyond the red brick house on the hill is Magdalena Peak, at 10:00 on the skyline. Near the middle of the slope, talus and vegetation form the face (side view, looking east) and bunned-up hair of "Mary Magdalene" for whom the Magdalena Mountains and the town are named. Magdalena Peak is capped by a thick rhyolite lava flow fed by an intrusive plug (dated at 13.1 Ma; Chapin et al., 1978) visible at its eastern end. This late Miocene rhyolite flow unconformably overlies Miocene Popotosa Formation and 28-Ma monzonite; the latter is part of a composite pluton related to the distended northern margin of the Magdalena-Sawmill cauldron (Chapin and Seager, 1975, Osburn and Chapin, 1983). **0.3**

23.3 Magdalena village limit. A major mining center at the turn of the century (silver, lead, zinc) and a key shipping point for cattle after WW I, Magdalena is now a quiet ranching community and a gathering place for the annual Old-timers Festival. **1.1**

24.4 Highway junctions at west end of Magdalena. **Continue straight ahead on US-60.** NM-169 on right leads to Alamo Chapter of the Navajo Indian Reservation; NM-107 on left goes to San Marcial at I-25. **0.1**

24.5 Road sign indicates Datil 34 mi, Springerville, 142 mi. Landmarks on the skyline ahead include the northern San Mateo Mountains at 11:00, Cat Mountain at 11:30, Gray Hill, with microwave tower, at 12:00, and Tres Montosas at 1:00. The Mt. Withington cauldron, source of the 27.4-Ma South Canyon Tuff, occupies most of the northern San Mateo Range and is also largely coincident with a strongly extended domain of the central Rio Grande rift (Ferguson, 1991). Tres Montosas, Gray Hill and Cat Mountain lie in a strongly extended and hydrothermally mineralized domain associated with a monzonite-granophyre stock (north of Tres Montosas; Wilkinson, 1976) and the western margin of the Magdalena-Sawmill cauldron (Osburn and Chapin, 1983). All these landmarks lie south of the relatively unextended and unmineralized Mogollon slope. See McLemore (this volume) for distribution of volcanic epithermal mining districts in west-central New Mexico. **0.5**

25.0 Roadcuts for next 2.6 mi expose gravelly to sandy alluvium of probable middle to late Pleistocene age. Red argillic zones and thin calcretes locally cap these gravels. Pebble imbrications suggest northeasterly paleoflow subparallel to Arroyo Gato, which trends east-northeast on the north side of the highway. These may be axial-stream deposits of ancestral Arroyo Gato or in some cases younger inset terrace gravels. Near here US-60 crosses the projected trace of a gently south-plunging synclinal axis defined by Oligocene ignimbrites a few miles to the north (Brown, 1972). To the west, Oligocene ignimbrites are strongly tilted to the east, as at Silver Hill (1:30) and east of the Tres Montosas (12:30). Another antiformal domain boundary separates west-tilted ignimbrites at Tres Montosas

and Gray Hill from this east-tilted domain. Similar synformal and antiformal tilt-block domain boundaries are common in moderately- to strongly-extended terranes of the Basin and Range (Stewart, 1980; Wernicke, 1992) and in the central Rio Grande rift (Chamberlin and Osburn, 1986; Chapin, 1989). **0.9**

25.9 Gravelly sand in roadcut on right shows pebble imbrications indicative of northeasterly paleoflow. **0.5**

26.4 Milepost 110. Silver Hill at 2:30 is comprised by Oligocene La Jara Peak Basaltic Andesite of the Mogollon Group. **1.2**

27.6 Enter large roadcut, mostly in hydrothermally altered, strongly sheared, and flow-banded La Jencia Tuff (28.8 Ma). Except near the west end of the cut, flow banding dips approximately 60° to the east-southeast. The light gray, phenocryst-poor tuff with sparse andesitic lithic fragments is locally bleached, iron stained and partially silicified (at southwest end of cut). Cubic limonites, pseudomorphs after pyrite, locally form 2 to 3% of the tuff. At the southeast end of the cut medium gray La Jara Peak Basaltic Andesite appears to conformably overlie the steeply-dipping La Jencia Tuff. Several north-trending normal faults, dipping steeply to east and west, cut the La Jencia Tuff. Fault gouges and breccias are as much as 6 ft thick, and dip-slip slickensides are prevalent. At the northwest end of the cut is a nearly vertical east-northeast-striking shear surface that exhibits subhorizontal slickensides (plunging 20° to S60°W) superimposed on older dip-slip slickensides that plunge 70° to S30°E. The sense of lateral slip on this late-stage shear surface is not readily apparent. If left lateral, it would tend to support Chapin and Cather (in press), who interpret the Colorado Plateau as having rotated 1.0° to 1.5° clockwise in Neogene time, in association with the formation of a zone of sinistral transtension along the San Agustin arm of the Rio Grande rift. **0.2**

27.8 Highway crosses projected trace of the down-to-the-west Hells Mesa fault and enters the Abbey Springs Basin of late Oligocene to middle Miocene age (Chapin and Cather, in press). Chapin et al (1979) estimated the maximum thickness of basin fill to be 2450 ft and assigned this fill to the Popotosa Formation. J. Abbott (oral commun., 1993) suggested that this basin-fill unit has a southerly trending axial-stream facies. Chapin and Cather (in press) refer to the Abbey Springs Basin fill as lower Santa Fe Group. Fanglomerate deposition within the Abbey Springs Basin is well constrained in time. Approximately 2 mi north of here, at Arroyo Montosa, 26-Ma dacite flows are interbedded with basal fanglomerates of the lower Santa Fe Group (Chapin and Cather, in press). Also, 5 mi to the west, subhorizontal lavas of the 16.3-Ma basalt of Council Rock (Bachman and Mehnert, 1978), rest conformably on top of the basin-fill fanglomerates near the western margin of the Abbey Springs Basin. **1.1**

28.9 Lower Santa Fe conglomerate in roadcut on right contains abundant basaltic andesite clasts. Pebble imbrications indicate westerly or southwesterly paleoflow. **0.3**

29.2 Roadcuts in gently west-tilted (3-4°), light brown conglomerate and conglomeratic sandstone of lower Santa Fe Group. Basaltic andesite clasts dominate; minor clasts of South Canyon-like ignimbrite and glassy flow-banded rhyolite lavas are present. Pebble imbrications indicate southwesterly or westerly paleocurrents. **0.2**

29.4 Flat-lying 16.3-Ma basalt of Council Rock forms rounded hills at 10:00. **0.9**

30.3 Roadcuts in non-indurated gravel and sand probably represent inset terrace deposits of middle to late Pleistocene age. **1.4**

31.7 Climbing hill of lower Santa Fe fanglomerate, roadcut on left in moderately indurated brown to buff conglomerate containing subequal concentrations of hydrothermally altered ignimbrite clasts and andesitic clasts. Pebble imbrication indicates easterly paleoflow. **0.2**

31.9 Note horizontal ledges of basalt of Council rock capping hill at 9:00. **0.5**

32.4 Milepost 104. Roadcuts in bouldery lower Santa Fe fanglomerate. Hydrothermally altered boulders of Hells Mesa Tuff, Rock House Canyon Tuff and andesitic conglomerate (lower Spears Group-type) are present and reflect increasing proximity to the western margin of the Abbey Springs Basin. **0.3**

32.7 Road cuts in subhorizontal 16.3-Ma basalt of Council Rock that caps the Santa Fe Group here. Approximately 22 mi to the northeast, the 16.2-Ma andesite of Silver Creek is tilted 35° to the west and *lies near the base* of the main body of the lower Santa Fe Group (Popotosa Formation). This relationship implies that the Magdalena-Abbey Springs-Tres Montosas extensional domain is relatively old and inactive in comparison to the Socorro-La Jencia Basin domain, which is distinctly active. Feeder dikes for the basalt of Council Rock are locally well exposed 4 mi north of here (Chamberlin, 1974). **0.4**

33.1 Road side picnic tables on right with USBLM-NMSHD sign commemorating the Magdalena Livestock Driveway. This sign reads as follows:

> "South across the road lies one of the west's historic "hoof highways" which was used annually from 1885 until 1971. Sheep and cattle were driven to and from the railroad at Magdalena, NM. The 125 mile driveway extended west to Datil, NM then forked leading to Horse Springs, NM or to Springerville, AZ. The driveway was 5-10 miles wide and covered 200 square miles. The peak trailing year 1919 saw 150,000 sheep and 21,677 cattle pass this point. In the 1930's the Civilian Conservation Corps fenced the driveway and drilled water wells every 10 miles. During the drives cowboys and herders moved cattle about 10 miles a day and sheep about 5 miles, allowing them to graze as they went with chuckwagons and remudas of horses following behind. Trailing gave way to trucking and the last portion of the driveway was officially closed in November, 1971." **0.1**

33.2 Crossing projected trace of the Puerticito fault zone, which bounds the western flank of the Abbey Springs Basin. **0.1**

33.3 Highway rises onto the Tres Montosas section of the

southern Gallinas Mountains uplift. Entering long roadcut in hydrothermally altered and structurally complex andesitic debris-flow deposits and sandstones of the middle Spears Group that are interbedded with light gray, 34.2-Ma Rock House Canyon Tuff of the Datil Group (McIntosh and Chamberlin, this volume). Compaction foliation in the silicified ignimbrite is locally apparent on the north side of the cut (0.15 mi from east end) and dips 40° to the east. Spears Group outcrops near the northeast end of the cut also contain a low-angle normal fault, dipping 28° west, and conjugate quartz veins with both vein sets dipping west, one steep and one shallow. These structural observations indicate this cut is part of a strongly extended domain on the east flank of Tres Montosas. Geologic maps of this area (Wilkinson, 1976; Chamberlin, 1974) show numerous down-to-the-west normal faults repeating strongly east-tilted Datil Group ignimbrites and interbedded Spears Group strata. Exposures of Permian Abo Formation a mile north of here are unconformably overlain by Spears Group conglomerate (Wilkinson, 1976); thus the Tres Montosas section is also on a Laramide uplift. Approximately 4 mi north of here the strongly east-tilted extensional domain terminates against a northeast-striking zone of scissors faults. North of this scissors zone the Hells Mesa Tuff is tilted about 5° to the west (Chamberlin, 1974). This scissors zone accommodates a dip reversal and apparently a greater degree of extension on the south side. It may be classified as an accommodation zone or a transfer fault. This accommodation zone locally defines the south margin of the Mogollon slope where it crosses the Gallinas uplift west-southwest of Council Rock. **0.4**

33.7 Three wooded hills of Tres Montosas at 11:00. An anticlinal tilt-block domain boundary trends north along the east foot of Tres Montosas. Tres Montosas is capped by moderately west-dipping (20°) Hells Mesa Tuff; the Hells Mesa is repeated by normal faults downthrown to the east (Wilkinson, 1976). To the north, this anticlinal axis intersects the Oligocene (?) monzonitic Tres Montosas stock. Domed and hornfelsed volcanic strata form a resistant annular rim around the stock. The accommodation zone west-southwest of Council Rock passes north of the stock thereby separating it from the Mogollon slope. **1.7**

35.4 Road to Montosa Cattle Company on right. Microwave tower marks the crest of Gray Hill at 9:30. Excellent exposures of beautifully flow-banded La Jencia Tuff are found along the road to the microwave tower (Fig. 1.2). The 28.8-Ma La Jencia Tuff fills a deep northeast-trending paleovalley here (Wilkinson, 1974) that is cut in the underlying 32.1-Ma Hells Mesa Tuff. The west rim of the Sawmill-Magdalena cauldron, source of the La Jencia Tuff, lies about 3 mi east of Gray Hill (Osburn and Chapin, 1983). **1.8**

37.2 Roadcuts in Hells Mesa Tuff within the west-tilted moderately extended domain that underlies Tres Montosas (Wilkinson, 1976). **0.6**

37.8 Road to North Lake and Dog Springs Canyon on right. Approximately 25 mi to the northwest, Dog Springs Canyon is the type area for the Dog Springs Member of the Spears Formation of Osburn and Chapin (1983), or the Dog Springs Formation of the Spears Group (Cather et al., this volume). Andesitic to dacitic (58-64% SiO_2; Cather et al., 1987) debris-flow deposits and breccias of the Dog Springs comprise much of the northern Gallinas Mountains, the Datil-Sawtooth Mountains, and the low hills along J-L Draw (west of Crosby Mountains). Highly contorted and chaotic bedding characterize the Dog Springs Formation, compared to gentle uniform dips in underlying and overlying strata (Osburn and Chapin, 1983). This deformation is attributed to widespread soft-sediment deformation, or liquefaction, possibly triggered by one or more seismic events. Rapid loading of saturated basin-floor sediments (early andesitic sandstones and mudstones) by thick debris flows may have also triggered soft-sediment deformation. Spectacular soft-sediment deformation in the Dog Springs Formation will be viewed at Stop 3 today, in the Sawtooth Mountains west of Datil. **0.2**

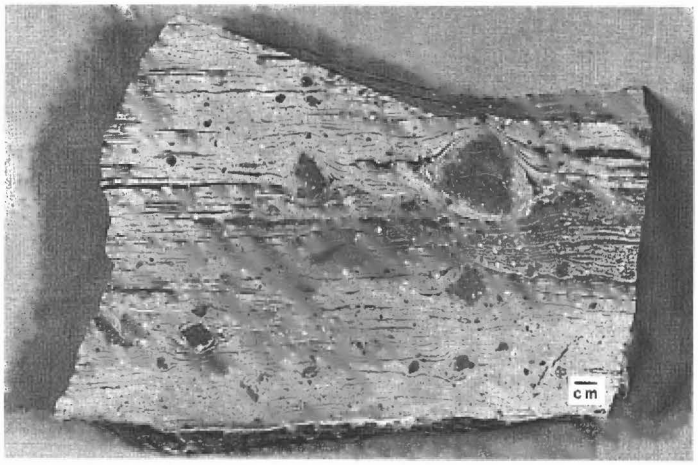


FIGURE 1.2. Flow-banded La Jencia Tuff showing effect of differential compaction and minor flowage around incompressible lithic fragments; sample from Gray Hill.

38.0 Entering northern section of the Plains of San Agustin, site of several late Pleistocene pluvial lakes, as described in the following minipaper by R. H. Weber. Highway crosses the projected high stand of these lakes near here, but shoreline features are locally masked by Holocene dune fields. Giant antennas of the VLA (Very Large Array) radio telescope dot the basin floor ahead. **2.4**

PLUVIAL LAKES OF THE PLAINS OF SAN AGUSTÍN

Robert H. Weber

New Mexico Bureau of Mines and Mineral Resources, Socorro, NM 87801

The 1994 Field Conference will cross the northern section of the Plains of San Agustín on the first day, and skirt the southwestern section on the third day. It is accordingly appropriate to summarize briefly some of the salient features of this structural and topographic intermontane basin that was inundated by an extensive lake system during at least the latest pluvial stages of the Pleistocene. Mapping on a scale of

1:24,000 of relict shorelines and surficial deposits of the floor and lower slopes of the basin by the present author has delineated a series of lake stages and associated littoral and lacustrine deposits of Pleistocene Lake San Agustín and subsequent Holocene playas.

Earlier investigations by Bryan (1926), Powers (1939, 1941), Hurt and McKnight (1949), Clisby and Sears (1956), Foreman (1956), Potter (1957), Foreman, Clisby, and Sears (1959), Stearns (1962), and Dick (1965) focused on various aspects of the geology, archaeology and palynology of the southwestern section of the area, herein designated as the Horse Springs (topographic) basin. Powers (1939) mapped a series of shorelines and associated littoral features in the Horse Springs basin extending to a maximum elevation of 6940 ft, recording the former presence of pluvial Lake San Agustin.

Later field investigations by Weber (1980, 1982) recognized a sequence of 16 principal lake levels ranging from 6800 to 7056 ft (later corrected to 7050 ft), the higher levels extending throughout three integrated topographic basins. These consist, from northeast to southwest, of the White Lake, C-N, and Horse Springs basins. North Lake, a very small, anomalous topographic basin, is linked to the northern end of White Lake basin. What here is designated as the Horse Springs basin formerly was shown as the limiting host for Lake San Agustín (Weber, 1980, fig. A-1). Later mapping of that basin indicated that the term Lake San Agustín should be extended throughout the conjoined topographic basins. At the 7050-ft maximum shoreline, the lake was approximately 57 mi long, with a maximum width of approximately 19 mi.

Absolute ages and chronology of the various lake stages remain essentially unknown. The degree of preservation of shorelines below the 7050-ft level (Fig. 1.3) and the presence of contiguous lake beds to these levels indicate a late classical Wisconsinan age, with a maximum stand at about 18,000 years B.P. Shorelines at 7005 ft, 7040 ft, and 7050 ft are highly fragmentary and lack contiguous lake beds. It therefore is suspected that these highest levels may reflect earlier pluvial stages; possibly early Wisconsinan (Bull Lake equivalent) or older. It should be noted that typical lacustrine deposits occur at 7060 ft in Nester Draw, indicating a higher lake stage than that recorded by the 7050-ft shoreline.

The present floors of the three contiguous basins are progressively higher in elevation from southwest to northeast: 6775 ft in Horse Springs basin, 6894 ft in C-N basin, and 6952 ft in White Lake basin. As a consequence, climatic changes toward the terminus of the Pleistocene resulted in desiccation and retreat of lake levels from northeast to southwest. On the basis of archaeological evidence, White Lake basin was reduced to a series of shallow ponds and marshes by ca 12,000 B.P. At 6960 ft, White Lake was separated from Lake San Agustín in C-N basin by a low sill, although a connection through a narrow channel, now covered by later deposits, is possible. The modern playa in White Lake basin is bounded by the 6955-ft level.

In the C-N basin, the reduced lake at the 6920-ft level connected with Lake San Agustín in Horse Springs basin through a narrow, steep-walled channel only 160 ft wide. The modern playa lies within the northern lobe of the area bounded by the 6895-ft shoreline (shown as 6900 ft in Weber, 1980, fig. A 2, as plotted on an uncorrected advance map sheet). A small lake may have persisted in the western part of Horse Springs basin well into the Holocene, possibly represented by a shoreline at 6810 ft, but this remains highly speculative. A probable playa shoreline is weakly expressed at approximately 6790 ft (Fig 1.3).

Drastically lowered lake levels resulted in vigorous eolian activity. Effective winds from the southwest drifted sands into sand sheets and

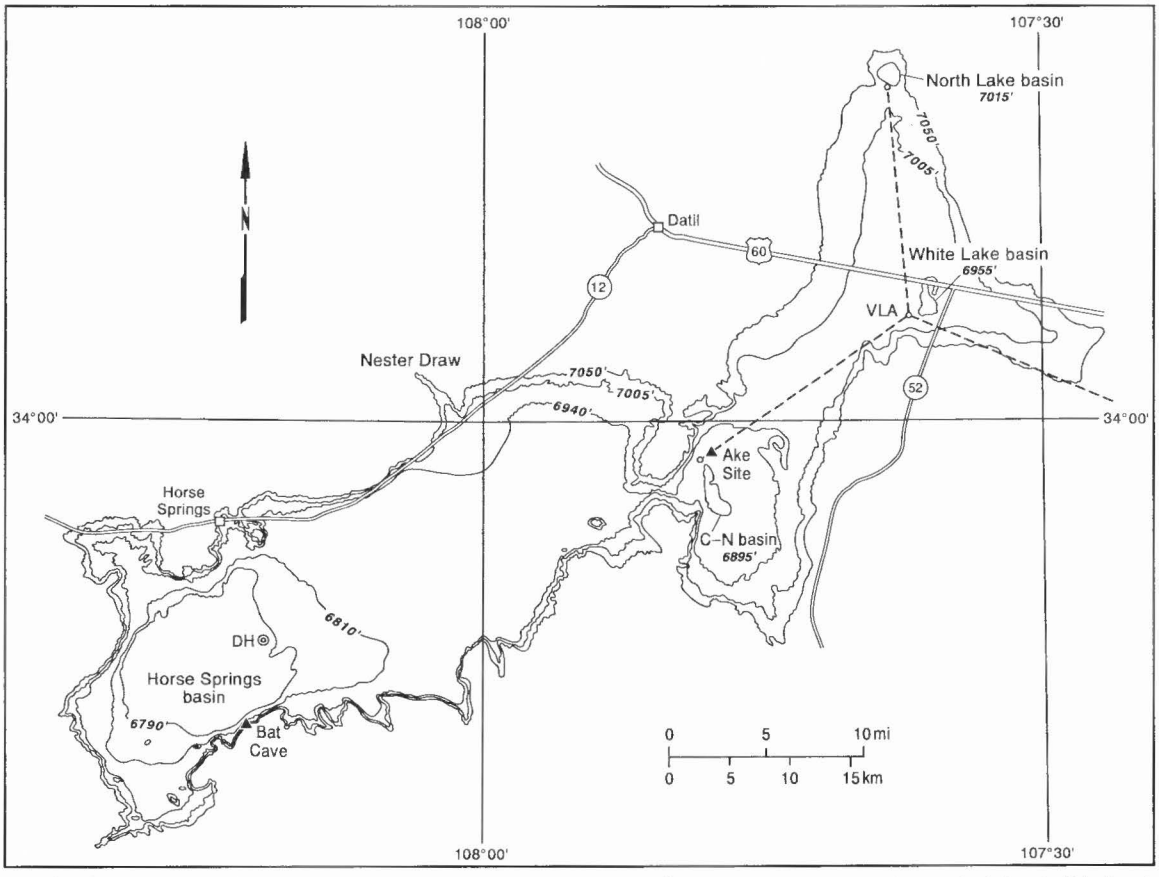


FIGURE 1.3. Map showing four stages of Pleistocene Lake San Agustin, Holocene playas (basins), and excavated archaeological sites (solid triangles). Oberlin core hole (Clisby and Sears, 1956) indicated by symbol labeled DH.

small dune fields on the northeastern side of Horse Springs basin, the northwestern edge of the C-N basin, and a much more extensive sand sheet and dune field on the northeastern side of White Lake basin (Osburn, et al., 1993). Sands driven over the crest of Lion Mountain cut pronounced northeasterly grooves in the Andesite of Lion Mountain (Osburn, et al., 1993, fig. 4). These dune fields are now largely stabilized by vegetation, although they were still active during the drought years of the 1950s. Several episodes of active dune formation have been recognized, extending back to ca 11,000 B.P.

The deeper stratigraphy of the basin fill is poorly known, except in the 2000-ft cored Oberlin hole on the basin floor south of Horse Springs (DH of Fig. 1.3). For details on this core see Clisby and Sears, 1956; Foreman, 1956; and Foreman et al., 1959. The lack of deep dissection that results from the closed internal drainage and low relief of the basin floor limit stratigraphic exposures to the uppermost few feet. Excavations for the Very Large Array (VLA of Fig. 1.3) radio-telescope facilities wave-guide trenches and antenna foundations exposed deeper strata that permitted documentation of the latest features of the stratigraphy. Alternating sands, silts, and clays indicate a complex sequence of rising and falling lake levels. Shrink-and-swell activity in deep-water clays results in unstable foundation conditions for highways and other engineering structural loads. In the central part of the Horse Springs basin this process is manifested in the hummocks and hollows of well-developed gilgai. Giant desiccation polygons are prominent in both the Horse Springs and White Lake basins, described and illustrated by Neal (1965) and Neal and Motts (1975). That these are actively opening and healing episodically was observed during mapping in the White Lake basin. Open fissures and associated conical soil pipes are effective in draining large volumes of surface water following thunderstorms.

Despite the complex faulted structure surrounding and probably underlying the lake basins, the undeformed, consistent elevation of shorelines throughout the area indicate structural stability during the latest Pleistocene and Holocene. Only one late fault was found to cut alluvial fan deposits of the western bajada of the San Mateo Mountains (Bruton Ranch fault of Weber; VLA faults of Menges et al., 1984). The fault does not truncate the oldest shoreline of the White Lake basin. None of the other late faults reported for the surrounding area could be confirmed on the ground. At least some of these were found to be based on linear air-photo images of gullied stock and ranch trails.

Further evidence reflecting past climatic and environmental conditions on the Plains of San Agustín derive from fossil faunal and floral assemblages. The megafauna of the surficial deposits includes extinct bison, horse, mammoth, mastodon(?), camel and short-faced bear of Rancholabrean aspect. Smaller faunal components include muskrat, pigmy rabbit, ground squirrel, vole, horned owl, water fowl, neotenic salamander, frog and fish. The molluscan fauna comprises more than 30 species of which only 6 are still living in the surrounding region. Abundant ostracodes and diatoms are proving useful in environmental reconstructions, as noted below.

Re-evaluation of the upper part of the original 2000-ft Oberlin core has yielded additional information on the pollen, ostracodes, diatoms, algae, magnetic polarity and isotopic ages, as reported by Markgraf et al. (1983, 1984). Additional analyses from a pit and shallow auger sample 4 mi northwest of the Oberlin core hole are from an area of gilgai and giant desiccation cracks that may have led to mixing of stratigraphic relationships.

Phillips and Campbell (1992) reviewed the geologic and hydrologic features of the Plains of San Agustín and reported analyses of two cores taken in the southwestern part of the Horse Springs basin. A chronology of paleoenvironmental reconstructions based on ostracode stratigraphy and oxygen isotope variations in ostracode tests was presented.

A recent geologic map of the Horse Springs West quadrangle illustrates some of the littoral features of the Horse Springs section of lake San Agustín (Ratté et al., 1991). In view southward across the basin toward Bat Cave from this area, in the vicinity of Horse Springs are a stacked series of relict shorelines, locally marked by prominent wave-cut cliffs. Some of the best examples of beaches, bay-mouth bars and spits are preserved along this section of the lake margin. Many of these are illustrated by Powers (1939).

Further information on the archaeology of Bat Cave, resulting from recent excavations by the University of Michigan, are found in Wills et al., (1984) and Wills (1988).

40.4 Milepost 96. Entrance to road-metal quarry ahead on right. This quarry provided ballast for trackways used to move VLA antennas into various configurations. The Oligocene andesite of Lion Mountain provided this ballast. A geologic map of the Lion Mountain and northern Arrowhead Well quadrangles (Osburn et al., 1993) provides detailed coverage of the Cenozoic geology from here north to Lion Mountain at 2:30. Structure sections of the Lion Mountain area illustrate a weakly extended domain (<3% extension) defined by gently folded and faulted Oligocene ignimbrites; thus, Lion Mountain is here placed on the Mogollon slope. A possible vent area for flow-banded rhyolite lavas (the rhyolite of Piñon well, Osburn et al., 1993), located about 3 mi south of Lion Mountain, lies along the projected accommodation zone that trends west-southwest from Council Rock. Osburn et al. (1993) also documented the intense scouring ability of sands blown across the crest of Lion Mountain with photographs of striated and grooved lava blocks. **1.0**

41.4 Entering Holocene dune field approximately 2 mi wide. Good view of Lion Mountain at 2:45. Other landmarks on the Mogollon slope skyline include the flat-topped Crosby Mountains from 11:30-12:30, the Datil Mountains from 12:15 to 2:00 and the Gallinas Mountains from 2:00 to 2:45. To the left and south of the San Agustin plains, high peaks mark late Oligocene to early Miocene volcanic centers aligned east-northeast along the Morenci lineament (Chapin et al., 1978; Ratté, 1989). Mt. Withington at 8:45 is at the apex of the Mt. Withington caldera, source of the 27.4-Ma South Canyon Tuff (Ferguson, 1991). Upper Oligocene to lower Miocene shield volcanoes composed of Bearwallow Mountain Andesite underlie Luera Peak at 10:00, Pelona Mountain at 10:15 and O Bar O Mountain at 10:20. Garmezy (1990) recognized the trend of the Morenci lineament as a major right lateral shear zone of Laramide age. Horse Mountain at 11:00 is a dissected upper Miocene dacitic to rhyolitic volcano (Ratté et al., 1991), summarized in the Third-Day road log of this guidebook. **2.4**

43.8 Junction with NM-52, to VLA visitor center and Dusty on left. **Continue straight ahead on US-60.** At 8:45 (looking along NM-52) the piedmont slope descending from Mt. Withington is offset approximately 100 ft down to the west, by the VLA fault of middle to late Pleistocene age. McFadden et al. (see following mini-paper) estimate the most recent offset on the VLA fault took place more than 100,000 years ago. The VLA fault and another Pleistocene fault scarp near North Lake (at 2:30, scarp not visible from here) are the most easterly indication of a late Miocene to Quaternary domain of extension in the Datil-Quemado-Springerville region that is temporally and, in part, spatially associated with the Jemez lineament (Aldrich and Laughlin, 1984). Tomographic mapping of the mantle across the southwestern U.S. indicates an

anomalously low velocity upper mantle under west-central New Mexico, generally coincident with the southwestern part of the Jemez lineament (Spence and Gross, 1990). This upper-mantle anomaly may represent a zone of extensional decompression and partial melting that has been feeding basaltic magmas to the Quemado-Red Hill volcanic field (McIntosh and Cather, this volume) and adjacent volcanic fields along the Jemez lineament for the past several million years. **0.6**

SOIL, TECTONIC AND CLIMATIC GEOMORPHOLOGIC INVESTIGATIONS IN THE SAN AGUSTIN PLAINS AREA, NM

Leslie D. McFadden[1], Richard P. Lozinsky[2], Christopher M. Menges[3], Jerry R. Miller[4], John Ritter[5]

[1]Dept. of Earth & Planetary Sciences, University of New Mexico, Albuquerque, NM 87131-1116; [2]Division of Natural Sciences, Fullerton College, Fullerton, CA 92632-2905; [3]U.S. Geological Survey, 101 Convention Center Dr., Suite 860, Las Vegas, NV 89109; [4]Desert Research Institute, University of Nevada, Reno, NV, 89506; [5]Department of Geology, Wittenberg University, Springfield, OH 45501

The San Agustin Plains area has been the site of numerous geologic investigations. Published Quaternary studies of the San Agustin Plains have focused primarily on the stratigraphy and paleoenviromental analysis of the deposits of pluvial lakes in the ancestral San Agustin Basin that episodically formed during the Pleistocene (Bryan, 1926; Powers, 1939; Clisby and Sears, 1956; Foreman et al., 1959; Weber, 1980; Margraf et al., 1983, 1984; Phillips et al., 1992; Johnson, 1992), which form a major part of the 1.6 Ma stratigraphic record. This mini-paper describes the results of studies of Quaternary alluvial deposits (particularly the piedmont deposits in the northeastern part of the basin derived from the San Mateo Mountains) geomorphic surfaces, soils and the VLA fault. We estimate age ranges for the geomorphic surfaces by comparing observed soil development with independently dated soils (soil chronosequences) formed in similar soil-forming circumstances, following methods of Jenny (1980) and modified and elaborated by Birkeland (1984).

Quaternary alluvial deposits in the study area consist primarily of lenticular to weakly stratified, poorly sorted, gravelly sandy alluvium derived from Oligocene to Miocene, basaltic to rhyolitic, volcanic and volcaniclastic rocks in the San Mateo and nearby mountains. The deposits, depicted as Qp by Osburn et al. (1993) on their map of the area just north of this study area, are alluvial fans or terraces inset into older Quaternary fan remnants. The piedmont deposits range in altitude from 2140 m (approximate height of pluvial shoreline features) to over 2300 m near the mountain front. Presently, the drainages are ephemeral, and graded to the San Agustin plains, where there are numerous shoreline features and locally extensive eolian dunes and sand sheets. Because the alluvial deposits are high-energy gravels, datable materials were found only at one site.

On the basis of field and photogeologic studies, four major geomorphic surfaces associated with Quaternary surficial fluvial deposits are recognized. The oldest such surface in the area is Q1. Although we did not study this surface in detail, field and photogeologic observations indicate that it is a deeply dissected constructional surface remnant associated with relatively thick alluvial-fan deposits composed of coarse, poorly-sorted bouldery alluvium. Fragments of petrocalcic horizons, some of which exhibit laminar character, occur on the surface and lower hillslopes. These are interpreted as remnants of a very strongly developed (stage IV, after Gile et al., 1966) calcic soil. This interpretation is supported by a massive K horizon (> 1 m thick) in deposits that underlie the eroded Q1 surface in a railroad construction-related exposure associated with the VLA facilities. The age of the deposits of Q1, given the very strong degree of soil development and the strong degree of soil development on the younger Q2 surface, is estimated to be middle Pleistocene. The preservation of constructional surface remnants suggests that it is not a pre-Quaternary deposit. This estimated age is also based on a correlation with the oldest Quaternary surface (altitude 1865 m) in the nearby La Jencia Basin, described by McGrath and Hawley (1987), who recognized the associated fluvial deposits as the final stage of early to middle Pleistocene basin aggradation. In other studies of Quaternary deposits and soils at similar elevations and climate (1800- 2150 m; ppt = 35 cm) in the Española Basin in northern New Mexico (Dethier and Dempsey, 1984; Dethier et al., 1988), the oldest Quaternary surface possessing soils with maximal stage IV carbonate morphology is estimated to be between 0.35 and at least 1.1 Ma. The stage IV soil of the Lower La Mesa surface in the Las Cruces region (Gile et al., 1981) is at least 0.5 Ma, but soil development in this altitudinally lower site has occurred in a more arid, warmer climate.

The next youngest surface, Q2, occurs primarily as a fluvial terrace inset as much as 25 m below the Q1 surface. The soil on this surface exhibits a moderately developed, moderately to strongly reddened (5YR 4/6) argillic (Bt) horizon and a calcic horizon with stage III morphology and a content of up to 34% $CaCO_3$ (Table 1). The ochric A epipedon is 8.5 cm thick, and some pedogenic carbonate occurs in the argillic horizon (Btk) at a depth of 27 cm. Morphological attributes of the soil indicate that at least part of the lower argillic horizon has been massively engulfed by the calcic horizon. The degree of development indicates that the soil has formed in alluvium no younger than about 75 to 100 kyrs, based on comparison with soils on the late Pleistocene deposits of the Española Basin and Las Cruces soil chronosequences.

A variety of surfaces, recognized as Q3 and Q4, are either inset in or bury deposits of the Q2 surface. The Q3 surface may be latest Pleistocene to early Holocene in age; whereas Q4 is clearly Holocene. A radiocarbon age of 3350 ± 110 yrs B.P. (DIC-2928) was obtained from charcoal recovered from alluvium associated with a Q4-associated deposit in which a soil that exhibited A-AB-Bw-Bk-2Bk horizon sequence had formed. The calcic horizon exhibits only stage I morphology and the Bw horizon only slight reddening and weak structure development. Other soils on Q4 surfaces in the study area possess even weaker soil development, although the ochric epipedon may have an organic carbon content as high as 2.7% (Table 1). Weakly to moderately developed cumulic soils, also inferred to be Holocene in age, have formed in colluvial aprons derived from erosion of older Quaternary deposits. These aprons locally bury Q2 or Q3 surfaces.

Soils have formed on prominent beach ridges associated with the most recent high stands of the pluvial lake of the San Agustin Basin. These beach ridges probably formed no earlier than the last high stand (about 18 ka) and no later than the early Holocene (8 ka; Phillips et al., 1992; Johnson, 1992), after which paleoenviromental data indicate increasingly stronger lake salinity, a more xeric regional vegetation, and lake desiccation. Soils developed in the littoral sand and high energy, gravelly shoreline deposits exhibit organic-matter rich epipedons, a moderately developed, reddened argillic horizon, and stage I to locally II calcic horizon morphology. Soils on surface Q3 exhibit relatively similar characteristics (Table 1), supporting the latest Pleistocene to early Holocene age estimate for the associated fluvial parent materials.

Deeply incised and recently formed continuous and locally discontinuous arroyos locally expose the stratigraphy of the uppermost 3 to 4 m of late Quaternary valley-fill deposits. Complex stratigraphic relations among Quaternary units, some of which are not expressed as geomorphic surfaces, are revealed in these exposures. For example, the Q2 surface is buried by a stratigraphic unit in which a soil with stage III to locally stage IV carbonate morphology is present. This unit clearly is older than the Q3-associated deposits. In addition, Bt lamellar bands are present in the soil associated with deposits of Q2, reflecting deep translocation of illuvial clay, which has accumulated in distinct, separate bands, rather than as a continuous, at least several meter-thick zone that typifies argillic horizons. The processes by which these lamellae form are not completely understood, but their origin is presumed to be pedogenic and is usually favored in sandy parent materials. In detailed studies of such deposits, the formation of the lamellae precedes

TABLE 1.1. Summary of morphological, textural and chemical data for soils on Quaternary deposits, San Agustin Plains, New Mexico.

TABLE 1. SUMMARY OF MORPHOLOGICAL, TEXTURAL AND CHEMICAL DATA FOR SOILS ON QUATERNARY DEPOSITS, SAN AGUSTIN PLAINS, NM												
Profile Horizon	Thickness	Color	Structure^	Consistence#	CaCO3 Stage	Clay Films***	Sand %	Silt %	Clay%	CaCO3 %	Organic	pH
	(cm)	(dry)		(wet)							Carbon (%)	
Q4 (Torriorthent)												
A1	0 to 4	10YR 4/3	sg	no, po	NO *	NO	62.9	30.4	6.7	nd	2.7	5.7
A2	4 to 56	10YR 3/2	1 gr	ss,sp	NO	NO	62.3	26.5	11.2	nd	1.2	6.9
A3	56 to 72	10YR 3/3	m	ss, sp	NO	NO	49.9	38.1	12	nd	1.1	7.3
Bk1	72 to 89	10YR 3/3	1fsbk	no,po	I	NO	51	37.1	11.9	nd	0.6	7.4
Bk2	89 to 139	10YR 3/2	1fsbk	no,po	I	NO	57.9	32.5	9.6	nd	0.5	7.5
Bk3	139 to 151	10YR 4/3	m	no,po	I	NO	59.7	30.9	9.4	nd	0.3	7.6
Q3 (Haplustoll)												
A	0 to10	10YR 4/3	sg	ss,sp	NO	NO	50.4	39.5	10.1	nd	1.7	6.1
Bt	10 to 46	10YR 3/3	1fsbk	ss,p	NO	cs	30.2	50.1	19.7	nd	0.8	6.9
Bw	46 to 60	10YR 4/3	1fsbk	ss,sp	NO	NO	60.4	28.4	11.2	nd	0.7	7.4
Bwk	60 to 100	10YR 3/3	2vc to fsbk	ss,sp	I+	NO	39.2	54.6	6.2	nd	0.6	7.4
Q3 (Calciustoll)												
A	0 to 4	10YR 5/3	1f&msbk	s,sp	NO	NO	46.1	26	23.7	0.2	nd**	nd
Bw1	4 to 19	7.5YR 5/4	1f&msbk	s,p	NO	NO	27.9	20.9	44	0.2	nd	nd
Bw2	19 to 40	7.5YR 5/6	2m&csbk	nd	NO	NO	20.5	30.4	31	0.7	nd	nd
Bwk	40 to 64+	7.5YR 5/4	1f&msbk	nd	II	NO	26.8	52.9	8.3	2.2	nd	nd
							21.9	23.6	8.5			
Q2 (Argiustoll)												
A	0 to 8.5	7.5YR 3/4	1m&csbk	s,p	NO	NO	46.4	26	23.7	nd	nd	nd
Bt	8.5 to 27	5YR 4/6	2m&csbk	vs,vp	NO	1vt&tgr;4tped	27.9	20.9	44	nd	nd	nd
Btk	27 to 37	7.5YR 4/6	1&2msbk	vs,p	I	1tped	20.5	30.4	31	nd	nd	nd
Bwk	37 to 46	7.5YR 5/6	2&3msbk	vs, p	II	NO	26.8	52.9	8.3	nd	nd	nd
K	46 to 111+	7.5YR 8/4	m	ss,po	III	NO	21.9	23.6	8.5	nd	nd	nd
Q2 (Calciustoll) ~'												
A1	0 to 4	7.5YR 4/2	1msbk	s,p	NO	NO	48.1	27.3	8.4	0.9	nd	nd
A2	4 to 11	7.5YR 4/2	1f&msbk	ss,sp	NO	NO	38.7	25.8	10.4	0.9	nd	nd
AB	11 to 19	7.5YR 5/4	1fsbk	ss,sp	NO	NO	37.2	21.3	14.1	1.6	nd	nd
Bwk	19 to 30	7.5YR 5/4	1fsbk	ss, sp	NO	NO	24	14.7	8.5	26.3	nd	nd
Bk1	30 to 70	7.5YR 7/4	m	s, sp	II	NO	27.5	14.6	12.1	34.2	nd	nd
Bk2	70 to 78+	7.5YR 6/4	m	ss,sp	II	NO	25.2	17.7	16.1	23.1	nd	nd
^ sg-single grain; m-massive; 1-weak; 2-mediu m; 3-strong; f-fine; m-moderate; s-strong; sbk-subangulary blocky												
#no-nonsticky; ss-slighty sticky; s-sticky; vs-very sticky; po-non plastic; sp - slightly plastic; p-plastic; vp-very plastic;												
* none observed												
** not determined												
*** cs-colloidal stains on grains;f-films; t-thin; mk-moderately thick; k-thick; 1-few; 2-common; 3 many; 4 -continuous; ped-ped face												
~ Described on scarp slope formed in Q2-associated alluvium												

coalescence and development of the argillic horizon. Such lamellae, however, are not observed in soils of younger deposits in the study area. This suggests that a strongly developed argillic horizon must be present before genesis of the lamellae is favored.

Very strongly reddened (3.75YR 6/6) clayey matrix occurs in gravelly lenses several decimeters below the slightly reddened (7YR 6/6) argillic horizon of the Q2 soil. In contrast to the Bt lamellae, accumulation of this clay is not attributed to pedogenesis, as the clay's color shows that it could not have been derived from the overlying argillic horizon. Also, this deposit does not exhibit other features typically associated with soil profiles; therefore, it does not represent buried soils. Instead, we attribute its formation to introduction of clay to the unit from an external source, perhaps via vadose-zone transport of suspended clay through hydrologically very transmissive gravels. The only possible source of such reddened, clay-rich material is a strongly developed argillic horizon once present on surface Q1, presumably associated with the well developed calcic horizon still partly preserved. The presence of the Q2-associated deposits topographically below the Q1 surface, and the presence of reddish clay colluvial deposits of Q1 slopes favor this process. Finally, the presence of a very strongly developed and reddened argillic horizon in the soil of the much less extensively dissected and oldest deposit of the La Jencia Basin described by McGrath and Hawley (1987) shows that such a horizon may well have been present on the Q1 deposit prior to its deep dissection and erosion during the late Quaternary.

Major horizon characteristics of soils in Holocene and latest Pleistocene deposits that were not subject to the effectively wetter, late Pleistocene (full glacial) climate reflect the currently semiarid (annual precipitation = approximately 35 cm) and moderately warm (annual average temperature = 8.5° C)) climate of area. Available soil moisture is sufficient to sustain locally abundant grasses, including Galleta and Blue Grama grasses. Biomass production rates are sufficiently large to provide the soil organic matter to enable Mollic epipedon development in many Holocene soils (Table 1.1) (Ritter et al., 1984). Within 3 ka of development, Bw horizons also have formed as iron oxyhydroxide accumulation and concomitant soil structural development progress. The weak argillic horizons in older Holocene and latest Pleistocene soils form via translocation of suspended silicate clay. Micromorphologic studies of such horizons show development of cutanic agglomeroplasmic or porphyroskelic fabrics, which reflects formation of oriented clay and clay bridging, accompanied by concomitant conversion of simple packing (interstitial) voids to channel and plain soil voids. Formation of the overlying Mollic horizon promotes substantial soil respiration, which favors development of a noncalcareous B horizon environment that, in turn, is conducive to clay translocation and the observed Bt horizon development. However, in all but a few soils, carbonate is leached

to depths typically no deeper than 40 cm, despite the relatively high permeability of the parent materials (Table 1.1). This is partly because a significant fraction of annual precipitation falls during the summer when the seasonally maximal soil evapotranspiration limits soil infiltration depth. The ultimate development of strongly developed calcic horizons, however, must also reflect a high influx and subsequent incorporation of calcareous dust. This conclusion is indicated by the relatively low calcium content of the parent materials and the minimal evidence of strong chemical alteration of the parent material. This process has apparently strongly influenced Quaternary soil development elsewhere in New Mexico (Gile et al., 1981; Machette, 1985) , where strong calcic horizons form in Pleistocene soils, even at elevations that exceed 2600 m. This is an elevation at which soils are typically noncalcic elsewhere in much of the southwestern United States. Certainly, during relatively arid periods of the Quaternary, the plains of San Agustin provide one obvious local source for at least some of the dust.

Tectonic geomorphic studies in the San Agustin Basin were concentrated in the area of a large fault scarp located in northernmost subbasin. This scarp, the VLA fault, had been recognized previously by R. Weber (personal commun., 1983) and Machette and McGimsey (1983), but had not been studied. The topographic scarp can be discerned over a distance of 10 km, and in some places it is as high as 30 m. The VLA fault thus reflects substantial Quaternary movement. In addition it is somewhat anomalous, in that it is separated by several kilometers from the mountain fronts and projects northward into the center of northern subbasin, rather than following the basin margin.

Evaluation of the VLA Fault integrated studies of the Quaternary alluvial deposits reported above, their relation to the fault, and morphological studies of the scarp, largely based on the scarp degradation model of Wallace (1977). Topographic profiles across the VLA scarp at 15 locations and geomorphological evidence show that surface Q1 has been offset 20-30 m along a composite scarp and Q2 by 2-5 m along a single-rupture scarp (Menges et al., 1984). Q3 and younger surfaces are unruptured by the fault, constraining the age of most recent rupture to late Pleistocene. Following the method of Bucknam and Anderson (1979), linear regression analysis of log scarp height versus maximum scarp-slope angle on single-event scarps (Fig. 1.4) also indicates an older late Pleistocene age (10 ka) for the most recent rupture. This estimate is supported by comparison of scarp-height—scarp-slope trends observed on reference scarps locally and regionally. For example, topographic profiles of a scarp (La Jencia fault) located north of the Magdalena Mountains by Machette and McGimsey (1983); Machette (1986, 1988) and Menges et al. (1984) indicate a Holocene age for most recent rupture (Fig. 1.4). In addition, the soil on the VLA fault scarp slope is better developed than Q3 soils, which are primarily Holocene in age, strongly suggesting that the late Pleistocene last-rupture age estimate is reasonable. Comparisons between the heights of composite and

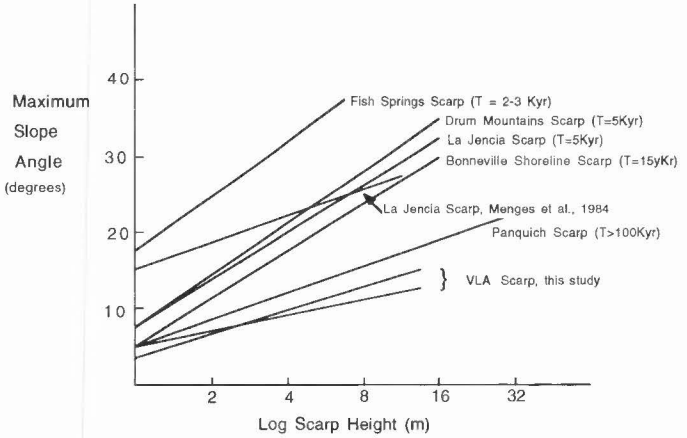


FIGURE 1.4. Composite "best-fit" lines for the VLA scarp and lines for the La Jencia scarp and other reference scarps described in studies noted in the text. T refers to the estimated age of the formation of the scarp. Best-fit line determined using simple linear regression analysis.

single-rupture VLA fault scarps indicate 5 to 10 events on the fault since formation of the Q1 surface, which suggests a 10,000 yr recurrence interval. This rate is consistent with those reported for Quaternary faults in southern New Mexico and Arizona (Menges and Pearthree, 1989).

Margraf et al. (1983) suggested that generally constant basin subsidence rates in the San Agustin Basin, calculated on the basis of paleomagnetic, radiometric and amino acid-racemization ages of basin sediments deposited during the last 0.75 Ma, imply a strong tectonic-subsidence control on sedimentation rates. Documentation of sustained Quaternary movement along the VLA fault through soil and geomorphic studies also indicates that tectonism has continued to influence San Agustin Basin evolution significantly. Formation of the 30-m-high scarp has also clearly influenced geomorphic evolution of the piedmont. Uplift of the Q1 deposits along the scarp has confined more recent deposition to valleys formed subsequent to their deposition. Uplift has also precluded burial of the older Quaternary deposits despite continuous base-level rise in the basin, where aggradation during the last 1.6 Ma might otherwise be expected to cause regional base-level rise and burial of older Quaternary units. Many valleys above the scarp associated with the largest drainages are strongly asymmetrical, with consistently steep south-facing slopes and gentle north-facing slopes. Given evidence for continued tectonic movement on the VLA fault in this area during the Quaternary, such valley asymmetry may reflect local tectonic tilting. Similarly asymmetric valleys also are present on the Taos Plateau and on the Pajarito Plateau in northern New Mexico. Such valley asymmetry also may be related to microclimately driven, aspect-related geomorphic processes. Exposures of stratigraphy of deposits of Q1 at one location, however, show that beds have strikes of N22° to 60°W, and tilts that range from 5 to 9° to the north. Such attitudes differ significantly from beds of younger Quaternary deposits, are steeper than those expected for medial piedmont channel deposits, and are inconsistent with the expected major northeast direction of channel orientation on the piedmont. This evidence is consistent with the observed pattern of valley asymmetry; thus, although microclimatic influences may favor maintenance of valley asymmetry, tectonically driven processes are more likely the fundamental cause.

The lack of movement on the VLA fault during the last 10,000 yrs implies that the major latest Pleistocene and Holocene aggradational-degradational cycles in this area are not tectonically controlled. Thus their origin might be explained instead by climate, another important factor that influences fluvial systems. In the San Agustin Plains, Pleistocene-to-Holocene climate changes not only caused the complete desiccation of a once-extensive pluvial lake, but also were associated with major changes in regional vegetation (Margraf et al., 1983; 1984). Many geomorphologic studies have demonstrated that such climate changes significantly impact soil formation, vegetation, and fluvial processes over large areas and in diverse climates. Throughout the southwestern United States, these changes induced a cycle of rapid and thick valley aggradation and channel incision, caused primarily by dramatic changes in drainage basin sediment supply and hillslope/channel discharge relations (Bull, 1991). The precise nature of the interrelationships among climate changes, long-term Neogene tectonism, lithology, local relief, and other factors that have influenced soil and fluvial system dynamics in this area, however, is complex and remains an important research problem.

We thank several students in the Department of Earth and Planetary Sciences Quaternary Studies Program who also helped to describe soils during studies in the field area: Mary Ann Joca, Glen Kawaguchi, Larry Smith, and Keith Kelson. Funding for part of this research was provided by a University of New Mexico Research Allocations Grant to the senior author.

44.4 Milepost 92. Entering playa of White Lake; US-60 crosses projected southeastern margin of the Mogollon slope near here. The Bouger gravity map of Keller and Cordell (1983) suggests that the Plains of San Agustin include three linked structural basins, two deep half-

graben basins coincident with the Horse Springs Basin and the C-N Basin (Fig. 1.3), and a third shallow basin north of US-60, between the White Lake Basin and the North Lake Basin. Local unconformities between Datil Group and Mogollon Group ignimbrites and thickness trends in the Dog Springs area at 2:00 (Harrison, 1980), suggest that the northern basin is a shallow, south-plunging, synclinal sag of late Oligocene age. This downwarp formed at about the same time (29-27 Ma) as initial extension in the Socorro segment of the Rio Grande rift (Chapin and Cather, in press), and presumably has been inactive during Neogene time. Uranium test wells drilled by Mobil Alternative Energy Inc. in the early 1980s indicate that basin-fill deposits in the area north of US-60 (HH Ranch area) are about 500-650 ft thick (G.R. Osburn, unpubl. report to Mobil Alternative Energy Inc., 1984). **0.4**

44.8 Low roadcuts in gray lacustrine muds. **1.3**

46.1 Trackway and tourist stop (on left) for one of the world's largest radio telescopes (Fig. 1.5). The Very Large Array, established in 1980, is now a sister instrument to the Very Long Baseline Array (established in 1993), which has its outermost antenna at Mauna Kea, Hawaii. The 10 VLBA antennas are electronically connected to and controlled by the National Radio Astronomy Observatory Array Operations Center located on the New Mexico Tech campus in Socorro. Each antenna weighs approximately 230 tons and has a reflecting dish 82 ft in diameter. The most distant stars, galaxies, quasars and other objects recorded by the VLA are 6×10^{21} mi away and are seen as they were more than 10 billion years back in time. The VLBA can measure image detail to better than one thousandth of a second of arc, or equivalent to being able to see a football on the surface of the moon. VLBA antenna stations are also able to measure their exact location in the universe to within one centimeter and can detect tiny variations in the earth's rotation. Self guided tours of the visitors center (near the ten-story building at 9:30) can be made from 8:30 a.m. to sunset every day. **3.1**

49.2 Road to old Augustine Well, (now B. and B. Gallaher Ranch) on left; road to HH Ranch on right. Augustine Well was a stop on the Overland Stage route of the 1880s and later a watering stop along the western New Mexico livestock driveway. Another important well 10 mi southwest of here (low hills at 2:00) is the 1966 Sun Oil Company No.1 Well, which was drilled to Precambrian gneiss and a total depth of 12,284 ft. This well intersected a nearly complete Tertiary stratigraphic section (Table 1.2), which is generally representative of the Datil-Crosby Mountains area (Osburn and Chapin, 1983). Only 590 ft of the basaltic andesite of Crosby Mountains (Lopez and Bornhorst, 1979) and 65 ft of the South Canyon Tuff (McIntosh and Chamberlin, this volume) are missing; presumably they were removed by Neogene erosion. Based on the Sun No. 1 Well and the above missing units, the total thickness of the Tertiary volcanic pile (Mogollon, Datil, and Spears Groups) in the Datil region was as much as 5000 ft. In addition, a 2095 ft intercept of Eocene Baca Formation indicates that the Sun No. 1 Well is in the Laramide Baca Basin (Cather and Johnson, 1984), probably near its southern structural margin. The total thickness of Eocene-Oligocene strata on the Mogollon slope near Datil is 6800 ft. A thick aplite intrusion of probable Miocene age was intersected within Permian rocks near the bottom of the Sun No. 1 well (Ratté, written commun., 1994). **1.2**

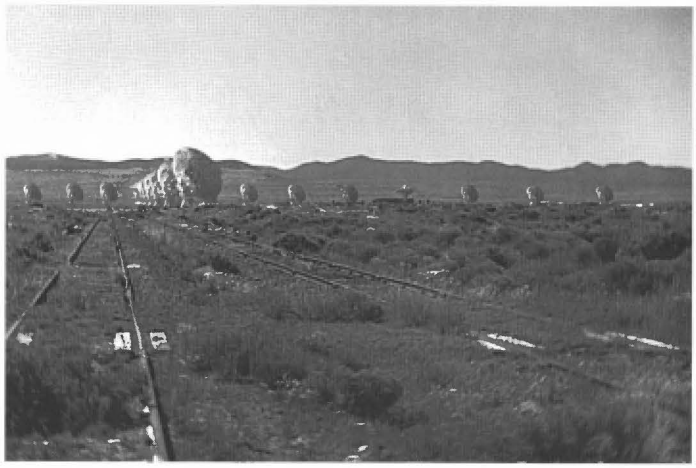


FIGURE 1.5. View to south along north arm of the VLA radio telescope. Quaternary scarp of the VLA fault offsets piedmont slope below lowest saddle on skyline (left center).

50.4 Begin ascent of low-gradient alluvial fan that emanates from White House Canyon, a major source of sediment to the northwestern San Agustin Plains. **1.3**

51.7 Entering Catron County (Fig. 1.6), named for New Mexico's first U.S. Senator Thomas B. Catron. It is the largest and least populated county in New Mexico. Cattle ranching is the primary economic activity. A

TABLE 1.2. Generalized Cenozoic stratigraphy of the Sun Oil Company No. 1 Well, San Agustin Plains (sec. 29, T3S, R9W; T.D. 12,284 ft). Based on an unpublished lithologic log by Roy Foster (New Mexico Bureau of Mines and Mineral Resources, Library of Subsurface Data) and a preliminary visual inspection of cuttings from Tertiary units by R. M. Chamberlin. All correlations are tentative; the more tentative correlations of Tertiary units are queried. Unit contacts and thicknesses are primarily based on Foster's log. Nomenclature of Tertiary units is after Osburn and Chapin (1983), Ratté (1989), Ratté et al., (1991) and Cather et al. (this volume). Ignimbrite ages from McIntosh et al., (1991); age of Dog Springs Formation from Cather et al., (1987) and McIntosh and Chamberlin (this volume).

Thickness (ft)	Unit
230	Quaternary alluvium
150	Vicks Peak Tuff (28.6 Ma), Mogollon Gr.
90	La Jencia Tuff (28.9 Ma), Mogollon Gr.
375	South Crosby Peak Fm., upper Spears Gr.
285	Hells Mesa Tuff (32.1 Ma), Datil Gr.
470	andesite of Dry Leggett Canyon (?), Datil Gr.
320	Rincon Windmill Fm. (?), middle Spears Gr.
220	tuff of Lebya Well (?), Datil Gr.
240	Kneeling Nun Tuff (?) (34.9 Ma), Datil Gr.
360	Chavez Canyon Fm., middle Spears Gr.
1760	Dog Springs Fm. (ca. 37-40 Ma), lower Spears Gr.
2095	Baca Formation (Bridgerian to Uintan)
6595 ft = (2005 m)	Total Cenozoic section



FIGURE 1.6. View west along US-60, the serene corridor to northeastern Catron County. Flat-topped Crosby Mountains on horizon to left. Gently south-dipping cuesta immediately right of road sign is underlain by 34.98-Ma Datil Well Tuff on the Datil Mountains block of the Mogollon slope.

generalized geologic map of the Quemado-Datil area (Fig. 1.7) provides the regional setting for today's stops. **1.7**

53.4 Milepost 83. View of flat-topped peaks of Crosby Mountains from 11:00 to 12:15 (Fig. 1.8). Twin Peaks in foreground are capped by the basaltic andesite of Deep Well directly overlying the La Jencia Tuff (Osburn and Chapin, 1983). These same units were originally mapped by Lopez and Bornhorst (1979) as the basaltic andesite of Twin Peaks overlying the A-L Peak Rhyolite. Lopez and Bornhorst's 1979 geologic map of the Datil area provides the best available data on outcrop distribution and structure in the Datil area, but most of their ignimbrite names have been abandoned because they are synonymous with previously named and mapped ignimbrites in the Socorro-Magdalena region (Osburn and Chapin, 1983; McIntosh et al., 1991; McIntosh and Chamberlin, this volume). Osburn and Chapin (1983) formally defined two ignimbrites named by Lopez and Bornhorst; the 34.98-Ma Datil Well Tuff and the 33.66 Ma-Blue Canyon Tuff. Lopez and Bornhorst's Tuff of Main Canyon is synonymous with the 34.17-Ma Rock House Canyon Tuff (Osburn and Chapin, 1983; McIntosh and Chamberlin, this volume). Lopez and Bornhorst's Tuff of Rock Tank and Tuff of Ary Ranch are both synonymous with the 32.1-Ma Hells Mesa Tuff; also their A-L Peak Rhyolite (as mapped) is now known to include the 28.8-Ma La Jencia Tuff, the 28.6-Ma Vicks Peak Tuff and the 27.4-Ma South Canyon Tuff (McIntosh et al., 1991; McIntosh and Chamberlin, this volume). All of the following identifications of stratigraphic units in the Datil area follow the nomenclature of Osburn and Chapin (1983) as redefined by Cather et al. (this guidebook). **0.3**

53.7 Route enters northeast portion of the geologic map of the Datil area by Lopez and Bornhorst (1979). **0.7**

54.4 Milepost 82. East-sloping cuestas at 3:00 in northeastern Datil Mountains include about 40-100 ft of South Crosby Peak Formation (conglomeratic sandstones and thin pumiceous ignimbrites) sandwiched between the La Jencia Tuff and the Hells Mesa Tuff (Harrison, 1980). Approximately 3 mi further west, within a structurally higher part of the Red Lake fault zone, the Hells Mesa and La Jencia tuffs fill west-trending paleovalleys and the South Crosby Peak Formation is absent (Harrison, 1980). In contrast, in the Crosby Mountains (11:00), the South Crosby Peak Formation ranges from 600 to 800 ft in thickness (Lopez and Bornhorst, 1979; Osburn and Chapin, 1983). In the Crosby Mountain area the South Crosby Peak Formation comprises all of the upper Spears Group volcaniclastic sedimentary rocks shown on the regional geologic map (Fig. 1.7) and contains less than 10% non-welded pumiceous ignimbrites by volume. The significant southward increase in thickness of the South Crosby Peak Formation is apparently associated with an east-trending zone of down-to-the-south normal faults that crosses the Datil-Crosby Mountains at the latitude of Datil (Lopez and Bornhorst, 1979). Based on thesis studies in the Datil-Horse Springs area (Lopez, 1975; Bornhorst, 1976; Jones, 1980), Elston (1978, 1984, 1989) interpreted the South Crosby Peak Formation as the cogenetic fill (intracaldera- or moat-fill) of the Crosby Mountains caldera or volcano-tectonic depression. As summarized in the following minipaper, the "Crosby Mountains caldera" might alternatively be described as the "Crosby Mountains volcano-tectonic collage", a seemingly disparate collection of temporally unrelated structural and volcanic elements. **2.0**

THE CROSBY MOUNTAIN "CALDERA": A VOLCANO-TECTONIC COLLAGE OF DISPARATE ORIGIN

Richard M. Chamberlin

New Mexico Bureau of Mines and Mineral Resources, Socorro, NM 87801

Elston (1989) described the Crosby Mountains caldera as one of the best documented ash-flow tuff calderas in the Mogollon-Datil volcanic field. As outlined by Elston, however, the Crosby Mountain caldera clearly lacks the thick, densely welded, intracaldera tuff, silicic intrusions and extrusions, and hydrothermal alteration or mineralization that are characteristic of large ash-flow calderas (Lipman, 1984). This minipaper summarizes current observations that indicate the Crosby Mountains caldera (or volcano-tectonic depression) as proposed by Bornhorst (1976), Jones (1980) and Elston (1978, 1984, 1989) represents a temporally unrelated collection of volcanic and tectonic elements (Fig. 1.9).

Except for block and ash deposits of the 33.7-Ma Horse Springs dacite (Ratté et al., this volume), all ignimbrites within and adjacent to the proposed Crosby Mountains caldera form thin sheets (0-130 ft) typical of distal ash-flow deposits (Chamberlin et al., 1994b; Osburn and Chapin, 1983a). Block and ash deposits of the Horse Springs dacite form a north-trending series of exposures between Horse Springs and the west flank of Alegres Mountain. Bornhorst (1976) originally interpreted these exposures to represent a vent zone (inside dotted line of Fig. 1.9) along the west flank of the "Crosby Mountains depression," later renamed the Crosby Mountains caldera (Elston, 1989). Exposures of the Horse Springs dacite become progressively finer grained and thinner from south to north (Ratté, 1989; Ratté et al., this volume). The 33.7-Ma Horse Springs dacite must have erupted from a source under the San Agustin Plains near Horse Springs and has no apparent relationship to the proposed Crosby Mountains caldera of Elston (1989). Two petroleum exploration wells to Precambrian basement (Fig. 1.9), a

regional seismic reflection profile (Armstrong and Chamberlin, this volume), and regional mapping (Chamberlin et al., 1994b), demonstrate that a normal volcanic apron sequence (ca. 40-26 Ma) overlaps a reverse-fault bounded (AMF, DF, Fig. 1.9) Laramide synclinal basin within the proposed caldera. Several arcuate normal faults, such as the Alegres Mountain fault (AMF), in the Datil-Quemado-Reserve region apparently represent Laramide transpressional structures that have collapsed under later regional extension.

Field observations (Ratté, oral commun., 1993) and regional seismic reflection profiles (Armstrong and Chamberlin, this volume; L. Garmezy, oral commun., 1993) imply that Permian rocks exposed on the south flank of Horse Mountain represent a fragment of a Laramide uplift that was buried by Spears Group volcaniclastic conglomerates. Limestone and granite clasts in these conglomerates (Ratté, oral commun. 1993) imply the presence of a nearby erosional unconformity developed on pre-Tertiary rocks about 37-35 Ma, prior to development of the putative caldera. Bornhorst (1976) suggested these Permian rocks represented a resurgent dome *within* the Crosby Mountains volcano-tectonic depression.

Elston (1989) indicated that the proposed Crosby Mountains caldera

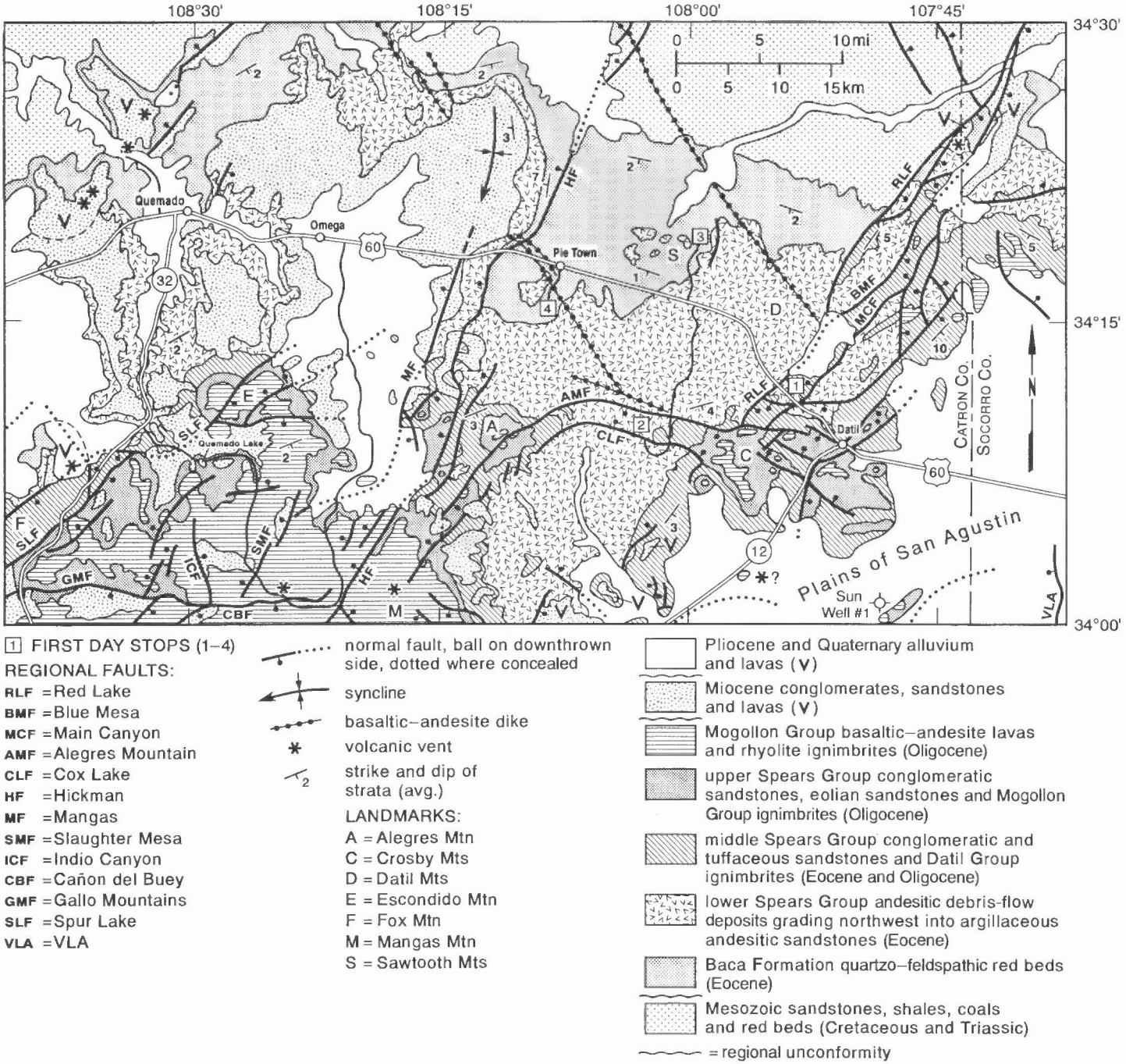


FIGURE 1.7. Generalized geologic map of the Quemado-Datil region, northeastern Catron County (modified after Chamberlin et al., 1994b; and unpublished digital data of the state geologic map project by O. J. Anderson and G. E. Jones, in prep.). As mapped here, the upper Spears Group locally contains thin ignimbrites of the Mogollon Group (McIntosh and Chamberlin, this volume). Eocene-Oligocene units generally intertongue, but unconformities are also apparent locally at several horizons within the volcanic pile.



FIGURE 1.8. The northern twin of Twin Peaks (left center) is underlain by light gray pumiceous ignimbrites (ca 29.7 to 28.9 Ma) intercalated with epiclastic conglomerates of the South Crosby Peak Formation of the upper Spears Group. Twin Peaks are capped by basaltic andesite of Deep Well and the La Jencia Tuff. Note absence of resistant ignimbrites on south twin peak, an indication that the pumiceous ignimbrites probably filled local paleovalleys.

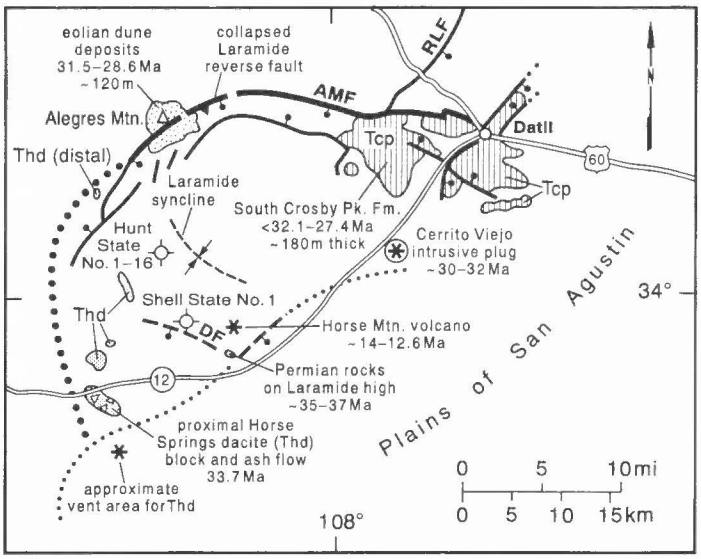


FIGURE 1.9. Sketch map of the Crosby Mountains caldera or volcano-tectonic depression (heavy line and dots), as proposed by Bornhorst (1976), Jones (1980) and Elston (1978, 1984, 1989). The distribution of volcanic and structural elements of their proposed caldera and currently available age constraints are summarized on the map. Data from McIntosh et al. (1991), McIntosh and Chamberlin (this volume), Ratté et al. (1991; this volume), third-day road log (this volume, mile 112.3), Lopez and Bornhorst (1979) and Chamberlin et al. (1994b). AMF = Alegres Mountain fault, RLF = Red Lake fault, and DF = Dutch Oven Pass fault zone.

formed between eruption of the 32.1-Ma Hells Mesa Tuff from the Socorro caldera and the 28.9-Ma La Jencia Tuff from the Sawmill Canyon-Magdalena caldera. A series of three thin (0-65 ft), nonwelded, pumiceous ignimbrites intercalated with epiclastic conglomeratic sandstone of the South Crosby Peak Formation are the only volcanic rocks of this age range within the proposed caldera (Lopez and Bornhorst, 1979; Osburn and Chapin, 1983; McIntosh and Chamberlin, this volume). The small volume (<4 km^3) of these ignimbrites in the South Crosby Peak Formation cannot account for collapse of the large diameter (25-30 mi) Crosby Mountains caldera proposed by Elston (1989). I propose that the dioritic hypabyssal porphyry (volcanic neck?) at Cerrito Viejo (Fig. 1.9), imprecisely dated at 30.56 ± 1.42 Ma, could represent a potential source of the lowest pumiceous ignimbrite in the South Crosby Peak Formation, which is imprecisely dated at 29.67 ± 0.86 Ma (McIntosh and Chamberlin, this volume). Regardless of possible genetic relationships, this small-volume pyroclastic unit cannot reasonably be linked to a large Crosby Mountains caldera as proposed by Elston (1989).

Detailed mapping and sedimentological studies of the South Crosby Peak Formation (32.1-27.4 Ma) will be necessary to evaluate why this unit thickens so rapidly to the south in the vicinity of Datil, New Mexico (cf. Lopez and Bornhorst, 1979; Harrison, 1980). Eolian sandstones in the Alegres Mountain area (Fig. 1.9), which are correlative to the South Crosby Peak Formation, span the proposed caldera margin fault (AMF) and show no apparent change in thickness (Jones, 1980; Chamberlin et al., 1994b).

At present, available stratigraphic relations, isotopic age data and regional mapping are contrary to the notion of a Crosby Mountains caldera, or a Crosby Mountains volcano-tectonic depression as proposed by Elston (1989, 1984, respectively). It is recommended that future maps of ash-flow calderas in New Mexico omit this apparent volcano-tectonic collage.

56.4 Milepost 80. Reconnaissance mapping by R. M. Chamberlin indicates that the east ridge of Twin Peaks, at 11:00, consists of three nonwelded pumice-rich (10-20%) and lithic rich (5-10%) ignimbrites, each about 30-50 ft thick, which are interbedded with andesitic conglomerates of the South Crosby Peak Formation. The lowest ignimbrite contains vitrophyric and andesitic rock fragments. The upper two ignimbrites contain a mixture of andesitic and welded-tuff fragments. Fragments of densely welded, crystal-rich, quartz-rich Hells Mesa Tuff are largest (~5 cm) and most abundant in the uppermost pumiceous ignimbrite. A similar sequence of three thin lenticular pumiceous ignimbrites on Anderson Mountain (peak at 11:45) has yielded $^{40}Ar/^{39}Ar$ ages confirming the presence of xenocrystic Hells Mesa sanidines in the upper two ignimbrites (McIntosh and Chamberlin, this volume). Also, at Anderson Mountain the lowest pumiceous ignimbrite has yielded an apparent eruptive age of 29.67 ± 0.86 Ma, as determined from plagioclase phenocrysts hand picked from cognate pumice clasts. Lopez and Bornhorst (1979) did not differentiate or map the distribution of these pumiceous ignimbrites within the South Crosby Peak Formation. Their age is bracketed by the underlying 32.1-Ma Hells Mesa Tuff and the overlying 28.8-Ma La Jencia Tuff. Similar pumice-rich ignimbrites, generally not associated with interbedded conglomerates, are commonly observed throughout the Socorro-Datil region (Osburn and Chapin, 1983). Where confined between the Hells Mesa and La Jencia tuffs, the thin pumiceous tuffs have been informally referred to as the tuff of South Crosby Peak (C. E. Chapin, oral commun., 1993). **0.7**

57.1 The northern twin of Twin Peaks at 9:00 is capped by 100 ft of basaltic andesite of Deep Well overlying 65 ft of densely welded La Jencia Tuff. Approximately 500 ft of conglomeratic sandstones and pumiceous ignimbrites of the South Crosby Peak Formation are exposed in the slopes below the La Jencia Tuff. **0.3**

57.4 Milepost 79. Highway descends onto flat floor of White House Canyon. North wall of canyon at 1:30 is cut in Hells Mesa Tuff. **1.0**

58.4 Milepost 78. New Mexico State Highway Department maintenance yard on right. **0.3**

58.7 Roadcuts on left in nonwelded pumice-rich ignimbrite within the South Crosby Peak Formation. The presence of large Hells Mesa-type lithic fragments (Fig. 1-10) indicates this is probably the uppermost pumice-rich ignimbrite in the Crosby Peak Formation. Zeolitization of the pumiceous ignimbrites and the presence of numerous lithic fragments have thwarted attempts to determine their paleomagnetic orientation. **0.3**

59.0 Roadcuts in conglomeratic sandstones of the South Crosby Peak Formation. **0.2**

59.2 Entering downtown Datil (Spanish, "date", as in fruit of the date palm), settled in 1884 (Pearce, 1965). Junction with NM-12 on left. **Continue straight ahead on US-60**. Third-Day road log will bring us back to Datil. Early travelers along the Ocean-to Ocean Highway (ca. 1912-1920) could have stayed at the luxurious Navajo Lodge near here (Fig. 1-11). Since 1933, the Eagle Guest Ranch has provided rustic and peaceful lodging, good food, and gasoline to tourists and local ranchers (Fig. 1.12). **0.2**

59.4 Milepost 77. For the next 9.3 mi, US-60 trends northwest along White House Canyon, a major drainage that generally cuts across the regional structural grain. **0.6**

60.0 Road to Datil Well campground on left. Highway crosses alluvium-covered trace of major down-to-south fault zone near here (Lopez and Bornhorst, 1979; Fig. 1.7). Thick South Crosby Peak Formation and Mogollon Group volcanic units are preserved on the south side of this fault zone. This arcuate, concave-to-the-south, normal-fault zone can be traced for 25 mi westward to Alegres Mountain, where it is referred to as the Alegres Mountain fault (Alegros fault of Jones, 1980; spelling and name changed to match that of Alegres Mountain 7.5' quadrangle). A regional north-trending seismic reflection profile (Armstrong and Chamberlin, this road log) shows that this fault was previously a zone of Laramide transpressional faulting, upthrown on the south, and then buried by the Eocene Baca Formation.

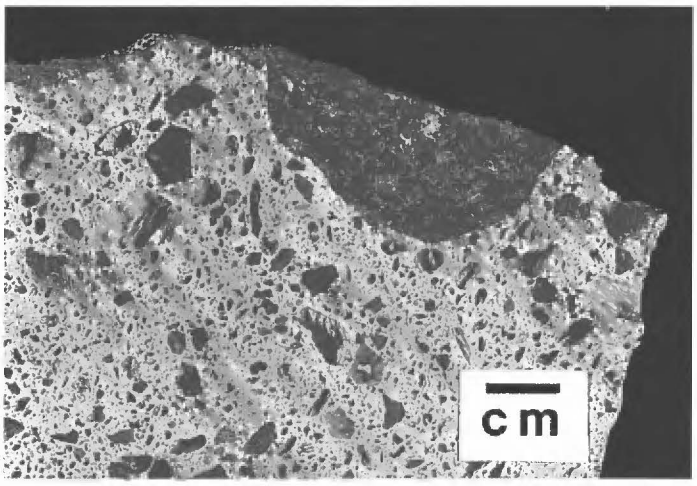


FIGURE 1.10. Slab of non-welded pumiceous and lithic-rich ignimbrite from the South Crosby Peak Formation; fragile zeolitic pumice forms striated pockets in rock face. Note large fragment of crystal-rich Hells Mesa Tuff (upper right).



FIGURE 1.11. Cowboys ready to ride, Navajo Lodge in Datil, ca. 1920. Photograph courtesy of Buz and Beverly Easterling, Quemado Lake Estates.

Near Datil, the Alegres Mountain fault zone merges in a complex pattern with the north-northeast-trending Red Lake fault zone, which also has indications of a Laramide ancestry (Cather, 1989). **0.2**

60.2 Dark ledges of coarsely porphyritic andesite of White House Canyon (Fig. 1.13) form southwest wall of canyon from 9:00 to 11:00. The andesite of White House Canyon and the immediately overlying Datil Well Tuff are interbedded in the Chavez Canyon Formation of the middle Spears Group (Osburn and Chapin, 1983; Cather el al., this volume). This gently southwest-dipping cuesta (9:00-11:00) locally marks the upthrown footwall of the Alegres Mountain fault. **0.2**

60.4 Milepost 76. Narrow ledge of 35.0-Ma Datil Well Tuff caps lower mesa at 2:00; Osburn and Chapin (1983) measured 31 ft of Datil Well Tuff at the type section approximately 200 ft east of the mesa corner. Upper mesa at 3:00 is capped by the 34.2-Ma Rock House Canyon Tuff. Volcaniclastic conglomerates and sandstones of the Chavez Canyon Formation typically underlie rubble-covered slopes below the Datil Group ignimbrites. Today's second stop provides an unusually good exposure of these widespread volcaniclastic sedimentary apron deposits assigned to the middle Spears Group. **0.7**



FIGURE 1.12. Local rancher George Farr and family at the Eagle Guest Ranch Trading Post in Datil, ca. 1935. Photograph courtesy of Kenneth and Carol Coker, Eagle Guest Ranch.

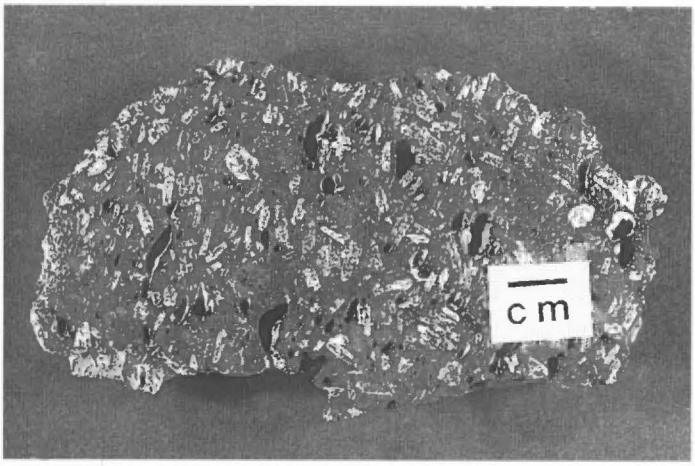


FIGURE 1.13. Vesicular turkey-track basaltic-andesite (55.3% SiO_2, anhydrous) lava from the andesite of White House Canyon.

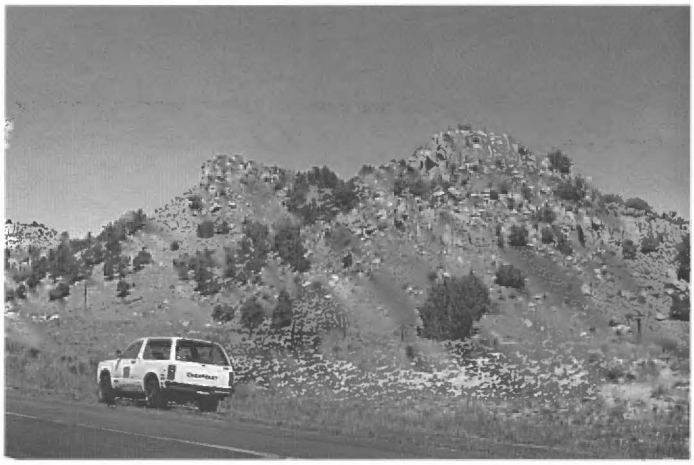


FIGURE 1.14. Ledge-forming andesite of White House Canyon caps knobby hill at Vega Well overlook. Vantage point of Stop 1 is at hill crest on right. A small east-northeast-trending normal fault passes through saddle and drops lavas down to north. View is to northwest.

61.1 Junction with Forest Road 100 on right. FR-100 follows Main Canyon to Blue Canyon and the type section of the 33.7-Ma Blue Canyon Tuff (Osburn and Chapin, 1983) about 7 mi north of here. **0.1**

61.2 Dead Horse Mesa at 12:00 is capped by Datil Well Tuff and andesite of White House Canyon (Lopez and Bornhorst, 1979). **0.1**

61.3 Road cuts and slopes on left expose light gray argillaceous feldspathic sandstones and andesitic conglomerates of the Chavez Canyon Formation. Lopez and Bornhorst (1979) recognized and described the mostly fluviatile unit exposed here, but did not differentiate it from the coarse andesitic debris-flow deposits and breccias of the underlying Dog Springs Formation (Osburn and Chapin, 1983). Several mapping projects (Harrison, 1980; Coffin, 1981; Brouillard, 1984; Chamberlin et al., 1994b) have differentiated the fluvial conglomerates of the Chavez Canyon Formation from the underlying Dog Springs debris-flow deposits and noted that the contact is often an angular unconformity. Angular unconformities are associated with soft-sediment deformation structures that are widespread within the underlying Dog Springs Formation (Osburn and Chapin, 1983). The Chavez Canyon Formation is about 400 ft thick in the Datil region. **0.9**

62.2 Road sign announces entering Cibola National Forest. Most of the woodland along White House Canyon, however, is private property, originally acquired as sections and quarter sections under the Homestead Act. **0.5**

62.7 Baldwin Cabin, named for 1880s rancher Levy Baldwin, on hill top at 2:00. **0.4**

63.1 **Slow down, prepare for Stop 1.** Southeast crest of knobby hill at 1:00 (Fig. 1.14) is site of Stop 1. **0.1**

63.2 **STOP 1. Park along right shoulder of US-60**, as directed by flagpersons. Walk northwest along highway to private road to Vega Well (at cattle guard). S. Taubman is the local landowner at Vega Well and permission to use the overlook (Fig. 1.15) is required. The high point west of the Vega Well overlook is an alternative view point within the Cibola National Forest. Enter Vega Well property through gate at cattle guard and walk to southeast crest of the low hill immediately north of the road. This hill is capped by ledge-forming coarsely porphyritic andesite of White House Canyon that conformably overlies andesitic sandstones and conglomerates of the Chavez Canyon Formation of late Eocene age.

At the Vega Well overlook, use the index map (Fig. 1.15) and the panoramic photo (Fig. 1-16) as your guide to locating landmarks and geologic features. To the north, the almost treeless hill in the left middle foreground of the panorama is reference point "A" on the index map. Winchester (1920) was the first to map the north-northeast-trending Red Lake fault where it cuts Mesozoic strata in the Acoma section of the Colorado Plateau. Later studies by Wengerd (1959) and Maxwell (1976) in the Acoma region showed that this normal fault zone is associated with northwest-trending en echelon folds and domes in Cretaceous strata; this suggests it had an earlier history of Laramide right-lateral transpression. Robinson (1981) estimated the stratigraphic throw of Cretaceous strata along the main strand of the Red Lake fault at D-Cross Mountain to be about 1180 ft. Observations of striated fault surfaces in Cretaceous rocks near Alamocito Creek imply a late-stage, dip-slip, normal displacement for the Red Lake fault zone.

The main purpose of this stop is to present an introduction to the Cenozoic stratigraphy and structure of the Mogollon slope in northeastern Catron County. Major Cenozoic stratigraphic units and regional structural patterns are illustrated on Figure 1.7. The most significant map pattern is one of gently (2-5°) south-dipping Eocene and Oligocene strata locally offset and distended by north-northeast-trending normal fault zones. Miocene conglomerates are preferentially preserved on the downthrown side of the Neogene normal fault zones. These epiclastic conglomerates were mostly derived from erosional remnants of Oligocene volcanic highlands (e.g., Mangas Mountains, Gallo Mountains, Alegres Mountain and Crosby Mountains). Eocene andesitic debris flows in the Datil Mountains

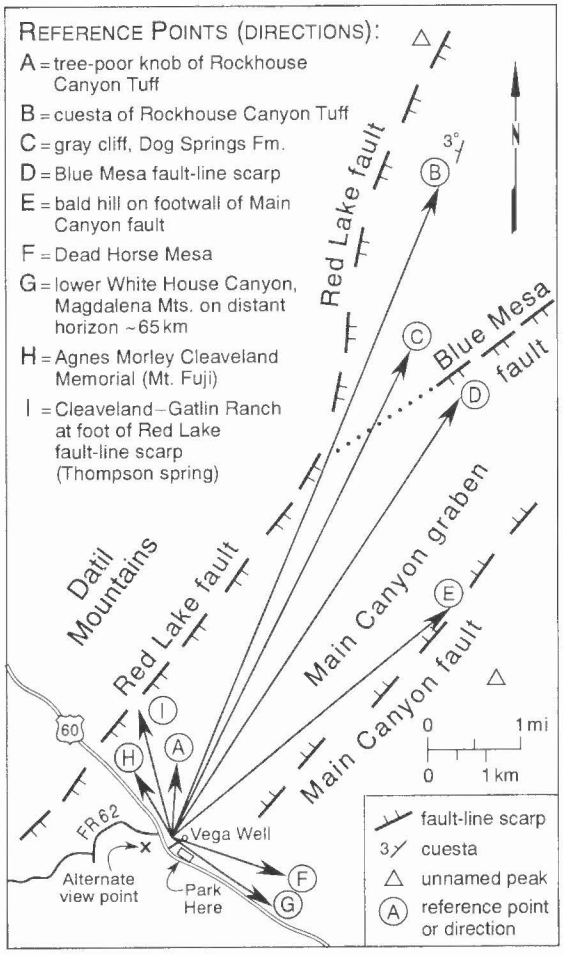


FIGURE 1.15. Panoramic index map of the Main Canyon graben area from the Vega Well overlook at Stop 1.

(lower Spears Group), which lie on a broad horst block between the Red Lake fault and the Hickman fault, were also a source of Miocene conglomerates in the Pie Town area. The estimated maximum Neogene normal displacement on the Hickman and Red Lake fault zones is about 2000 ft. Miocene units include the Fence Lake Formation, west of the Hickman fault zone; the Gila Group, south of the Spur Lake and Cañon del Buey faults; Santa Fe Group, south of the Alegres Mountain fault; and the conglomerate of Rock Tank Canyon (Robinson, 1981) east of the Blue Mesa fault.

Regional thickness trends of the middle to upper Eocene Baca Formation (nonvolcanic fluvial red beds) and upper Eocene andesitic debris flows of the Dog Springs Formation (Cather and Johnson, 1984; Cather, 1989) indicate that the Neogene Datil Mountains horst was a depressed synclinal trough between reverse faults along the Red Lake and Hickman fault zones during late Laramide transpressional deformation. Increasing evidence indicates that Laramide transpressional welts (uplifts) in west-central New Mexico have collapsed to form Neogene extensional or transtensional basins approximately contemporaneous with similar inversion of Laramide uplifts along the axis of the Rio Grande rift (Cather, 1989; Garmezy, 1990; Chapin and Cather, in press). However, the possibility of *local* Laramide trantensional basins at releasing bends in lateral or oblique slip regimes (e.g., Cather, 1992) should not be overlooked, because they may have preserved Paleozoic and Mesozoic sedimentary strata favorable for hydrocarbon exploration.

Andesitic debris-flow deposits of the Dog Springs Formation (ca. 40-37 Ma, Osburn and Chapin, 1983; Cather et al., 1987; McIntosh and Chamberlin, this volume) are widespread in the Gallinas and Datil Mountains and along the west flank of the Crosby Mountains (J-L Draw area). Debris flows of the Datil Mountains area appear to intertongue with and grade

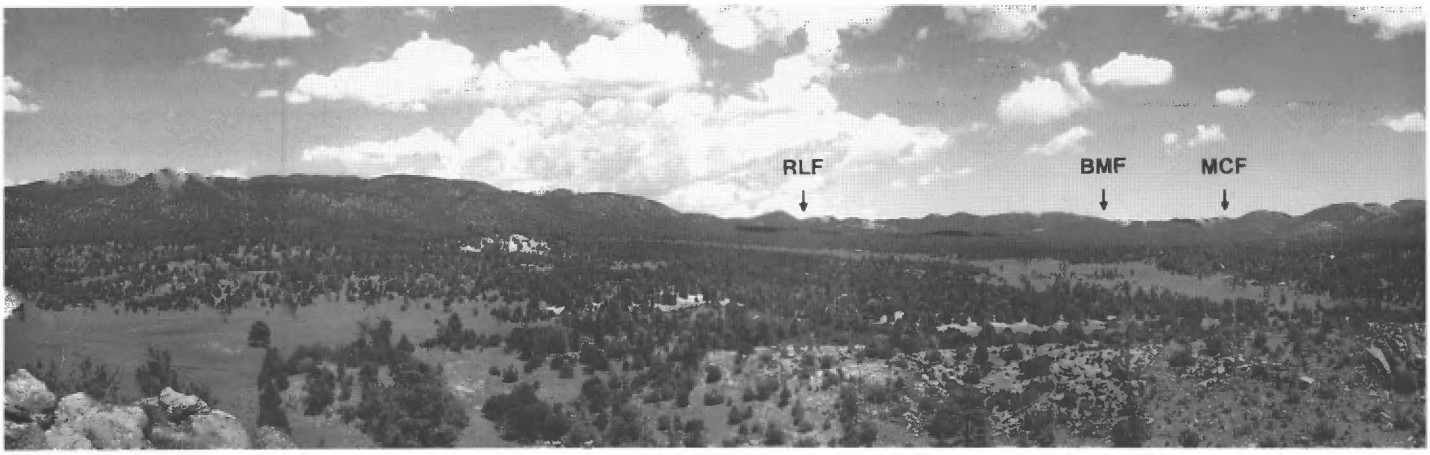


FIGURE 1.16. Panorama of the Red Lake fault zone and topographic low of the Main Canyon graben; view to north from Vega Well overlook. Arrows indicate where major fault traces cross the horizon. Compare with index map, Fig. 1-15. Abbreviations are: RLF= Red Lake fault, BMF= Blue Mesa fault, and MCF= Main Canyon fault.

northwestward into andesitic sandstones and mudstones of the volcaniclastic unit of Largo Creek (new name, Chamberlin and Harris, this volume). Both of these upper Eocene andesitic units are informally assigned to the lower Spears Group. Regional distribution patterns of the lower Spears Group in the Datil-Quemado region suggest an andesitic source area located under the southern San Agustin Plains in the vicinity of the C-N Basin.

Volcaniclastic alluvial apron deposits of the middle Spears Group are mostly epiclastic conglomerates deposited by north-flowing braided stream systems emanating from andesitic to rhyolitic eruptive centers to the south. Outflow sheets of Datil Group ignimbrites derived from calderas to the south and east (McIntosh et al., 1991) are interbedded with the volcaniclastic sedimentary units (e.g. Chavez Canyon and Rincon Windmill Formations) to form a multi-story sediment and ignimbrite layer cake collectively lumped together here as the middle Spears Group and Datil Group. Porphyritic basaltic andesite to andesite lava flows (e.g. andesite of White House Canyon and andesite of Dry Leggett Canyon) are also interbedded in this upper Eocene to lower Oligocene interval (ca. 35 to 32 Ma). A major eruptive center for the andesite of Dry Leggett Canyon has been documented in the San Francisco Mountains area southwest of Reserve by Ratté (1989). As will be observed at Stop 2, syneruptive tuffaceous sandstones and pumiceous mudstones of rhyolitic composition are another significant lithology in the middle Spears Group. Syneruptive tuffaceous sandstones (terminology after Smith, 1991) largely define the middle Spears Group in the Quemado-Escondido Mountain area where Datil Group ignimbrites are locally absent (volcaniclastic unit of Cañon del Leon, new name, Chamberlin and Harris, this volume).

Epiclastic conglomerates and thin, non-welded, pumiceous ignimbrites in the South Crosby Peak Formation disconformably overlie the Hells Mesa Tuff (32.1 Ma) in the Crosby Mountains area (Osburn and Chapin, 1983). These non-welded lithic-rich ignimbrites must be older than the overlying 28.9-Ma La Jencia Tuff. However, additional epiclastic conglomerates that occur above the La Jencia Tuff, to the base of the South Canyon Tuff (27.4 Ma) have been mapped with the South Crosby Peak Formation in the Crosby Mountains (Lopez and Bornhorst, 1979). This dominantly sedimentary interval (ca 32-27.4 Ma) in the Crosby Mountains is here informally assigned to the upper Spears Group. A thick interval (400-800 ft) of massive and commonly high-angle cross-bedded sandstones occupies the same stratigraphic interval in the Mangas-Alegres Mountains region. Distal ignimbrite sheets, including the Caballo Blanco Tuff (31.7 Ma), Vicks Peak Tuff (28.6 Ma) and Bloodgood Canyon Tuff (28.0 Ma) locally fill paleovalleys in the massive fine- to medium-grained sandstones, and demonstrate that this unit is contemporaneous with the South Crosby Peak Formation. These massive cross-bedded to planar-bedded sandstones of apparent eolian origin (cross beds indicate prevailing westerly winds) have been informally assigned to the sandstone of Escondido Mountain (new name, Chamberlin and Harris, this volume). Presumably these sands once intertongued with distal alluvial apron deposits of the South Crosby Peak Formation in the erosional gap between the Crosby Mountains and Alegres Mountain. The Mogollon Group ignimbrites also erupted from calderas to the south and southeast of the Datil-Quemado area (McIntosh et al., 1991).

Upper Oligocene to lower Miocene(?) basaltic andesite lavas of the Bearwallow Mountain Andesite and the basaltic andesite of Crosby Mountains generally cap the middle Tertiary volcanic pile in the Datil-Quemado region. Erosional remanents of stacked basaltic andesite flows in the Mangas, Alegres and Crosby Mountains are commonly about 600 ft thick. Individual flows are typically about 30 ft thick. A much thicker pile of basaltic andesite lavas under Mangas Mountain (1200 ft) implies that this was a major eruptive center for the Bearwallow Mountain lavas.

Large basaltic-andesite dikes at Pie Town (Stop 4) and Lehew (aka Hickman) are lithologically similar to the Bearwallow Mountain lavas and yield K-Ar ages of 27.7 ± 0.6 and 27.3 ± 1.3 Ma, respectively (Laughlin et al., 1979) . Basal Bearwallow flows in the Mangas Mountains area have been dated at 27.8 ± 1.7 Ma (K-Ar, Baldridge et al., 1989) and at 26.0 ± 0.1 Ma ($^{40}Ar/^{39}Ar$ total gas isochron, McIntosh and Chamberlin, this volume). Considering analytical error of the K-Ar method these basaltic andesite dikes might be equivalent to the Bearwallow. These long (30-45 mi) dikes mark the onset of regional southwest-directed extension across the southeastern Colorado Plateau (Laughlin et al., 1983). Incipient regional extension, however, may have begun in the Datil area as early as 35-36 Ma (Cather, 1989). Relatively few regional normal faults in the Datil-Quemado area parallel the initial basaltic andesite dikes. Ancient colluvial breccias derived from Bloodgood Canyon Tuff adjacent to the Indio Canyon Fault (Fig. 1.7) suggest that it may have been active as early as 28 to 26 Ma.

On returning to vehicles note that the depositional contact of the andesite of White House Canyon on conglomerates of the Chavez Canyon Formation is well exposed on the southwest side of the Vega Well overlook (Fig. 1.17). Andesitic cross- bedded sandstones of the Chavez Canyon Formation are also well exposed in the roadcuts of US-60 west of the overlook.

Return to vehicles and continue west on US-60. 0.3

63.5 Roadcut on right in low-angle cross-bedded sandstone and andesitic conglomeratic sandstones of the Chavez Canyon Formation. A thin debris flow is also exposed near the northwest end of the cut, but this formation is dominantly fluviatile. Well-developed pebble imbrication in Chavez Canyon conglomerate at 11:00 (immediately below lava cap) indicates northwesterly paleoflow. **0.2**

63.7 Cuts on right and left in light gray conglomeratic sandstones of the Chavez Canyon conglomerate. Well-rounded clasts of medium-gray plagioclase-hornblende-biotite dacite porphyry, typical lithology of the underlying Dog Springs Formation, are ubiquitous in the lower Chavez Canyon Formation of the Datil area. **0.3**



FIGURE 1.17. Road logger (and honorary NMGS piano player) points to andesite of White House Canyon resting conformably on andesitic conglomeratic sandstones of the lower Chavez Canyon Formation. View to south on southwest side of Vega Well overlook.



FIGURE 1.18. Massive outcrop of andesitic debris-flow-breccia deposit in the upper Dog Springs Formation in upper White House Canyon.

64.0 Marble column at 10:00 marks memorial site for William Ramond Morley (1848-1884), pioneer railroad construction engineer for the Santa Fe Railroad, famous for designing and building the rail line through Raton Pass in northeastern New Mexico. He was accidentally shot and killed while working for the Mexican Central Railroad in old Mexico. His widow, Ada, and three young children came to the Datil area in 1886, later to become well-known successful cattle ranchers. Morley's tomboy daughter, Anne Morley Cleaveland, tells many tales of pioneer ranching experiences in the Datil region in her quasi-biographical book *No Life for a Lady*. Although rare, Ms. Cleaveland's brief geological notes are accurate and insightful. For example, she states "Datil is not a mineralized country. Not an ounce of valuable ore has ever been dug from its igneous mountains" (Cleaveland, 1941, p. 325). A brass plaque in memory of Anne Morley Cleaveland (1874-1958) is present on the hill at 1:00. Considering the view east down White House Canyon from the top of this hill, locally known as "Mt. Fuji", it is no wonder that "she loved this country". **0.6**

64.6 Road to Cleaveland-Gatlin ranch on right. Highway crosses alluvium-covered trace of the Red Lake fault near here. Roadcut on left in massive dacitic breccia (autoclastic?) of the Dog Springs Formation. For the next 5 mi, the relatively narrow upper reach of White House Canyon cuts across resistant dacitic debris flows and breccias of the upper Eocene Dog Springs Formation. **0.5**

65.1 Roadside table on right. Low cliffs of massive Dog Springs breccia at 1:30 (Fig. 1-18) have yielded an $^{40}Ar/^{39}Ar$ age of 36.94 ± 0.07 Ma from a single sanidine crystal and a less precise age of 37.57 ± 1.29 Ma from plagioclase crystals (McIntosh and Chamberlin, this volume). Some aspects of this dacitic breccia (Fig. 1-19) suggest a pyroclastic origin. The angular clasts of plagioclase-hornblende-biotite dacite porphyry float in a nonsorted massive matrix of similar composition. The microcrystalline matrix contains abundant broken slivers of phenocrysts and sparse angular fragments of

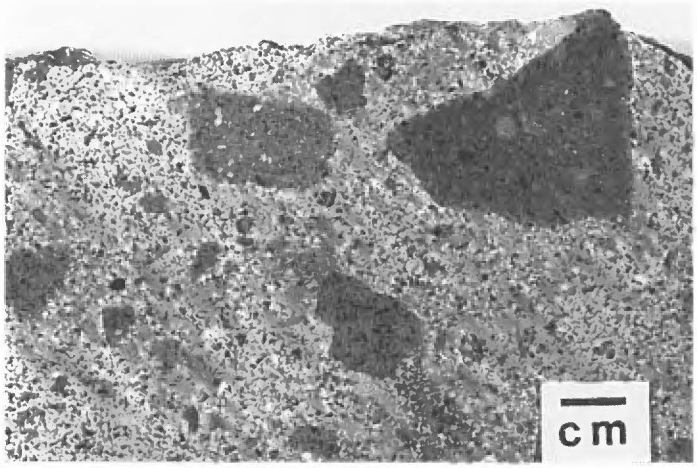


FIGURE 1.19. Typical plagioclase-hornblende-biotite porphyry clasts in Dog Springs debris-flow breccia deposit.

granular sandstone and mudstone. The sedimentary fragments are soft and tend to weather out, leaving angular pock marks, which can easily be mistaken for pumice. However, pumice and glass shards are not evident in thin section. These massive breccias are commonly interbedded with thick debris-flow deposits containing well-rounded cobbles of dacite porphyry. Attempts to determine emplacement temperatures of Dog Springs volcaniclastic breccias using paleomagnetic properties have been unsuccessful. By association with sedimentary-looking debris-flow deposits, these dacitic breccias are generally regarded to be of volcaniclastic sedimentary origin as opposed to hot pyroclastic deposits (Cather, 1986). **0.8**

65.9 Rock fin at 11:00 is formed by a resistant debris-flow bed that is standing on end. Although hard to find, bedding in the adjacent hillside, like the rock fin, is nearly vertical and strikes N45°W. Lopez and Bornhorst (1979) erroneously mapped this fin and other similar outcrops as pyroclastic dikes. **0.3**

66.2 Massive dacite breccia of Dog Springs Formation in roadcut on left lacks discernible bedding. **0.7**

66.9 Roadcut on left in Quaternary valley fill. Little is known about the thickness and age of valley fill here. Approximately 130 ft of Pleistocene to Pliocene (?) valley-fill deposits are exposed near Monument Saddle, at the head of Davenport Canyon, about 5 mi north of here. **1.3**

68.2 Bedded dacitic breccias in roadcut on left show attitude of N22°W, 84°NE at south end of cut and are subhorizontal at north end of cut. FR-6 to Davenport Canyon and Monument Saddle on right, just beyond. **0.2**

68.4 Milepost 68. White House Spring, near valley wall at 12:15, was original site of Ada Morley's 10 room white log house built in 1886. **0.2**

68.6 Highway begins ascent through narrow reach of upper White House Canyon. **0.3**

68.9 Remnants of old roadcut and road bed of Ocean-to-Ocean Highway parallel powerline on north side of US-60. This old road bed, in use in the 1920s (Fig. 1.20) was abandoned in the mid-1950s. **0.2**

69.1 Roadcut of US-60 on right (Fig. 1-21) exposes thick-bedded, dacitic, debris-flow deposits of the Dog Springs Formation dipping 30° to east-southeast. Well-rounded cobbles and boulders of dacite porphyry (Fig. 1-22) were presumably derived from mountain-stream bottoms and imply a relatively low-temperature environment of deposition for these deposits. **0.2**



FIGURE 1.20. Buttress and wooden beams of old Ocean-to-Ocean Highway bridge over drainage of upper White House Canyon. Carbide-lamp graffiti of W. H. Creamer Sep. 4, 1922 shows little or no fading over the last 71 years. Note medium to large pines growing from road bed.



FIGURE 1.21. Andesitic debris-flow deposits in Dog Springs Formation at Mile 69.1.



FIGURE 1.22. Close-up view of rounded stream cobbles and boulders of plagioclase-hornblende porphyry in massive debris-flow deposit of Dog Springs Formation.

69.3 Cut on right in interbedded argillaceous dacitic sandstones and dacitic debris-flow deposits dipping 30° to east-southeast. Small displacement conjugate normal faults exposed here strike N70°E and imply a local north-northwest oriented tensile stress axis. About 4 mi north of here, a 0.6-mi-long, 30-ft-wide, red mudstone dike cuts vertically across Dog Springs debris-flow deposits. This clastic injection dike, presumably derived from liquefied upper Baca Formation, strikes N50°E and also implies a northwest oriented tensile stress axis. All of these features are attributed to regional soft-sediment deformation and liquefaction in late Eocene time, shortly after or during deposition of the Dog Springs Formation. **0.1**

69.4 Milepost 67. Roadcut on left in Dog Springs debris-flow deposits and sandstones. The next 11-mi segment of US-60 was widened and "modernized" (roadcuts converted to rubble and then seeded) in a construction project completed in July 1993. **0.6**

70.0 Highway crests at West Pass; approximate elevation is 8100 ft. Headwaters of White House Canyon at 3:00. Entering drainage area of Z Slash Draw, which

becomes Z Slash Canyon about 5 mi to the south. Dog Springs beds at 2:00 look horizontal from here. **1.3**

71.3 **Turn left onto FR-63 and head south. 0.1**

71.4 Alegres Mountain on skyline at 1:00 is the highest point on the Mogollon slope of west-central New Mexico. It rises to an elevation of 10,220 ft and is capped by the Mangas Mountain member of the Bearwallow Mountain Andesite of the Mogollon Group. This erosional remnant of late Oligocene basaltic andesite lavas is approximately 650 ft thick.

For the next 5 mi FR-63 follows the drainage of Z Slash Draw, which generally parallels and defines an upper Eocene facies transition from dominantly Dog Springs debris-flow deposits on the east (higher hills to left) to dominantly argillaceous fluviatile sandstones on the west (lower hills on right). These poorly-sorted sandstones, compositionally equivalent to the coarser Dog Springs deposits, are newly assigned to the upper Eocene volcaniclastic unit of Largo Creek (Chamberlin and Harris, this volume). Most of the poorly-sorted, planar-bedded Largo Creek sandstones probably represent distal hyper-concentrated flow deposits derived from downstream transformation of the medial Dog Springs debris-flow deposits. Similar transitions (transformations) are commonly observed in the overall facies lineage of continental volcanic terranes (Fisher and Smith, 1991). The Dog Springs Formation and the volcaniclastic unit of Largo Creek are both assigned to the lower Spears Group (Fig. 1.7).

Willard's (1959, fig. 1) reconnaissance geologic map of northern Catron County shows that his "latite facies (Tdl) of the Datil Formation" is essentially equivalent to the Dog Springs Formation as presently defined. Willard's "volcanic sediment facies (Tds)" is also generally equivalent to the volcaniclastic unit of Largo Creek. However, the Miocene Fence Lake Formation was not discriminated on Willard's map where it unconformably overlies the volcaniclastic unit of Largo Creek in the Quemado-Pie Town area. **0.8**

72.2 Flat-topped Crosby Mountains at 12:00 and gently west-tilted top of Sugarloaf Mountain at 12:15. Both are capped by undated late Oligocene(?) basaltic andesite lavas assigned to the Mogollon Group. These basaltic andesites locally overlie the 27.4-Ma South Canyon Tuff (McIntosh and Chamberlin, this volume) and are probably correlative with the Bearwallow Mountain Andesite. They are, however, presently assigned to the informal unit of the basaltic andesite of Crosby Mountains (Lopez and Bornhorst, 1979). **0.4**

72.6 Cliffs and pinnacle of Dog Springs Formation in wooded hillside at 11:00. **0.4**

73.0 Cox Peak on middle skyline at 1:00 is capped by 250 ft of gently south-dipping (undeformed) Dog Springs debris-flow deposits overlying at least 300 ft of andesitic sandstones of the volcaniclastic unit of Largo Creek (Chamberlin et al., 1994b). **0.7**

73.7 Profile of upper Miocene Horse Mountain volcano is visible on skyline at 12:15. Cuesta with white stripe in middle slope just below and left of Horse Mountain is near site of Stop 2. Cuesta is capped by 33.6-Ma Blue Canyon Tuff and the white stripe is formed by the 34.2 Ma Rock House Canyon Tuff. **1.0**

74.7 Bumpy road crosses outcrop of light gray andesitic sandstones of the volcaniclastic unit of Largo Creek. **0.7**

75.4 **Bear right at fork in road**. Primitive Forest Road 62 on left leads to Flying V Draw. **0.3**

75.7 Wooded hills in foreground from 11:00 to 1:00 are underlain by Dog Springs Formation. **0.2**

75.9 Cattle guard. Entering private land; road curves to right. **0.4**

76.3 Road enters Quemado 30′ x 60′ quadrangle, area of the reconnaissance geologic map of Chamberlin et al. (1994b), the source of much of the geologic information presented from here on. **0.2**

76.5 Road begins sweeping S curve, first right then left, around windmill at Black Well. **0.2**

76.7 Road enters narrows of upper Z Slash Canyon. Wooded hills to east and west are mostly capped by Dog Springs Formation debris-flow deposits that are locally interbedded with and overlie andesitic sandstone of Largo Creek lithology. On a reconnaissance level, these hills are mapped as Dog Springs Formation. **0.7**

77.4 Ledge-forming Dog Springs beds at 10:00. **0.6**

78.0 Butte at 2:30 is capped by apparently horizontal debris-flow-breccia deposit overlying Largo Creek-type sandstones; this horizontal-looking breccia bed actually lies on the crest of a complex isoclinal fold system that is well exposed on the south flank of the butte (Fig. 1-23). On the west limb of this fold system, the breccia bed dips 60° to the west-northwest; and subhorizontal axes of isoclinal folds trend N20°E. **0.2**

78.2 Cattle guard. Enter T. L. Mannering ranch. **0.4**

78.6 Rounded peak on skyline at 10:30 is capped by 33.6-Ma Blue Canyon Tuff, just slightly older than the Eocene-Oligocene boundary, which has recently been shifted from 36.6 Ma (Palmer, 1983) to 33.4 Ma (McIntosh et al., 1992). This peak and underlying section of Datil Group ignimbrites and middle Spears Group conglomeratic sandstones are preserved on the downthrown side of the Alegres Mountain fault in a narrow east-west trending graben approximately 2 mi wide. **0.3**

78.9 Axes of tightly-folded Dog Springs beds dip about 50° to south-southwest at 9:00. Just beyond, the road crosses projected trace of Alegres Mountain fault (AMF, Fig. 1.7) with an estimated local stratigraphic throw of 600 ft, downthrown to the south. Displacement on the AMF apparently increases toward the east, where it may be as much as 1200 ft in the northern Crosby Mountains. The AMF forms the north margin of what is here termed the Cox Lake graben. The east end of the Cox Lake graben is downwarped to the east-southeast at an angle of about 4°; this accounts for the progressive easterly increase of stratigraphic throw on the AMF. To the west of Alegres Mountain the AMF displaces the Bearwallow Mountain Andesite about 400 ft (Jones, 1980). **0.1**

79.0 Red ledges of Chavez Canyon Formation conglomerates at 9:00 to 9:30. Datil Well Tuff is locally absent here. **0.2**

79.2 Road to Mannering ranch house on right. Blue Canyon Tuff of the Datil Group caps cuestas at 12:30 and 1:00, and Rock House Canyon Tuff of the Datil Group forms

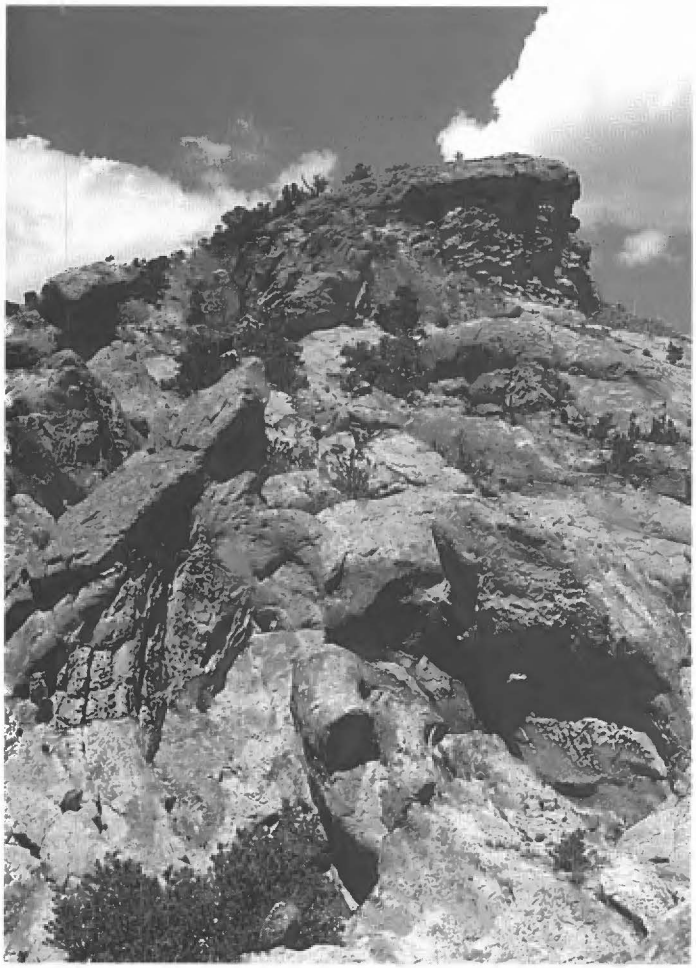


FIGURE 1.23. Isoclinal fold in the Dog Springs Formation, NW¼ sec. 31, T1S, R11W; view to northeast. Note fold noses above brushy piñon on lower left. Small sausage-like nose, just above brush is approximately 2 ft wide. Subhorizontal debris-flow breccia bed on skyline is at crest of broader anticlinal fold.

white band in middle slope. Slope-forming interval between Blue Canyon and Rock House is the Rincon Windmill Formation of the middle Spears Group. **1.0**

80.2 White ledge forming Rock House Canyon Tuff is at road level on the left. **0.3**

80.5 Beds of Rincon Windmill Formation exposed at road level on left. Blue Canyon Tuff caps ridge on left, but descends to road level ahead. **0.4**

80.9 Cattle guard. Road crosses projected trace of the Cox Lake fault. This down-to-the-north normal fault has an estimated stratigraphic throw of 800 ft and forms the south margin of the Cox Lake graben. **0.2**

81.1 Cattle guard. Low hills at 2:45 to 3:00 are underlain by Dog Springs Formation in the footwall of the Cox Lake fault. **0.5**

81.6 Entrance to Jay Saulsberry Ranch on right. **0.4**

82.0 Cattle guard. **Prepare for hard right turn 0.2 mi ahead. 0.2**

82.2 **Make hard right turn,** onto ranch road that heads north along Nester Draw. **0.1**

82.3 Road forks at side-by-side gates. Take right fork; the right gate is usually open. Now on private land of the Fred Saulsberry ranch; permission to enter this area may be obtained at the ranch headquarters 1.2 mi to the south. **0.1**

82.4 Dog Springs Formation exposed on hillside to left. **0.3**

82.7 Datil Group ignimbrites form resistant ledges and caprock in hills at 12:00 (Fig. 1.24). **0.1**

82.8 Gate across ranch road, normally closed. Continue straight ahead. Folded Dog Springs beds at 2:00. **0.2**

83.0 Lower Chavez Canyon Formation is faulted against Dog Springs Formation at 3:00. **0.1**

83.1 Gate across ranch road, usually open. **0.1**

83.2 Cross projected trace of Cox Lake fault. Note gentle synclinal trough at 2:00. **0.3**

83.5 Ravine above small alluvial fan at 3:00 is site of Stop 2. **Continue straight ahead to turn around at triangular intersection. 0.2**

83.7 **Take right fork at Y intersection, make counterclockwise U turn, and head south to Stop 2. 0.4**

84.1 **STOP 2. Park at side of road, remain headed south,** for return to US-60. The purpose of this stop is to provide a hands-on look at three distal ignimbrite sheets of the Datil Group and interbedded volcaniclastic sedimentary rocks of the middle Spears Group that are unusually well exposed here at Saulsberry Ranch.

These upper Eocene rocks on the west flank of the Crosby Mountains are locally preserved in the Cox Lake graben, between the Alegres Mountain fault and the Cox Lake fault. For orientation, see photograph and measured section through these upper Eocene rocks (Figs. 1.25, 1.26). Correlation of the ledge-forming ignimbrites has been verified by $^{40}Ar/^{39}Ar$ geochronology (McIntosh and Chamberlin, this volume) and by determination of thermal remanent magnetic directions. These new $^{40}Ar/^{39}Ar$ ages, based on multiple analyses of individual sanidine crystals, are superior to previous bulk-sample sanidine analyses of the Datil Well Tuff and the Rock House Canyon Tuff, which were apparently contaminated by older



FIGURE 1.24. View to north of ledge-forming Datil Group ignimbrites at Saulsberry Ranch. Site of Stop 2 is at light-colored area on far left. Blue Canyon Tuff caps mesas, white ledges in mid-slope are formed by Rock House Canyon Tuff and narrow ledge in lower third of slope is Datil Well Tuff. Volcaniclastic sedimentary rocks of middle Spears Group between ignimbrites are poorly exposed, except for low cliff of andesitic conglomerate at base of section.

xenocrysts of sanidine. These new isotopic age data strongly suggest that the Datil Well Tuff is correlative with the Bell Top Tuff No. 4 (McIntosh et al., 1991), but more data are needed to confirm this possibility. If this tentative correlation is correct, the Datil Well Tuff (34.98 ± 0.19 Ma) may represent an initial (premonitory) phase of eruption from the Emory caldera area that culminated in eruption of the Kneeling Nun Tuff at 34.89 ± 0.05 Ma (McIntosh et al., 1991).

With the correlation of the ignimbrites at Saulsberry Ranch firmly established by isotopic ages and paleomagnetic directions, these formations may be mapped regionally on the basis of their physical characteristics. The Datil Well Tuff is a light gray, moderately phenocryst-rich (~15%) partially to densely welded, pumice-poor rhyolite ignimbrite. Medium-grained phenocrysts of sanidine are dominant and minor green pyroxene is distinctive; plagioclase and quartz are rare to absent. The light gray to white, phenocryst-poor (~2%), pumice-rich Rock House Canyon Tuff, is poorly

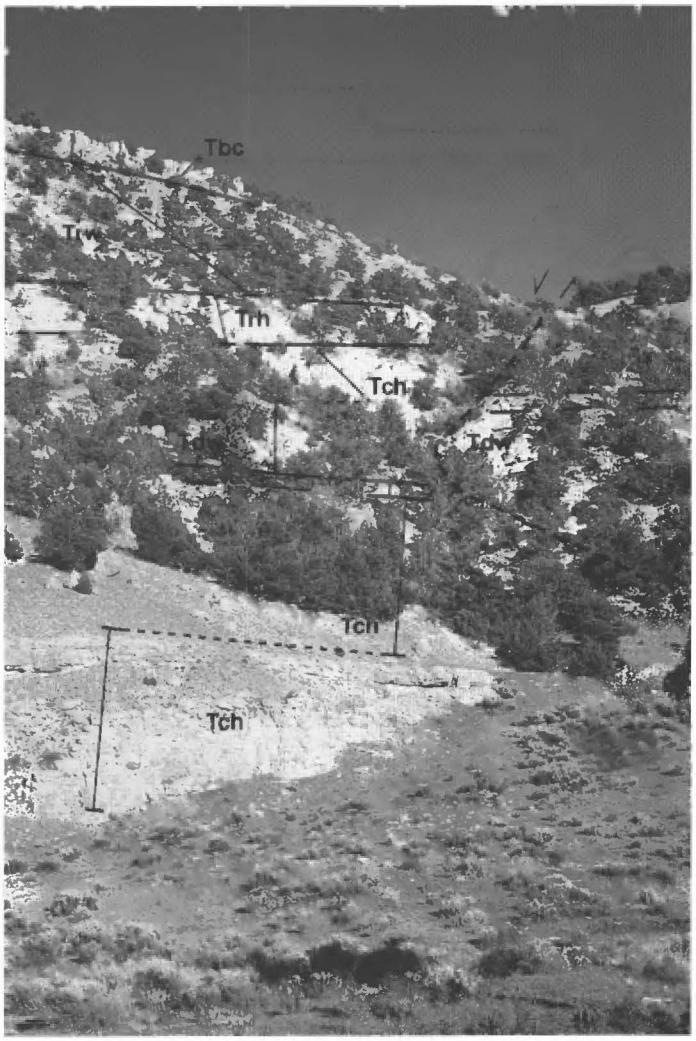


FIGURE 1.25. View showing location of measured stratigraphic section at Saulsberry Ranch. Distal ignimbrites of the Datil Well Tuff (Tdw), Rock House Canyon Tuff (Trh) and Blue Canyon Tuff (Tbc) are interbedded with and cap volcaniclastic sedimentary rocks of the Chavez Canyon Fm. (Tch) and the Rincon Windmill Fm. (Trw), of the middle Spears Group. Finer lines show approximate path of measured section (Fig. 1.26).

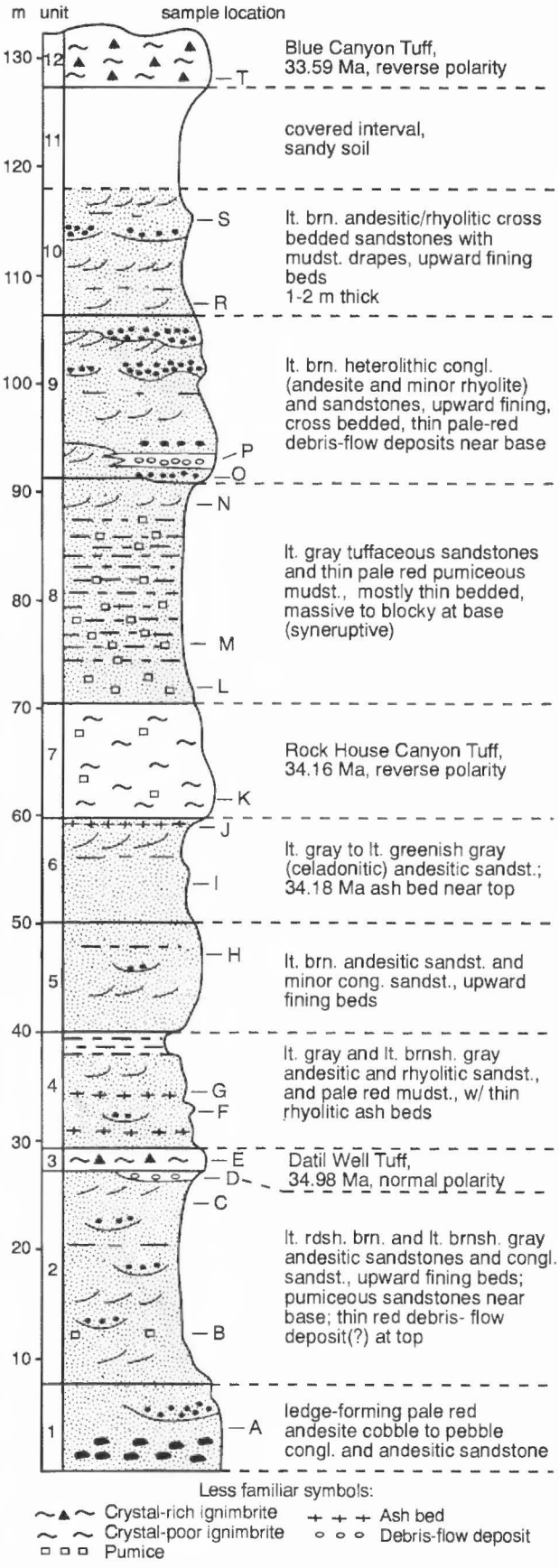


FIGURE 1.26. Measured section of Datil Group ignimbrites and middle Spears Group at Saulsberry Ranch; section measured by R. M. Chamberlin and O. J. Anderson. Rock House Canyon Tuff separates underlying Chavez Canyon Formation from overlying Rincon Windmill Formation (Osburn and Chapin, 1983).

welded to nonwelded. Small sparse phenocrysts of sanidine and plagioclase with minor quartz and biotite are typical. Unusually large phenocrysts of plagioclase (5-6 mm) and smaller sanidine phenocrysts comprise about 20% of the Blue Canyon Tuff. Biotite and sparse quartz are also present. Plagioclase in the Blue Canyon at Saulsberry Ranch is mostly altered to clay minerals; probably a reflection of deuteric or vapor-phase alteration. The partially to densely welded, light to medium gray Blue Canyon Tuff generally contains 2-4% small andesite lithic fragments; small lithic fragments also occur in the Rock House and Datil Well Tuffs but tend to be more sparse. All of the ignimbrites are ledge-forming units and locally form caprocks.

Thickness variations in these distal ignimbrites (typically 0-100 ft) can be an important indicator of paleotopography. The 6-ft-thick Datil Well Tuff locally pinches out to the northeast of the measured section; also the Rock House Canyon Tuff, about 30 ft thick in this region, is abruptly truncated at a local normal fault-controlled unconformity approximately 1.2 mi east of this site. The field relationships there (SW¼ sec. 32, T1S, R11W) indicate down-to-the-south normal faulting along the Alegres Mountain fault zone as early as 34.2 Ma. A similar normal fault appears to truncate the Hells Mesa Tuff 1.8 mi farther east (Lopez and Bornhorst, 1979). Abrupt thickness changes of ignimbrites at ancient fault scarps are key indicators of contemporaneous displacement because ignimbrites are emplaced essentially instantaneously and produce a mold of the underlying paleotopography (Chamberlin, 1983). Distal ignimbrites also fill paleovalleys in the Quemado-Datil region; paleovalley margins should not be confused with local fault-controlled unconformities.

The general lithology and compositional character of Spears Group volcaniclastic sedimentary rocks at Saulsberry Ranch are summarized in Fig. 1.26. Upward fining beds of volcaniclastic conglomerate to sandstone, low-angle trough crossbedding, and thin mudstone drape deposits indicate that the Chavez Canyon and Rincon Windmill Formations were primarily deposited by braided channel systems on a broad alluvial apron peripheral to volcanic highlands. Limited observations of pebble imbrications at widespread sites suggest that paleoflow was dominantly northerly. This is consistent with the general recognition that major late Eocene volcanic centers were primarily south of the Datil region, although specific source cauldrons for the Datil Well, Rock House Canyon, and Blue Canyon Tuffs have not yet been located. Both the Chavez Canyon and the Rincon Windmill formations consist of intercalated beds of andesitic to rhyolitic composition and variable mixtures of heterolithic conglomerates containing both andesitic and rhyolitic clasts.

The Rock House Canyon Tuff is locally overlain by 70 ft of mostly thin-bedded, light gray, tuffaceous (shard-rich) sandstone and thin, pale, red, pumiceous mudstones (unit 8, Fig. 1.26). Preferential concentration of pumice in the mudstone drapes (Fig. 1.27) provides convincing evidence that the pumice was floating and therefore freshly introduced into the fluvial system at the time of deposition. In the terminology of Smith (1991), this pumiceous unit is a syneruptive deposit, presumably derived from the non-welded top of the Rock House Canyon Tuff. Similar late Eocene syneruptive units are newly assigned to the volcaniclastic unit of Cañon del Leon in the Quemado area where the Datil Well, Rock House and Blue Canyon ignimbrites are locally absent. Tuffaceous Cañon del Leon beds are intercalated with andesitic sandstones and conglomerates that must be laterally equivalent to the Chavez Canyon beds observed here.

Another noteworthy lithology in the Saulsberry Ranch section is a rhyolitic sandstone bed (sample location F, Fig. 1.26), that probably represents reworked, nonwelded, crystal-rich Kneeling Nun Tuff. This interpretation is supported by its stratigraphic position and its mineralogy (sanidine-and plagioclase-rich with about 10% quartz and 5% biotite). Occurrences of heterolithic conglomerates (Fig. 1.28) and thin muddy debris-flow beds (Fig. 1.29) in the Rincon Windmill Formation are also notable.

The above observations and regional mapping suggest little difference in the general lithology, provenance or depositional environment of the Chavez Canyon and Rincon Windmill formations. They would be essentially indistinguishable where the Rock House Canyon Tuff is not present. Some revision in the nomenclature of these middle Spears Group formations may be appropriate when the Datil-Quemado region is mapped in detail. Considerably more sedimentological data is needed to evaluate the possible influence of contemporaneous normal faulting on upper Eocene and Oligocene depositional systems in the Datil region. For example, Mack et al. (this volume) have used detailed sedimentological data from the Bell Top Formation to define a large half-graben type basin of late Eocene to Oligocene age in the southern Rio Grande rift. Sedimentary units of the Bell Top Formation are similar in age and lithology to those observed here at Saulsberry Ranch.

Field conference attendees should use proper caution when climbing through the section at Saulsberry Ranch. Be careful not to dislodge loose rocks and watch your footing. Quick climbers may enjoy the view of Horse Mountain (to the south) and Alegres

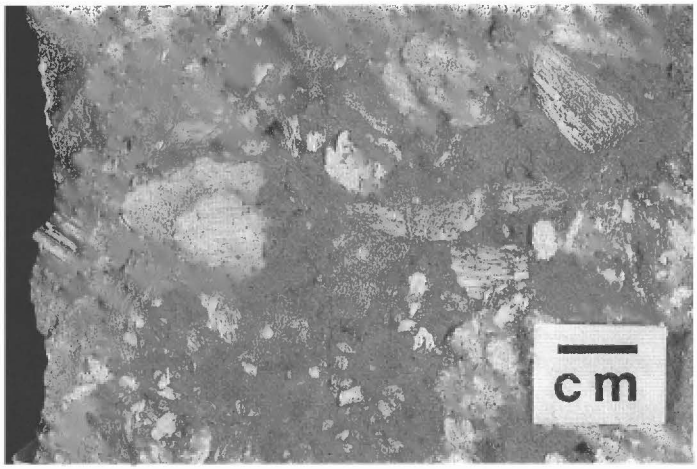


FIGURE 1.27. Pumiceous mudstone (Fig. 1-26, sample location M) as exposed on a bedding plane.

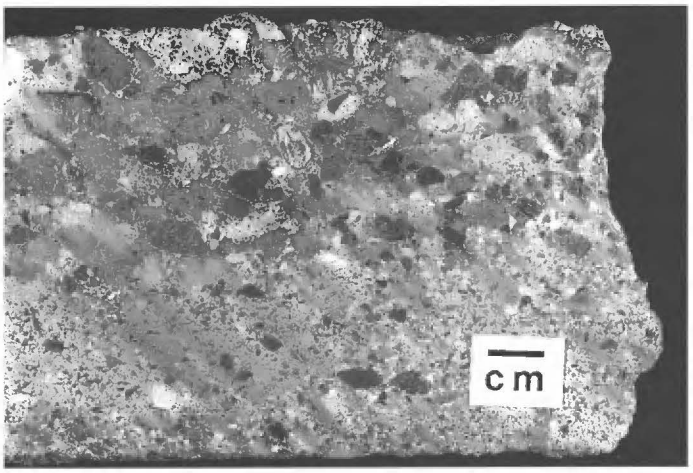


FIGURE 1.28. Heterolithic conglomerate (Fig. 1.26, sample location O) showing mixture of mostly darker andesitic clasts, and lighter rhyolitic clasts. Some rhyolitic clasts are densely welded ignimbrites.

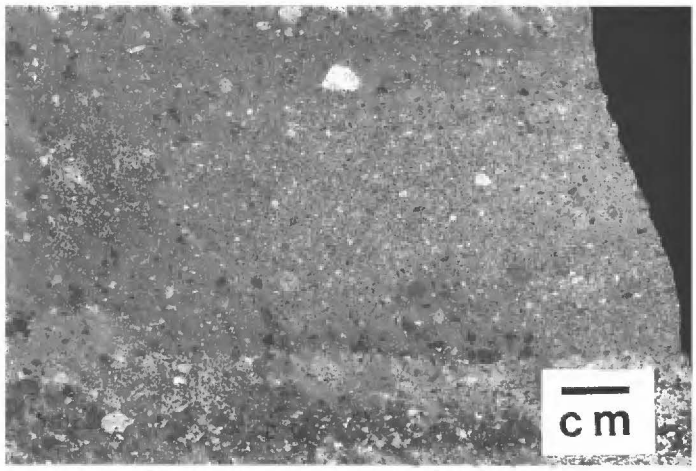


FIGURE 1.29. Contact between muddy debris-flow deposit and underlying coarse-grained sandstone (Fig. 1.26, sample location P). Note diffuse lighter-colored mixing zone at base of debris flow. Total thickness of debris-flow bed approximately 10 in.

Mountain (to the west) from the top of this mesa.

After stop return to vehicles and retrace route to US-60. 12.2

96.3 Stop sign at junction of FR-63 and US-60. **Turn left onto US-60. 0.2**

96.5 **Turn right onto Forest Road 6A.** Next stop is the lunch stop, below spectacular cliffs of the Sawtooth Mountains. For the next 1.9 mi route traverses andesitic sandstones of the volcaniclastic unit of Largo Creek of the lower Spears Group. **0.7**

97.2 Road crests hill of andesitic sandstones locally exposed to west. **1.2**

98.4 Road crests ridge line of basal Spears Group sandstones; view of central Sawtooth Mountains at 12:00 to 12:30. **0.1**

98.5 At north base of ridge line; bottom of hill. This slope break marks the approximate contact of the upper Eocene Baca Formation and the conformably overlying unit of Largo Creek. For purposes of reconnaissance mapping, where cliff-forming debris-flow deposits overlie Largo Creek type sandstones in the Sawtooth Mountains, this same contact with the Baca is mapped as the base of the Dog Springs Formation (Fig. 1.7). At this point we are on the Madre Mountain 7.5′ quadrangle just east of the Quemado 30′ x 60′ quadrangle mapped by Chamberlin et al., (1994b). The Madre Mountain quadrangle was mapped in reconnaissance by Chamberlin (1981b). **0.2**

98.7 Low roadcut on right in red sandstone of the Baca Formation, which contains abundant quartz in comparison to the nearly quartz-free beds of the overlying lower Spears Group. **0.6**

99.3 Good view of pinnacles and cliffs of Dog Springs Formation overlying moderately folded argillaceous andesitic sandstones in central Sawtooth Mountains at 12:00. Baca Formation underlies gentle wooded slopes at base of cliffs. **0.6**

99.9 Large pedestal, called Monument Rock, at 2:00 is capped by undeformed Dog Springs Formation with Baca locally exposed at the break in slope. Cliffs of Dog Springs Formation from 12:00 to 1:30 are focal point of Stop 3. From this vantage point these cliffs look deceptively like a simple layer cake. **0.3**

100.2 Road curves to left; road cuts and natural exposures of Baca Formation. **0.2**

100.4 Road sign indicates Sawtooth Mountain looking north and Sawtooth Mountains when looking south (Fig. 1.30). Area of Stop 3 is at 2:30. **0.2**

100.6 **Turn right on Forest Road 325.** Monument Rock to southeast at 1:00. **0.8**

101.4 **STOP 3. Make counter clockwise U-turn, as directed by flagpersons,** in open meadow. Park headed west for return to US-60. This is our lunch stop, timed for slightly after noon when these west-facing cliffs are out of the morning shadows. Spectacular soft-sediment structures well exposed within these cliffs of Dog Springs Formation are the focus of this stop.

The snaggle-toothed peak to the north-northeast attains a height of 8919 ft and the notched cliff to the

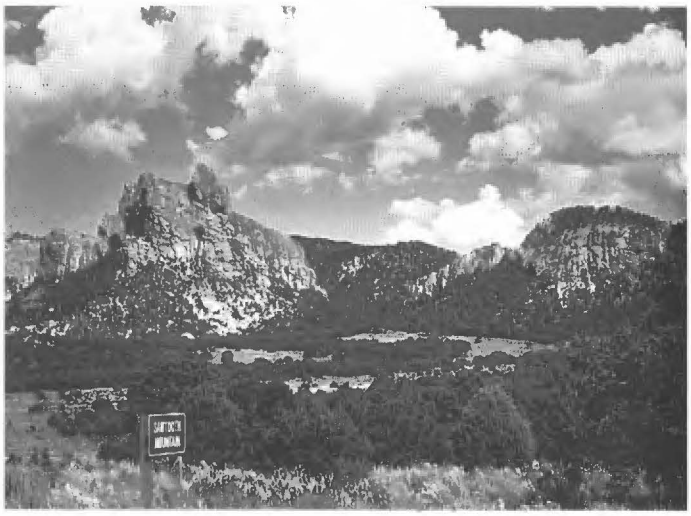


FIGURE 1.30. View of unnamed peaks and cliffs in the eastern Sawtooth Mountains from mile 100.4. Intensely folded andesitic sandstone beds, a low-angle fault, and overlying nearly vertical debris-flow deposits are all locally well exposed in these cliffs. This low-angle fault forms a distinct line (rising to left) approximately two-thirds of the way up the southern cliff, and projects across the canyon to just under the tooth-like spire. Gently dipping red beds of the Eocene Baca Formation. underlie the wooded slopes at the base of the cliffs.

east of it reaches 8761 ft. These unnamed cliffs and peaks are simply referred to here as peak 8919 and peak 8761, respectively. These bold cliffs of internally deformed Dog Springs Formation have not been mapped in detail. The following discussion is derived largely from Chapin and Cather (1989).

The early Ecocene (36.9 to 39.6 Ma) Dog Springs Formation consists primarily of andesitic to dacitic debris flows that commonly overlie and intertongue with argillaceous andesitic sandstones near its base (Cather, 1986; Cather and Chapin, 1989). Plastically folded sandstone beds, chaotic and steep dips in thick-bedded debris-flow deposits and numerous clastic injection dikes occur throughout the Dog Springs outcrop belt (Cather and Chapin, 1989). This outcrop belt forms a south-facing arc about 40 mi long and about 6-9 mi wide from the central Gallinas Mountains, west to Greens Gap (15 mi west of Datil). Estimated thicknesses of the total debris-flow section range from 1000 to 2000 ft (Cather, 1986), and the lower sandstones may be 100 to 200 ft thick where undeformed (e.g., Monument Rock). Regional mapping demonstrates that the underlying Baca Formation and overlying Chavez Canyon Formation and Datil Group ignimbrites dip gently to the south; thus regional deformation in the Dog Springs must be intraformational and of late Eocene age. Cather and Chapin (1989) emphasized that the Dog Springs debris-flows were deposited in an actively subsiding area between the Hickman and the Puerticito fault zones near the hydrographic center of the Baca Basin. The anomalously thick debris-flow sequence (>1000 ft) may have enabled fluidization of the sediments due to the presence of shallow groundwater. Rapid loading and overpressurization of unconsolidated sediments during accelerated debris-flow sedimentation, and basal shear by overriding debris flows, are possible mechanisms to trigger widespread soft-sediment deformation.

Similar soft-sediment deformation and liquefication structures of regional extent have been described in the Eocene Absoraka Volcanic Supergroup of Wyoming by Decker (1990). Decker aptly noted that historic regional soft-sediment deformation and liquefaction events have been triggered by major seismic shocks such as the 1811 New Madrid earthquake and the 1964 south-central Alaskan earthquake. Cyclic loading associated with earthquake vibrations was cited by Decker as the most likely cause for widespread liquefaction. Sudden deposition of lava flows, debris flows and explosive volcanic eruption are also possible triggers for liquefaction events. Thick intervals of rapidly deposited, low-permeability volcaniclastic sediments are particularly susceptible to liquefaction-related deformation. Following liquefaction of a sedimentary unit, the associated chaotic deformation patterns are primarily caused by gravitational collapse and diapirism (Decker, 1990).

As viewed from the southwest, the soft-sediment or liquefaction-related deformation visible in peak 8919 and peak 8761 can be divided into four structural zones or elements. From the base of the cliffs to the top, these elements include (1) a lower zone of undeformed Baca beds and basal Dog Springs fluvial sandstones



FIGURE 1.31. View to east-northeast of cliff-face below peak 8761 from Stop 3. Gently-dipping Baca Formation and light gray basal Dog Springs sandstones are poorly exposed in the lower slope on the right. Note intensely folded bedding in middle slope below gently south dipping fault surface (line between folded beds and massive looking top of cliff).

(Fig. 1.31), (2) a medial zone of intensely folded and sheared fluvial sandstones (Fig. 1.32) (3) a gently southeast-dipping low-angle detachment fault or decollement (Fig. 1.31) and (4) an upper zone (or plate) of steeply-dipping debris-flow deposits, of which only the massive-looking base of a single bed is visible in the upper cliff of peak 8761. The 60-70° east-northeast dip of these debris-flow deposits and truncation by the low-angle fault is much more impressive when viewed looking north from peak 8761 to the south face of peak 8919 (Fig. 1.33). This cross-section view shows all of the above-mentioned structural elements in one single frame. However, the crudely bedded and massive character of the debris-flow deposits is more safely observed and accessible in the notch of peak 8761 (Figs. 1.34, 1.35). The primary evidence of liquefaction at this stop is the zone of nearly recumbent and isoclinal folds in the medial zone below the low-angle fault. Clastic injection dikelets in flat lying dacitic-breccia beds about 1.2 mi northeast of here (Fig. 1.36) provide additional evidence of liquefaction in this area.



FIGURE 1.32. Close-up view of intensely folded fluvial sandstone beds of the lower Dog Springs Formation below low-angle fault in west-face of peak 8761. Noses of at least 8 nearly isoclinal folds can be recognized. Photograph from Cather and Chapin, 1989.

After lunch and a discussion of these spectacular cliffs, field conference attendees may hike to the notch in peak 8761 and get a close view of the folded beds, the low-angle fault and the nearly vertical debris-flow deposits above the fault. Alternatively, the south face of peak 8919 can be viewed by walking up the canyon between these cliffs. **After stop, return to vehicles and retrace route to US-60. 4.9**

106.3 Stop sign at junction of FR-6A and US-60. **Turn right and head west on US-60. 0.1**

106.4 Sandstones of the volcaniclastic unit of Largo Creek are locally exposed in low hills, in part the Airplane Hills, for next 2.8 mi. Recently reconstructed road cuts for next 8 mi consist of pulverized bedrock and smoothed soils that have been manicured and seeded so as to blend(?) into the environment. **2.1**

108.5 Leaving Cibola National Forest. Highway begins descent from the Airplane Hills into broad valley of Red Flats. **0.3**

108.8 Stream cut on right exposes light gray, medium- to coarse-grained argillaceous sandstone beds about 1-3 ft thick, separated by thin, pale red, mudstone drapes. Petrographic analysis of a medium-grained sandstone from this outcrop (Chamberlin and Harris, this volume; sample MP-62.4) shows that in decreasing order of abundance it consists of plagioclase, andesitic rock fragments, ferromagensian minerals (mostly hornblende and biotite with minor opaques) and very sparse quartz. Volume percentages of the above framework grains are 41.4, 40.8, 15.2 and 2.6 respectively. Low-birefringent clay minerals or zeolites (?) comprise about 10-15% of the matrix of this sandstone. **0.3**



FIGURE 1.33. View to north of peak 8919 from northwest flank of peak 8761. This cliff is approximately 500 ft high along the west face (left side). This spectacular cliff provides a cross-section view of a low-angle fault (rising to left) that juxtaposes steeply-dipping debris-flow beds (upper right) against strongly folded fluvial sandstones (note fold nose on lower right). Folded sandstones grade downward into essentially undeformed sandstone beds (lower left). Bedding in the upper plate appears to become more massive or obscure from right to left and the true character of the tooth-like spire is presently unknown.



FIGURE 1.34. Crudely bedded debris-flow deposits well exposed in notch of peak 8761; view to south. Beds dip approximately 70° and presumably are not overturned. Height of visible outcrop is about 50 ft.

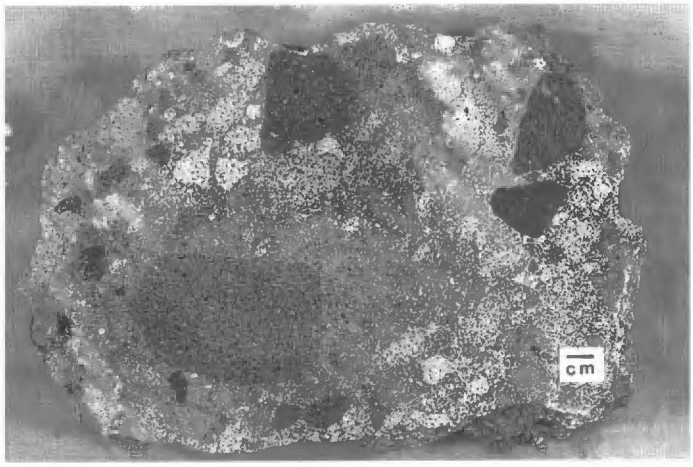


FIGURE 1.35. Slabbed andesitic debris-flow deposit from notch area of peak 8761. Note mixture of rounded and angular plagioclase-hornblende porphyry clasts floating in matrix of similar composition.

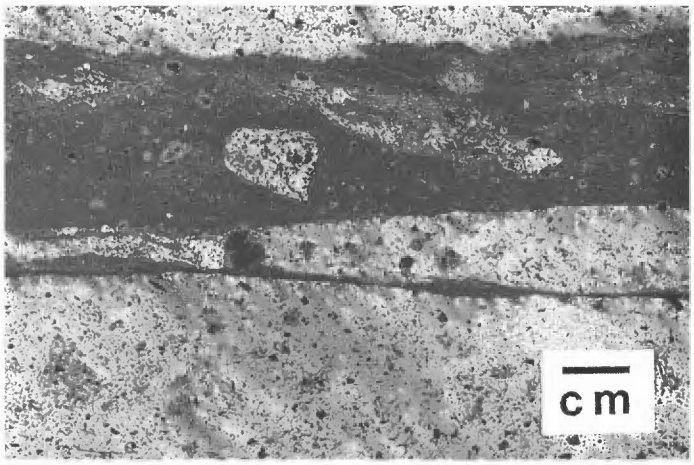


FIGURE 1.36. Clastic dikes within andesitic debris-flow breccia of the lower Dog Springs Formation. Sample collected near the head of Hay Canyon about 1.2 mi northeast of Monument Rock. Red muddy matrix of fluidal looking veinlets may have been partly derived from liquefaction of red mudstones in the uppermost Baca Formation, 200 ft stratigraphically below this site. Clastic dikes are subparallel to local bedding here, which is subhorizontal.

109.1 Rubble pile and small exposure on right used to be a revealing roadcut (Fig. 1.37). **0.2**

109.3 Good view of serrate Sawtooth Mountains to north. Highway descends across lower Spears Group/Baca Formation contact, which is locally concealed by Quaternary alluvium. Red Baca sandstones are poorly exposed on flanks of low hill at 1:00. **0.7**

110.0 Red soil in smoothed and seeded cut on right represents the Baca Formation. **0.2**

110.2 Milepost 61. Rounded hill at 1:00 provides good exposure of the base of the lower Spears Group overlying Baca Fm red beds. Local soft sediment deformation, expressed as low amplitude folds (~30 ft) in the Largo Creek sandstones might suggest that this is an angular unconformity, but only the *younger* volcaniclastic sandstone beds are visibly deformed. **0.3**

110.5 Manicured cuts in Baca Formation as indicated by red soil. **0.5**

111.0 Capitol Dome at 3:00 is the westernmost erosional monolith of the Sawtooth Mountains; it is formed by the Dog Springs Formation. **0.7**

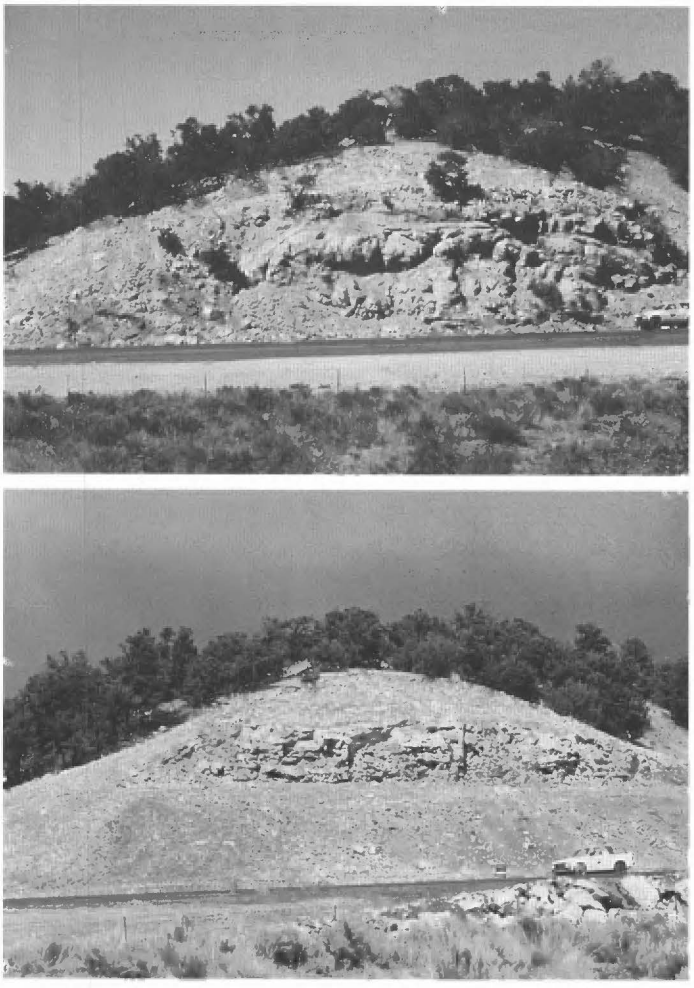


FIGURE 1.37. Roadcut on north side of US-60 in volcaniclastic unit of Largo Creek at west end of the Airplane Hills. Upper photograph shows old fashioned pre-1993 roadcut. Lower photograph shows new manicured roadcut at completion of construction project in July 1993.

111.7 Road to West Pie Town Tank on right. A regional seismic reflection profile, the ARMA Baca Basin Line No. 1, crosses US-60 here (see following minipaper). **0.3**

PRELIMINARY GEOLOGIC INTERPRETATION OF THE ARMA BACA BASIN SEISMIC REFLECTION PROFILE, NORTHEASTERN CATRON COUNTY, NEW MEXICO

Rodney M. Armstrong[1] and Richard M. Chamberlin[2]

[1]ARMA Geophysical Co. Inc., 907 N. Poplar St. Suite 230, Casper, WY 82601
[2]New Mexico Bureau of Mines and Mineral Resources, Socorro, NM 87801

Data of the ARMA Baca Basin seismic reflection profile No. 1 were acquired in 1987 as a speculative survey underwritten by Hunt Oil Company. A cooperative petroleum exploration venture of Shell (SWEPI), Elf Aquitane and BP was active in the region at that time (Kopacz, 1989; Garmezy, 1990). The location of the ARMA Baca Basin seismic line No. 1 and its relationship to regional structures are shown on Figure 1.38. The profile is approximately 47.1 mi long, mostly followed existing roads, and thus contains several moderate to tight bends. The seismic line is roughly parallel to the south-southwest regional dip in the Datil Mountains block.

The ARMA Baca Basin data were acquired using the Vibroseis source and recorded 30-fold. The recording system had 120 channels which recorded 24 geophones per group at a 110 ft group interval with a symmetric split spread. The four vibrators took 8 8-second sweeps each per vibrator point. The total array length was 220 ft and the vibrator point interval was 220 ft.

The data were processed by ARMA using a standard flow-through migration. For the purpose of this preliminary interpretation the original seismic sections were reduced by plotting every fourth trace and then filtered and phase rotated 90°. The generalized interpretation of the filtered data set has been reduced by an additional factor of about 5.5 times in order to produce a book-sized cross section (Fig. 1.39). Here, we describe the general construction of this preliminary pick section and discuss the regional structure and stratigraphy of northeastern Catron County as revealed by this line. Cenozoic extensional collapse (structural inversion) of a Laramide compressional zone near Alegres Mountain (AMF; Figs. 1.38, 1.39) and Laramide basement uplift southwest of Horse Mountain (DF, Figs. 1.38, 1.39) are significant aspects of this preliminary interpretation.

The major seismic reflection events picked on the seismic profiles have been identified by synthetic seismograms derived from the Shell (SWEPI et al.) No. 1 State, the Hunt Oil Co. No. 1-16 State and the Tenneco Oil No. 1 Federal petroleum exploration wells. For a description of the stratigraphy in the Hunt Oil Co. No. 1-16 well, see Broadhead (this volume). In addition to this well control, the top of the Baca and top of the Cretaceous (Crevasse Canyon Formation) were correlated to mapped outcrop locations. Angular unconformities at the top of the Cretaceous and the top of the Triassic were also identified by event terminations below the unconformities. In both cases, reflectors appear to terminate toward the south under these regional unconformities.

Strata of the lower Spears Group (upper Eocene) appear to be massive and produce no internal reflections. The top of the Baca Formation (middle to upper Eocene) is the shallowest continuous reflective horizon. Although there are numerous reflectors in the Baca, none of them are continuous across the section. Presumably this reflects the lenticular nature of fluvial sandstones and mudstones in the Baca Formation. In general, the top of the Baca looks parallel to the top of the Cretaceous section, but the top of the Cretaceous seems to have been a topographically rough surface that is filled in by the lower Baca. Assuming a uniform seismic velocity of about 10,000 ft/sec for the Baca Formation yields a thickness of approximately 2000 ft for this formation along US-60 near Pie Town. The calculated dip of the Baca Formation here is approximately 100 ft/mi to the south-southwest.

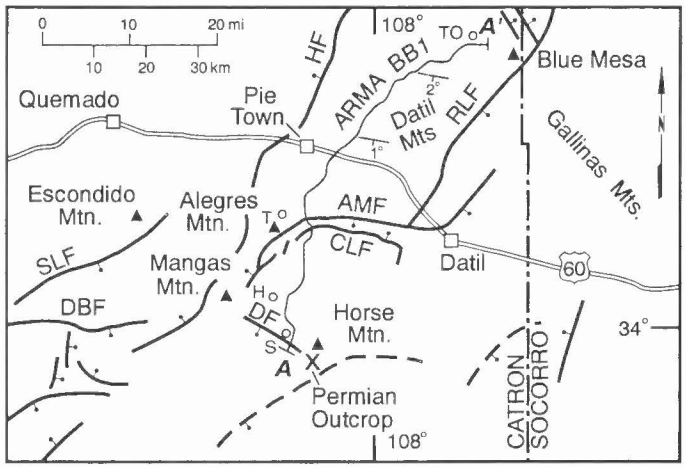


FIGURE 1.38. Location map of ARMA Baca Basin seismic reflection line No. 1 (A-A') and its relationship to regional structures in northeastern Catron County. RLF = Red Lake fault, HF = Hickman fault, AMF = Alegres Mountain fault, CLF = Cox Lake fault, DF = Dutch Oven Pass fault zone, DBF = Cañon del Buey fault, SLF = Spur Lake fault. S, H, T, and To indicate the approximate locations of the Shell (SWEPI et al.) No. 1 State, Hunt Oil Co. No. 1-16 State, Tenneco Oil No. 1 Federal, and Transocean Oil No. 1 Santa Fe RR petroleum exploration wells, respectively.

The unconformity at the top of the Cretaceous is tightly constrained in the Shell (SWEPI et al.) No. 1 State and the Hunt Oil Co. No. 1-16 State wells. It is clearly a major erosional surface associated with the Cretaceous section thinning fairly rapidly to the south. The exact event on the seismic section is difficult to identify but the angular unconformity between the Cretaceous and Baca is obvious. Numerous event terminations below the unconformity are obvious on the southern third of the line. The Baca reflectors and top of the Cretaceous dip rather steeply adjacent to the Alegres Mountain (AMF) and Cox Lake (CLF) normal faults. Rapid thinning of the Cretaceous section to the south across this fault zone demonstrates that the southern blocks were uplifted in a Laramide reverse-fault zone, prior to Baca deposition in middle Eocene time (Cather and Johnson, 1984). Lateral-slip may have occurred along this Laramide reverse-fault zone but cannot be demonstrated here.

The top of the Triassic (Chinle Formation) appears to be an erosional unconformity with the total Triassic section thinning to the south. It seems to be a rough surface that was overlain and filled in by the lower Dakota Formation, much like the basal Tertiary unconformity.

The San Andres event (top of Permian San Andres and Glorieta Formations) is not as obvious as it should normally be for a carbonate unit. It may be that the top of the San Andres is an erosional surface that is irregular and karsted. The San Andres event does appear to be more continuous north of US-60.

The Yeso event is a fairly easy pick and is closely tied to the Shell State No. 1 and Hunt well. The Tenneco well is also in reasonably good agreement, but the San Andres to Yeso interval is thicker on the seismic than indicated in the Tenneco well. This interval also thickens to the north. Several basement structures and faults appear to terminate in the San Andres-Yeso interval, suggesting a period of tectonic deformation in the lower to upper Permian (ancestral Rocky Mountains deformation?). Comparison of the Trans Ocean Well data and the seismic profile suggests the presence of a late Permian normal fault near the northeast end of the line. A strong lenticular reflection in the Yeso interval near the Hunt well is most likely equivalent to the diorite sill that was intersected in this well (Broadhead, this volume).

The Abo event is nearly conformable to the unconformity at the top of the Precambrian. Numerous changes in the seismic character of the whole Yeso–Abo interval occur along the section between the basement and the top of the Yeso. These changes might reflect variations in depositional environment and the influence of late Paleozoic structures.

Although tentative, the basement reflection at the southern end of the line appears to rise considerably to the south across the west-northwest-trending normal fault zone mapped by Ratté et al. (1991) near Dutch Oven Pass (Dutch Oven fault, DF, on Figs. 1.38, 1.39). If this is correct, the Dutch Oven fault zone may also have been a Laramide reverse fault zone that has partly collapsed under extension in Neogene time. Local Laramide uplift to the south would help explain the general rise in the basement south of the Hunt Oil Co. No. 1-16 well, and exposures of Permian rocks on the southeast flank of Horse Mountain.

112.0 Resistant outcrops of Largo Creek sandstones form low bluffs at 10:00 and 11:00; wooded slopes at base of bluffs are underlain by poorly exposed Baca Formation. Bare knob of Baca Formation at 1:30. **1.3**

113.3 Road sign, (well below crest of hill) declares that this is the Continental Divide, elevation 7796 ft. Apparently for next 650 ft water runs up hill to west, a local phenomenon presumably limited to the Pie Town area. **0.1**

113.4 Road crests at Continental Divide. **0.8**

114.2 Milepost 57. Forested hillside at 1:00 hides the Pie Town antenna of the VLBA. **0.1**

114.3 Road to Pie Town VLBA antenna on right. Visitors are welcome to tour this site, locally supervised by Kelly Gatlin and associates. **0.7**

115.0 Crest of hill in downtown Pie Town. Candelaria's Trading Post ahead on right carries on tradition of serving pie, mainly to tourists. Sign at entrance to park on left shows mountain-sized pies of the good old days. Pie Town was established by World War I veteran, Clyde Norman, who homesteaded here (ca. 1918) and began baking pies and serving coffee to local ranchers. Thus Norman's settlement was to become known as Pie Town. Hard times of the great depression and futile attempts at pinto bean farming in the Pie Town area were recorded by Farm Security Administration photographer Russell Lee (Smith, 1983). Slow, prepare for left turn ahead. **0.6**

115.6 **Turn left and head south on unpaved county road to Greens Gap.** NM-603 on right goes to Tres Lagunas and on to Grants. **0.2**

115.8 Four-way stop sign in west Pie Town. Continue straight ahead on county road. **0.1**

115.9 Hilltop to right is held up by small basaltic-andesite dike, which terminates just south of here as road curves to right. This dike is simply referred to here as the "small" Pie Town dike. It lies east of the larger dike referred to as "the Pie Town" dike. **0.2**

116.1 Late Oligocene (27.7 Ma) Pie Town dike of basaltic andesite composition forms ridge line from 1:00 to 2:30 (Laughlin et al., 1979). Volcaniclastic sandstones of the unit of Largo Creek are intermittently preserved here along the walls of the dike; Baca Formation underlies the gentle wooded slopes. A broad open syncline is partly visible in the Largo Creek beds from 3:00 to 4:00; north-northwest-dipping beds at 3:00 define the south limb of this syncline. Regional dips of Largo Creek beds in the Pie Town-Quemado area are about 2° to the south. Gentle open folds and minor faults, however, occur locally in the Largo Creek beds between Pie Town and

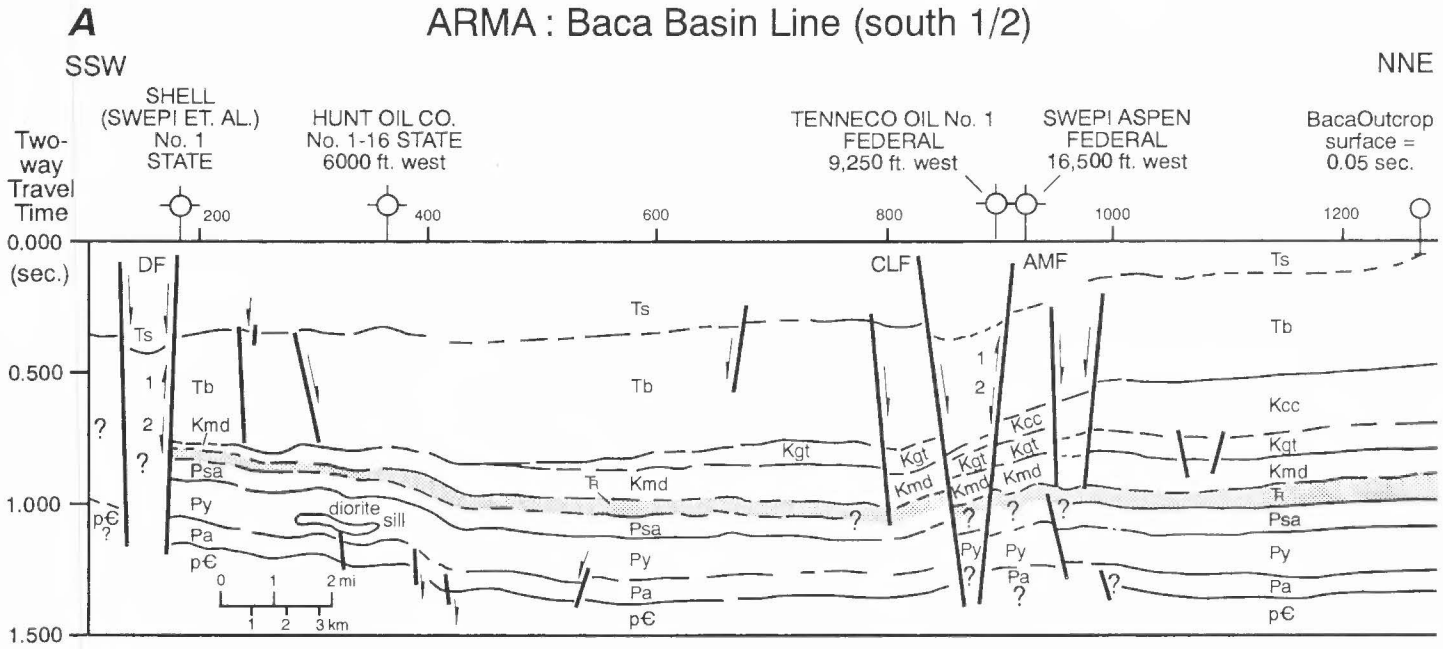


FIGURE 1.39. Generalized geologic section along the ARMA Baca Basin seismic reflection profile (A-A'; Fig. 1.38). Approximate vertical exaggeration in the Tertiary section is 5.5; in Paleozoic section vertical exaggeration decreases to about 3.7. Formations identified are: Ts = lower Spears Group, Tb = Baca Formation, Kcc = Crevasse Canyon Formation, Kgt = Gallup and Tres Hermanos Formations, Kmd = Mancos and Dakota Formations, TR = Chinle Formation, Psa = San Andres

Quemado Lake. The tectonic significance of these minor isolated(?) structures is presently uncertain; they may be contemporaneous with soft-sediment structures in the Dog Springs Formation, or they may reflect late Laramide deformation. **0.1**

116.2 Road to Pie Town landfill ahead on right. **0.1**

116.3 Cattle guard; entering W-Bar Ranch. **0.4**

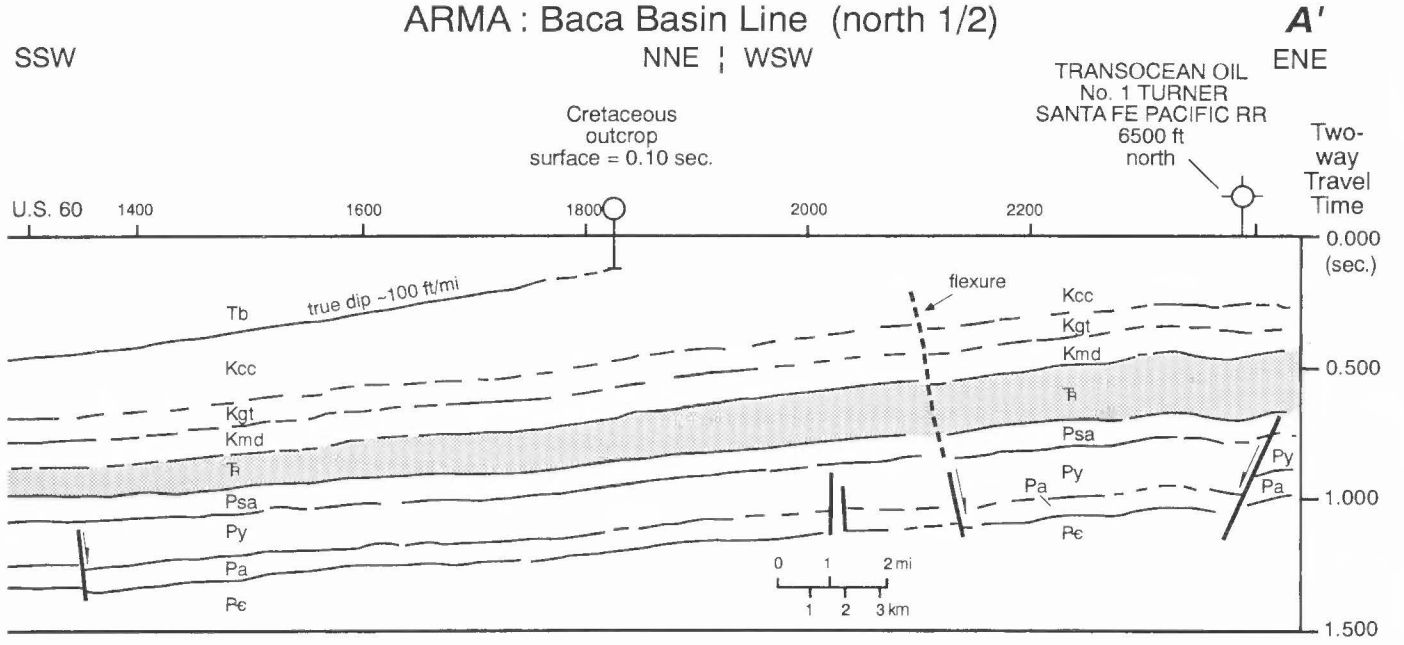
116.7 Depression east of dike at 11:00 is Bright Lake (cattle tank) near the site of Stop 4. The Pie Town dike forms a great wall-like outcrop for at least 6 mi to the south of Pie Town (Fig. 1.40). North of Pie Town the late Oligocene dike disappears under the Miocene Fence Lake Formation in the Omega Basin syncline (Fig. 1.7). **0.2**

116.9 Note gently south-dipping Largo Creek beds across valley at 9:00 to 10:00. **0.3**

117.2 Road crosses through gap in ridgeline of dike. Remnants of unit of Largo Creek are present on the



FIGURE 1.40. Aerial view along the Pie Town dike, looking north-northwest. Site of Stop 4 at Bright Lake in open area on east side of dike. Pie Town at right center. White calcrete ledge above end of dike on left marks top of the Fence Lake Formation on the downthrown northwest side of the Hickman fault.



Limestone and Glorieta Sandstone, Py = Yeso Formation, Pa = Abo Formation and pC = Precambrian basement rocks. Arrows along faults indicate inferred Laramide component of reverse movement (1), followed by Neogene component of normal movement (2). Abbreviated designations of faults are explained in caption to Figure 1.38.

east side of dike; Baca Formation is wall rock (host rock) on west side. The contact between these units is near road level in the gap. **0.1**

117.3 Volcaniclastic unit of Largo Creek forms ledges on skyline at 2:30. **0.1**

117.4 Sandstone of Baca Formation exposed in bar ditch on left. Red Baca-derived soils on hillside to left are generally shown as outcrop on regional maps (Fig. 1-7). **0.2**

117.6 **Turn left** and head east on road to Bright Lake Dam to view wall-like exposures of the Pie Town dike and adjacent country rock. This is private land of the W-Bar Ranch. Permission to visit this locality may be obtained at the W-Bar headquarters 2 mi south of here on the west side of the Greens Gap road. **0.2**

117.8 **STOP 4. Follow directions of flagpersons, make U-turn in flat to be headed west for return to US-60.** Walk to Bright Lake Dam on east side of the Pie Town dike. The purpose of this stop is to discuss the petrology and tectonic significance of the Pie Town dike and its relationship to other regional structures such as the Hickman fault zone. Conference participants may then climb the east flank of the dike to examine the chilled dike contacts and hornfelsed blocks of Baca Formation and Largo Creek-type sandstone within the dike. **All observers should be cautious and not get too close to the 30-ft-high wall on west side of dike.**

The Pie Town dike at Bright Lake forms a large resistant wall (Fig. 1.41) where it cuts poorly exposed Baca Formation and overlying andesitic sandstones of the volcaniclastic unit of Largo Creek (upper Eocene). The dominant strike of the 15-20-ft-wide basaltic andesite dike is N32°W and it dips approximately 85°NE. Locally, the dike makes a sharp bend to the right just north of the Bright Lake Dam. Wall rocks consisting of baked (locally reddened) Largo Creek sandstones are well exposed on the east side of the dike near the bend. This bend represents a minor deviation in this magma-filled tension fracture that is approximately 45 mi long; and presumably just as deep.

A sample of the Pie Town basaltic-andesite dike collected about 3 mi to the northwest provided a K-Ar whole rock age of 27.67 ± 0.59 Ma (Laughlin et al., 1979). This aphyric basaltic andesite, lacking in olivine microphenocrysts, contains about 53.5% SiO_2 and is distinctly higher in TiO_2 (2.26%) and P_2O_5 (1.6%) than



FIGURE 1.41. View along the Pie Town dike at Bright Lake. The chilled eastern margin of the nearly vertical basaltic andesite dike is locally well exposed where it bends sharply to the right adjacent to a small light-colored knob of baked andesitic sandstones in the volcaniclastic unit of Largo Creek. The dike contains a 3x3 m block of hornfelsed quartzo-feldspathic Baca sandstone just left of the Largo Creek knob. Ledge-forming Largo Creek sandstones on horizon; wooded slopes are underlain by Baca Formation. Largo Creek-Baca depositional contact is discontinuously exposed near mid-slope on flanks of wall-forming dike.

most other late Cenozoic basaltic andesites in the region (Laughlin et al., 1983). Xenocrystic quartz (largely resorbed) is a significant component (~ 0.5%) of the dike at Bright Lake.

The Pie Town dike is one of a group of three long north-northwest-striking late Oligocene basaltic andesite dikes that cut across the southeast margin of the Colorado Plateau. The great length, similar composition (high TiO_2; 51-53% SiO_2) and analytically equivalent K-Ar ages of these subparallel dikes has led to the conclusion that they formed orthagonal to the regional least principal horizontal stress (LPHS=S55-60°W) in late Oligocene time (Laughlin et al., 1983). More recent investigations using isotopically-dated dikes to determine secular variations in LPHS have documented a shift from west-southwest directed extension to west-northwest extension during a regional magma lull in early Miocene time (~ 22-17 Ma; Aldrich et al., 1986; Baldridge, et al., 1989).

Based on apparent similarity in age and chemical composition Laughlin et al (1983) suggested that basaltic andesite lavas of the Squirrel Springs Canyon Andesite (Rhodes and Smith, 1976) might be genetically linked to the Pie Town dike. More recent observations show that the suggested Pie Town-Squirrel Springs link is unlikely and that the basaltic andesite lavas of the Bearwallow Mountain Andesite are a more likely candidate to be the extrusive equivalent of the Pie Town dike, if any exists.

Lavas of the Squirrel Springs Canyon Andesite are texturally distinct turkey-track flows that contain abundant tabular plagioclase phenocrysts as much as 3 cm long. Regional mapping has also shown that the source area of this unit must lie somewhere to the southwest of Mangas Mountain and Escondido Mountain. Since the Pie Town dike lies to the northeast of both mountain ranges, it seems physically impossible for the Pie Town dike to be a source of the Squirrel Springs Canyon Andesite.

Aphyric to phenocryst-poor basaltic andesite lavas of the Bearwallow Mountain Andesite in the Mangas Mountain area *could* be an eruptive equivalent to the Pie Town dike. However, the Bearwallow lavas appear to be somewhat younger (26.1 ± 0.1 Ma) and lower in TiO_2 (1.14%, Ratté, 1989) than the Pie Town dike. A similar, but much shorter 0.6 mi basaltic-andesite dike is present on Escondido Mountain, where it cuts an ash bed equivalent to the 28.6-Ma Vicks Peak Tuff (Fig. 1-7). This dike could have been a feeder for the adjacent Bearwallow flows.

Regional mapping has shown that the Hickman fault zone offsets and downwarps the Pie Town dike. The dike is buried by the Fence Lake Formation where it is preserved in the Omega basin syncline between Pie Town and Adams Diggings. Near Adams Diggings the Pie Town dike appears to transect the west limb of a gently north plunging Laramide anticline. Likewise, the Fence Lake Formation unconformably overlaps the west flank of this Laramide anticline. The Pie Town dike terminates to the north near Fence Lake, which is also near the south end of the southwest facing Laramide Atarque monocline (Anderson, 1987). As interpreted by Laughlin et al. (1983), southwesterly directed dilation of the Pie Town dike probably represents a significant relaxation of northwest-directed Laramide compressional stress in late Oligocene time.

Return to vehicles and retrace route to US-60. 2.2

120.0 Stop sign at junction of Greens Gap road and US-60 in west Pie Town. **Turn left and head west on US-60. 0.8**

120.8 Roadcuts on right expose the "small" Pie Town dike. Red sandstones of the Baca Formation are locally bleached adjacent to this 6-ft-wide dike that dips about 80° to the southwest. The "small" Pie Town dike has been sampled for paleomagnetic analysis and $^{40}Ar/^{39}Ar$ age dating by W. C. McIntosh, R. M. Appelt and R. M. Chamberlin. An isotopic age is not available, but the paleomagnetic data indicate that the "small" Pie Town dike was downwarped and rotated (about a horizonal axis) with the adjacent Baca beds in post-late Oligocene time. **0.5**

121.3 Highway passes through water gap in the Pie Town dike at Wyche Draw. The dike is relatively well exposed south of the highway, where it cuts locally bleached and reduced (greenish) Baca Formation sandstones. It is about 15 ft wide here and dips approximately 85° to the northeast. **0.6**

121.9 Baca Formation in cut on left. Ridge on skyline from 12:00 to 1:00 is designated as the "Top of the World" on the Pie Town 7.5′ quadrangle. Although not quite as impressive as the Himalayas, this ridge line marks the top of the Fence Lake Formation on the downthrown northwestern side of the Hickman fault (Fig. 1-7). A subhorizontal laminar calcrete about 6 ft thick locally caps this ridge and has been quarried for road metal. **0.5**

122.4 Highway descends onto alluvial valley floor of Chavez Draw and crosses projected trace of the Hickman fault zone that locally strikes northeast as opposed to north-northeast for the overall fault trend. Northeast of here the Hickman fault zone offsets of the Pie Town dikes (100 to 200 ft), in both a right lateral and a left lateral sense. Stratigraphic displacement and northwesterly down-warping of Miocene Fence Lake beds here at Pie Town is estimated to be about 1000 ft, well in excess of the observed offsets. Similar apparent horizontal offsets of the late Oligocene dike at Lehew (aka Hickman) occur along the Hickman fault zone approximately 12 mi northeast of here. Some researchers (Aldrich and Laughlin, 1984; Baldridge et al., 1983) have interpreted the apparent horizontal offsets of the 27.3-Ma basaltic andesite dike at Lehew (Laughlin et al., 1979) as the expression of left-lateral strike slip. Regional mapping (Chamberlin et al., 1994b), however, has shown that the Hickman fault zone has a post-28-Ma-stratigraphic throw of as much as 2000 ft (down to the west) near Mangas. Rough estimates of the down-to-west stratigraphic throw at Lehew range from 800 to 1600 ft depending on the regional dip used in cross sections to determine the offset of the base of the Baca Formation. It should be noted that *pure* normal dip slip of Neogene age could have produced the apparent 500 ft of left offset (total of three offsets) of

the nearly vertical dike (N28°W, 85°NE) at Lehew, because the Hickman fault zone intersects the dike at an acute angle of about 53°. The Hickman fault zone here strikes N25°E; thus a pure dip-slip normal fault vector would plunge to N65°W and lie to the left of the dike trend (N28°W). Assuming a pure dip-slip normal displacement for the Hickman fault zone and a dip of 60° to the west-northwest; the observed 500 ft of apparent left offset at Lehew would require a dip-slip displacement of 1600 ft. A few observations of essentially dip-slip slickensides on post-Oligocene faults near Mangas and the above constraints near Lehew suggest that the Neogene displacement of the Hickman fault zone is essentially dip-slip; however, a minor component of left-oblique slip remains a possibility. A previous estimate of Neogene net slip on the Hickman zone by Chamberlin (1993) was incorrect.

Laramide reverse displacement on the Hickman fault zone, upthrown on the west, has been previously recognized (Cather and Johnson, 1984, Cather, 1989) by differences in thickness of the Baca Formation between Quemado (600 ft; Guilinger, 1981) and the Datil Mountains (1875 ft, Chamberlin, 1981b). More recent thickness data for the Baca Formation at Adams Diggings (0-400 ft; Chamberlin et al., 1994b) and near Pie Town (2000 ft; Armstrong and Chamberlin, this road log), both of which lie closer to Hickman fault zone, substantiate the previous interpretation.

Laramide deformation patterns (contractional strain) in the Zuni Mountains region (Chamberlin and Anderson, 1989; Chamberlin, 1991) also suggest that a significant component (>0.6 mi) of Laramide right-lateral slip occurred on the Hickman zone. **0.5**

122.9 Highway crosses Chavez Draw on upper Quaternary alluvial valley fill. **0.5**

123.4 Flat-topped Alegres Mountain on skyline at 9:00. Low mesa, with light gray landslide scar on its side at 10:00, is capped by basaltic boulder conglomerates of the middle to upper Miocene Fence Lake Formation unconformably overlying upper Eocene volcaniclastic unit of Largo Creek, (light gray beds in scar). Main trace of Hickman fault offsets the Fence Lake caprock to right of the landslide scar. The total post-Fence Lake displacement across two down-to-the-west faults of the Hickman zone in this area is about 500 ft. **0.5**

123.9 Volcaniclastic unit of Largo Creek forms small hill just north of highway. Petrographic analysis of framework grains in the medium-grained volcaniclastic sandstone yields 74.4% plagioclase, 14.4% andesitic rock fragments, 8.8% Fe-Mg minerals (hornblende, biotite and opaques), and 2.8% quartz (Chamberlin and Harris, this volume, sample MP-51.8). Clay minerals comprise about 10-15% of the matrix of this argillaceous sandstone. **0.5**

124.4 Low cuesta in foreground at 10:00 is composed of pebbly conglomeratic sandstones of the lower Fence Lake Formation dipping about 5-10°. At least 300 ft of lower Fence Lake beds are exposed here. An abrupt facies change occurs at Thaeger Draw on the south end of this cuesta. North of Thaeger Draw the lower Fence Lake beds consist of trough-cross-bedded, pebbly conglomerates and sandstones. Pebbles are mostly hornblende plagioclase porphyry dacites (Dog Springs type) mixed with less abundant basaltic andesite and rare ignimbrite clasts. South of Thaeger Draw the Fence Lake Formation is a subhorizontal basalt boulder to cobble conglomerate about 65 to 100 ft thick. Both facies unconformably overlie the unit of Largo Creek in this area. These facies relationships reflect different stream systems and different provenance for the Fence Lake Formation. Pebbly lower Fence Lake sediments were derived from the Datil Mountains area, and bouldery beds south of Thaeger Draw were derived from Alegres Mountain. A preliminary structure section in the Pie Town area (Chamberlin et al., 1994b) suggests that the lower Fence Lake pebble conglomerates may be locally 600-900 ft thick adjacent to the downwarped western flank of the Hickman fault zone. These moderately tilted lower Fence Lake beds near Pie Town may be somewhat older than the middle to upper Miocene Fence Lake conglomerate described by Lucas and Anderson (this volume) in the area southwest of Quemado. **0.2**

124.6 Roadcut on right in pale red muddy siltstones in unit of Largo Creek. **0.4**

125.0 Highway crosses approximate basal contact of the Fence Lake Formation. This regional unconformity is well exposed along the road to "Under the Mesa Well" in the Tres Lagunas 7.5′ quadrangle about 7 mi to the north. **0.1**

125.1 Lower Fence Lake Formation poorly exposed in roadcut on right. **0.1**

125.2 Lower Fence Lake pebble conglomerates and conglomeratic sandstones are well exposed in the upper bench of the road cut on the right. Note 25° dip. Pebble imbrications indicate westerly to northwesterly paleoflow. Hornblende-dacite clasts are mixed with basaltic andesites and rare ignimbrite clasts. **0.3**

125.5 Projected trace of north-northwest-trending, down-to-the-west Mangas fault (Fig. 1.7) passes under alluvial valley fill of Tres Lagunas Draw here. **0.4**

125.9 Roadcut on right is in poorly consolidated pebbly sandstone of the Fence Lake Formation; bedding attitude not discernible here. **0.9**

126.8 Milepost 49. Escondido Mountain at 10:30 on the skyline is capped by upper Oligocene Bearwallow Mountain Andesite of the Mogollon Group. **1.0**

127.8 Low roadcuts for next 1.2 mi are in light gray, poorly- to moderately-consolidated, pebbly sandstones of the upper Fence Lake Formation; bedding is approximately horizontal. **1.1**

128.9 Piñon-juniper covered hills on skyline from 1:00 to 2:00 are underlain by Fence Lake Formation. **0.1**

129.0 Highway begins descent onto Pliocene to early Pleistocene alluvial deposits of the Quemado Formation (Cather and McIntosh, and McIntosh and Cather, this volume). Within this area of the topographic Omega Basin (not to be confused with the Omega basin syncline), Quemado Formation deposits are derived from and inset against the Miocene Fence Lake Formation. Quemado deposits are generally poorly consolidated, often buff colored, and occupy lower levels in the landscape. Clast compositions are essentially the same as in the Fence Lake Formation, which is their primary source. **0.6**

129.6 Low roadcut on right in sandy Quemado Formation alluvium. **0.2**

129.8 Milepost 46. Cuestas that slope west and east at 2:30-3:00 respectively are capped by Fence Lake Formation. Knob in middle is undated late Miocene(?) basaltic volcanic neck of Techado Mountain. Cuestas may define a Pliocene(?) anticlinal axis near Toms Rock, 2.5 mi west of Adams Diggings. Upper Eocene volcaniclastic sandstones of the unit of Largo Creek are discontinuously exposed on the flanks of these mesas between Adams Diggings and Mariano Springs. One resistant andesitic debris flow is present within the unit of Largo Creek, 1.2 mi west of Toms Rock. It forms a distinctive elongated pedestal resting on typical Largo Creek sandstone beds (Fig. 1.42). Judging from its elongation, a distant volcanic source to the south or southeast seems likely. **0.4**

130.2 Grassy plains along Mangas Creek from 9:00 to 10:00 are underlain by Quemado Formation. Mangas Mountain, on the horizon at 9:00 was probably an eruptive center for the Bearwallow Mountain Andesite. **0.4**

130.6 Low cuts on right and left in sandy Quemado Formation. **0.5**

131.1 Windmill for well on right produces fresh water probably from saturated Fence Lake Formation conglomerates that project under the Quemado Formation here (see minipaper by Newcomer in Second-Day road log). **0.2**

131.3 Low roadcuts in medium-grained loamy sand. Landscape position suggests that this is an upper Pleistocene terrace deposit of San Ignacio Creek, which locally parallels the south side of US-60. **1.4**

132.7 County road to Mangas on left. First-Day road log overlaps with miles 38.2 to 47.5 of Second-Day road log for next 9.3 miles. The more detailed discussions of features along this stretch are in the Second-Day log. **1.1**

133.8 Milepost 42 at Omega Village limit. **1.1**

134.9 Roadcuts in sandy Quemado Formation alluvium. **0.3**

135.2 Road rises onto Fence Lake Formation. **0.4**

135.6 Site of Stop 1 on second day is at top of hill behind borrow pit at 1:00. **0.2**

135.8 Milepost 40. Begin descent of steep grade into valley of Rito Creek and Escondido Creek. Roadcut ahead on right exposes Fence Lake Formation unconformably overlying sandstones and mudstones of the volcaniclastic unit of Largo Creek. **1.2**

137.0 Roadcut on left exposes the Quemado Formation unconformably on volcaniclastic unit of Largo Creek. **0.7**

137.7 Cuts in the volcaniclastic unit of Largo Creek. **0.3**

138.0 Roadcut on left in pebbly stream sand of early Pleistocene to late Pliocene age. **0.2**

138.2 Round knob on right is the volcaniclastic unit of Largo Creek (upper Eocene). **1.0**

139.2 Cut on left in Quemado Formation. **0.5**

139.7 Cliffs of Fence Lake Formation capping lower Spears Group, 9:00 to 10:00. **1.2**

140.9 Old town of Quemado on left. Well-exposed Fence Lake Formation over slope-forming lower Spears Group on horizon (Fig. 1.43). **0.2**

141.1 Roadcuts on right in upper Baca Formation. **0.2**

141.3 Junction, NM-36 to Fence Lake on right. **Continue straight ahead on US-60.** Boundary stratotype for the base of the volcaniclastic unit of Largo Creek (upper Eocene) conformably overlying the Baca Formation (middle to upper Eocene) is well exposed on a low peak above the Quemado Community Cemetery 1.3 mi north-northeast of here. **0.1**

141.4 Quemado Post office on left. Downtown Quemado has changed some in the last 60 years (Fig. 1.44) but still has good food, comfortable lodging, gas and friendly Quemadans. **0.6**

142.0 Junction with NM-32 on left. **Turn left and head south on NM-32.** Road follows valley of Largo Creek for next 12 mi. Mesas on skyline at 12:00 and 1:00-4:00 are capped by commonly cliff-forming basaltic conglomerates of the Fence Lake Formation. The base of the Fence Lake Formation is a regional angular unconformity. The underlying Baca Formation and



FIGURE 1.42. Singular debris-flow deposit forms pedestal in the volcaniclastic unit of Largo Creek west of Adams Diggings near Tom's rock, in SE¼, sec. 25, T3N, R15W.

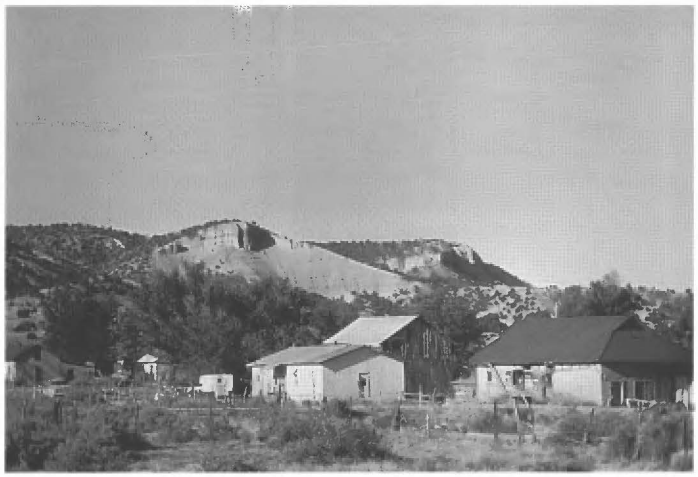


FIGURE 1.43. Cliff-forming conglomerate of Miocene Fence Lake Formation unconformably overlies upper Eocene slope-forming beds of the volcaniclastic unit of Largo Creek to create a geologic backdrop to old east Quemado in foreground.



FIGURE 1.44. A great depression era scene of downtown Quemado in February 1933; looking east-northeast. Building of Engle Mercantile Co. and Tavern remain standing. Photograph courtesy of Jimmy and Irene Jaramillo, El Sarape Cafe.

Spears Group strata near Quemado generally dip about 2° to the south-southeast; thus the Fence Lake rests on progressively older strata as it extends northward from source areas near Escondido Mountain and Agua Fria Mountain. The Fence Lake Formation is commonly 60-80 ft thick where well exposed in landslide scars on these mesa flanks. **0.3**

142.3 Low hill at 10:30 exposes red Baca Formation on its flanks, capped by Quemado Formation gravels. Landslide scar on mesa point exposes light gray andesitic sandstones of the volcaniclastic unit of Largo Creek. The depositional contact of the unit of Largo Creek on Baca Formation is approximately located at the foot of the mesa. **1.3**

143.6 Road curves to left and crosses concealed basal contact of the volcaniclastic unit of Largo Creek near here. Axis of Largo Creek valley ahead at 12:15; route on middle(?) to late Pleistocene valley fill for next 5 mi. **0.4**

144.0 Dissected graded surfaces, at 10:00 and 2:00, about 65-130 ft above the valley floor, are underlain by Quemado Formation piedmont gravels mostly derived from the Fence Lake Formation and lower Spears Group. Similar remnants of Quemado Formation can be observed in the middle landscape position along Largo Creek valley for the next 9.5 mi. **0.5**

144.5 Crest of Escondido Mountain (elev. 9854 ft,) on skyline at 10:30 consists of aphanitic basaltic-andesite lavas of the Bearwallow Mountain Andesite (26.1 Ma), disconformably overlying 28.05-Ma Bloodgood Canyon Tuff (not visible from here) and porphyritic Squirrel Springs Canyon Andesite, which locally forms 200 ft-high cliffs on the shoulders of Escondido Mountain. Vicks Peak Tuff (28.56 Ma) locally underlies the Squirrel Springs Canyon Andesite. All of these Oligocene volcanic units are assigned to the Mogollon Group (Cather et al., this volume).

Two newly named informal volcaniclastic units are locally well exposed along the upper reaches of Cañon del Leon, the deep cut below the west shoulder of Escondido Mountain. Upper Cañon del Leon is designated as the type section for approximately 600 ft of pumiceous and tuffaceous sandstones and intercalated andesitic conglomeratic sandstones of the volcaniclastic unit of Canyon del Leon (new name, Chamberlin and Harris, this volume). Sanidine phenocrysts from pumice in basal and uppermost pumiceous siltstones (presumably fresh and floating when deposited) have yielded $^{40}Ar/^{39}Ar$ ages of 35.33 to 34.17 Ma and imply this new map unit is of late Eocene age. The unit of Cañon del Leon conformably overlies andesitic sandstones and minor pumiceous sandstones of a 200-ft-thick transition zone at the top of the Largo Creek. As much as 800 ft of buff, massive planar-bedded to high-angle cross-bedded sandstones of the sandstone of Escondido Mountain (new name, Chamberlin and Harris, this volume) appear to disconformably(?) overlie the volcaniclastic unit of Cañon del Leon. Uniform grain size (fine- to medium-grained sandstone) and high-angle cross beds, generally facing east, indicate that the sandstone of Escondido Mountain is largely an eolian deposit. Ignimbrites of the Vicks Peak Tuff and Bloodgood Canyon Tuff locally occur as paleovalley fills within the sandstone of Escondido Mountain. Near Mangas, the 31.65-Ma Caballo Blanco Tuff occurs just 60 ft above the base of the sandstone of Escondido Mountain. These data indicate that sandstone of Escondido Mountain is Oligocene in age. As shown on the geologic map of the Datil-Quemado region (Fig. 1.7), the volcaniclastic unit of Largo Creek, the volcaniclastic unit of Cañon del Leon, and the sandstone of Escondido Mountain are informally assigned to the lower, middle and upper Spears group, respectively. Datil Group volcanic units, namely the tuff of Bishop Peak, the andesite of Dry Leggett Canyon and the tuff of Luna are locally intercalated with the unit of Cañon del Leon in the Fox Mountain area west of Escondido Mountain. **1.0**

145.5 Volcaniclastic unit of Largo Creek well exposed in deep scar at 8:45. These volcaniclastic sandstones consist primarily of andesitic rock fragments and oscillatory zoned (volcanic) plagioclase, with minor hornblende and biotite, and usually little or no quartz. **0.5**

146.0 Headquarters of Jim Williams ranch on left. The Williams family has been ranching along Largo Creek for several decades. White cliffs of pumiceous sandstone in Cañon del Leon at 11:00. **1.0**

147.0 Cross arroyo of lower Cañon del Leon. **1.1**

148.1 Roadcut on left in light brownish-gray andesitic sandstone and red mudstones of the volcaniclastic unit of Largo Creek. Just beyond is entrance to Apache National Forest; mostly private property along Largo Creek from here to Quemado Lake. **0.2**

148.3 Largo Creek sandstones and mudstones on left. **0.2**

148.5 Upper(?) Pleistocene gravel in channel over Largo Creek beds in cut on left. **0.2**

148.7 Volcaniclastic unit of Largo Creek in cut on left is unconformably overlain by Quemado Formation gravel and colluvium. **0.5**

149.2 Slight angular unconformity visible on mesa side at 9:00. Largo Creek sandstone beds are noticeably truncated by the gently north-sloping Fence Lake conglomerates. **0.1**

149.3 Low roadcuts expose sands and gravels of Quemado Formation **0.4**

149.7 Enter zone of gently folded and faulted Largo Creek beds, apparent in road cuts for next 1.7 mi. Gentle anticlinal warp on left is cut by numerous calicite-filled tension fractures (joints) that are nearly vertical and strike N20°E. Intersection of joints and bedding gives outcrop a pseudo-cross-bedded appearance. **0.6**

150.3 Note open synclinal fold in interbedded sandstones and mudstones of the unit of Largo Creek well exposed in roadcut on right. (Fig. 1.45). **0.2**

150.5 White crest of local landmark known as the Hub is barely visible through low saddle in foreground at 9:15 (Fig. 1.46). **0.3**

150.8 Roadcuts ahead for next 0.2 mi in essentially horizontal Largo Creek sandstones unconformably overlain by Quemado Formation gravels; note channel fill on left. **0.6**



FIGURE 1.45. Road logger points to sandstone-mudstone contact that defines open synclinal fold in the unit of Largo Creek. View is to west-northwest along axis of fold. Slope wash was scraped from part of the exposure to improve visibility of bedding.



FIGURE 1.46. View of the west shoulder of Escondido Mountain, on skyline, and the barely visible white crest of the Hub, in middle slope through saddle in left foreground. Cliff-forming outcrops on Escondido Mountain consist of Squirrel Springs Canyon Andesite disconformably overlain by Bearwallow Mountain Andesite, capping ridge crest. The Hub is topped by pumiceous sandstones of the volcaniclastic unit of Cañon del Leon. Large scar on right exposes subhorizontal Largo Creek beds unconformably overlain by cliff-forming Fence Lake Formation.

151.4 Enter large roadcut that provides a cross section view on left of two cut and fill units of the Quemado Formation that unconformably overlie anomalously north-tilted Largo Creek beds locally cut by a low-angle fault (Fig. 1.47). Close examination of the low-angle fault at the southeast end of the roadcut shows that it is a dip-slip thrust fault (Fig. 1.48). Total displacement on this southwest vergent thrust is probably not more than 30-100 ft. Moderate deformation in Largo Creek beds observed over the last 1.7 mi (folds, tension fractures and a small thrust) are all consistent with local northeast-directed shortening and northwest extension. This is a typical orientation for late Laramide compressional deformation in the southern Colorado Plateau (Davis, 1978, Chapin and Cather, 1981). These northwest-trending structures appear to be relatively local and were not observed along trend in the Cañon del Leon area. The orientation of these structures and the pre-35.3 Ma age (late Eocene) of the volcaniclastic unit of Largo Creek would allow this area to be interpreted as a minor zone of late Laramide deformation. **0.6**

152.0 Route enters narrow valley cut by Largo Creek. Bouldery colluvium caps unit of Largo Creek in roadcut on left. **0.4**

152.4 Paleocanyon fill of Quemado Formation is well exposed in roadcut on left. Pebble imbrications indicate both westward and northward paleotransport, suggesting that this exposure contains both axial deposits of ancestral Largo Creek and tributary deposits from the adjacent canyon that leads eastward to Leon Tank. This paleo- canyon was cut through the Fence Lake Formation and the volcaniclastic unit of Largo Creek to a depth of about 300 ft and then backfilled by about 100 ft of Quemado Formation in Pliocene to late Pleistocene time. **0.3**



FIGURE 1.47. Roadcut along NM-32 showing two cut and fill units of the Quemado Formation (Pliocene to upper Pleistocene), unconformably overlying north-dipping andesitic sandstones and mudstones of the volcaniclastic unit of Largo Creek; view to east. A low-angle fault juxtaposes dark-colored muddy Largo Creek beds over light-colored Largo Creek sandstone at the south end (right side) of the cut. A 6-ft-thick basaltic gravel bed of the Quemado Fm. caps the south end of the roadcut; note south-facing channel wall at north end of gravel bed. Another northeast-facing channel wall is locally defined by a stone-line, which cuts obliquely down to the left, from just above the left edge of the gravel bed. This younger(?) channel is back filled with 30-40 ft of buff sand and basaltic gravel of the Quemado Formation. The latter channel wall is exposed on both sides of this roadcut and trends N37°W. Both of these channels probably represent tributary arroyos to ancestral Largo Creek that were entrenched and back filled in Pliocene to early Pleistocene time.

152.7 Roadcut on left in light gray, well-sorted, fine-grained, moderately quartz-rich (10-20% quartz) andesitic sandstone assigned to a transition zone in the upper part of the unit of Largo Creek. This transition zone, approximately 200 ft thick, is locally characterized by the upsection appearance of moderately quartz-rich andesitic to rhyolitic sandstones, thin pumiceous mudstone and a general coarsening upward into light brown and blue-green (celadonite cemented) andesitic conglomerate and conglomeratic sandstone. This transition is exposed in roadcuts for the next 4 mi. **1.4**

154.1 Roadcut on left in subhorizontal moderately quartzose andesitic sandstones in transitional zone in the upper part of the volcaniclastic unit of Largo Creek. **0.3**



FIGURE 1.48. Close-up view of low-angle fault in the unit of Largo Creek (at mileage 153.5; about 7 ft above top of slope wash), view to east. The fault strikes N50°W and dips 32°NE. Fibrous calcite along the fault plane shows a lineation plunging 31° to N35°E, and indicates dip slip. Small secondary shears below the main fault surface displace thin mudstone beds with a hanging-wall up (reverse) sense of shear. Collectively these observations confirm that this is a dip-slip thrust fault.

154.4 Concrete retainer wall protects roadway on left for next 0.1 mi. Conglomeratic sandstone beds near middle of roadcut are offset by a small high-angle fault. Approximately 3 ft of reverse throw is indicated by displacement of a cobble conglomerate bed. Fault surface lacks striations necessary to evaluate slip characteristics. Both andesitic and minor rhyolitic tuff clasts are present in the conglomeratic beds. A thin pumiceous mudstone occurs near the base of the roadcut. This outcrop reflects the coarsening upward and local first appearance of rhyolitic pumice within the transition zone of the upper unit of Largo Creek. Bouldery Quemado Formation fills channel at top of cut and grades into colluvium. **0.6**

155.0 Roadcut on right in brownish to greenish gray (celadonitic) conglomeratic sandstones with abundant pebbles of andesite porphyry and minor rhyolitic tuff clasts, the transition zone at the top of the unit of Largo Creek. Route temporarily leaves valley of Largo Creek. **0.2**

155.2 Transition zone conglomeratic sandstones in cut on right. **0.3**

155.5 Roadcut and gully ahead on right exposes light gray andesitic sandstone and pumiceous mudstone of the transition zone of the unit of Largo Creek. At 9:00 on skyline, bluish-green sandstones of the transition zone are unconformably overlain by coarse Fence Lake Formation conglomerates. **0.2**

155.7 Agua Fria Mountain on skyline at 10:30 is capped by Squirrel Springs Canyon Andesite and Bloodgood Canyon Tuff. **0.2**

155.9 **Slow down for left turn.** Unnamed butte at 1:00 is capped by Fence Lake Formation. Castle Rock in

foreground at 11:00 is capped by cliff-forming basal pumiceous and tuffaceous sandstone of the volcaniclastic unit of Cañon del Leon. **0.1**

156.0 Junction with NM-103. **Turn left and head south on NM-103 to Quemado Lake. 0.5**

156.5 The cliff-forming basal marker bed of the volcaniclastic unit of Cañon del Leon is well exposed on the east side of Castle Rock at 8:30 (Fig. 1.49). For practical mapping purposes the base of the volcaniclastic unit of Cañon del Leon is placed at the bottom of the angular, jointed, cliff-forming marker bed, just above the thin white tuffaceous sandstone bed. Although locally offset by faults, this pumiceous marker bed can be traced for 9 mi to the east along the north foot of Escondido Mountain and for 12 mi to the west along the north foot of Fox Mountain where it lies below the andesite of Dry Leggett Canyon. Phenocrysts of sanidine from pumice in muddy siltstone near the base of the marker bed at Castle Rock have yielded an $^{40}Ar/^{40}Ar$ age of 35.33 ± 0.06 Ma. This bed is interpreted as the sedimentary response to rhyolitic pyroclastic eruptions that saturated the regional fluvial system with ash and pumice; this then lead to a rapid sheet-like aggradational event. Larger pumice fragments are preferentially concentrated in slackwater mudstones and siltstones in the marker bed. Presumably most of the pumice was freshly introduced into the stream system shortly before the time of deposition (Fig. 1.50). According to the terminology of Smith (1991) this tuffaceous marker bed would be classified as a syneruptive deposit. **0.3**

156.8 **Caution, slow for dangerous curve to right ahead. 0.1**

156.9 Roadcut on right in thin bedded pumiceous sandstones and mudstones at the base of the volcaniclastic unit of Cañon del Leon. **0.3**

157.2 Pumiceous sandstone of basal Cañon del Leon and greenish sandstones of upper transitional unit of Largo Creek in roadcuts on left. **0.7**

157.9 Road to Buz and Beverly Easterling Ranch on right. Base of the volcaniclastic unit of Cañon del Leon is well exposed in side of mesa on left. Mesas at 9:00, 12:00 and 3:00 are capped by Fence Lake Formation. **0.1**

158.0 Re-enter valley of Largo Creek. **0.3**

158.3 Road crosses perennial flow of middle Largo Creek; apparently fed by natural springs and seepage under Quemado Lake dam about 2 mi southeast of here. **0.2**

158.5 Fence Lake Formation unconformably overlies unit of Cañon del Leon at 3:00. **0.3**

158.8 Cattle guard. Red fence around Buz Easterling's polo field at 2:00. **0.1**

158.9 Road rises along cuts on right in thin-bedded pumiceous sandstones and mudstones of the volcaniclastic unit of Cañon del Leon. **0.1**

159.0 Road crosses poorly exposed north wall of a locally west-trending paleocanyon filled with as much as 200 ft of Fence Lake Formation conglomerates. Reconnaissance mapping indicates that this upper Miocene paleocanyon was in part controlled by an east-trending segment of the Spur Lake fault, which is downthrown approximately 600 ft to the south in this area. **0.1**

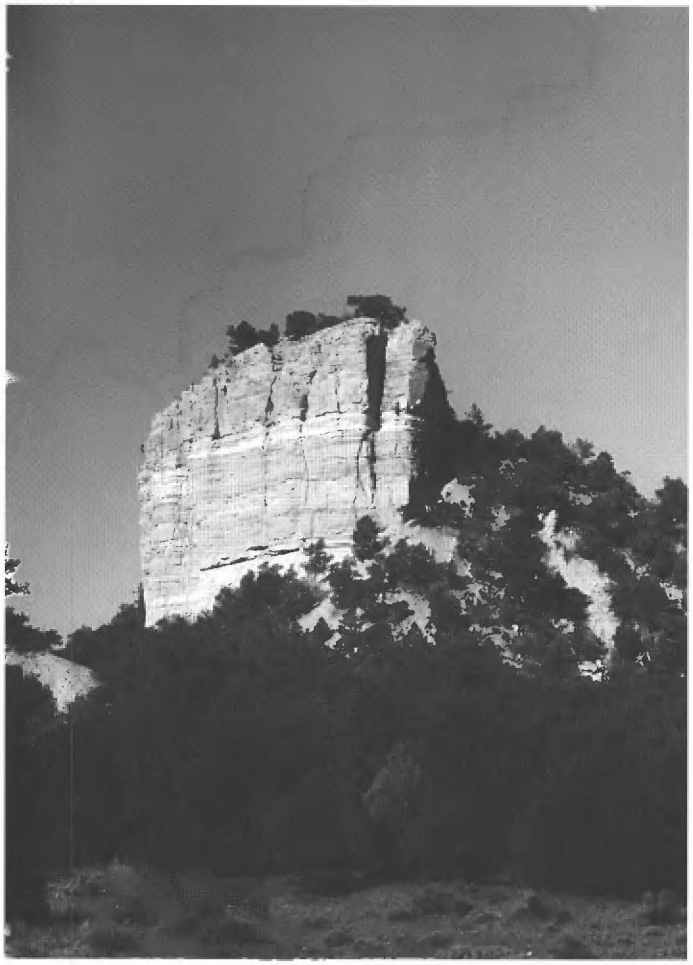


FIGURE 1.49. Castle Rock provides easily accessible boundary stratotype for the base of the volcaniclastic unit of Cañon del Leon. Basal contact is immediately below jointed cliff-forming marker bed of tuffaceous sandstone and pumice mudstones. Underlying thin white tuffaceous sandstone and tan to bluish green (celadonitic) andesitic conglomerate and conglomeratic sandstones are within transition zone in the upper part of the volcaniclastic unit of Largo Creek.

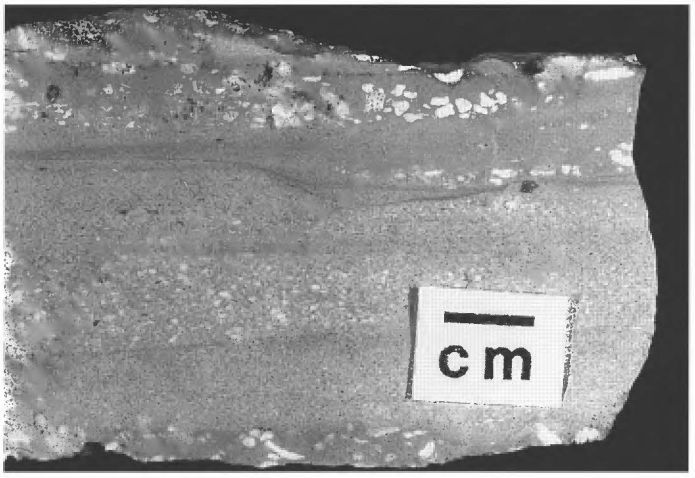


FIGURE 1.50. Tuffaceous sandstone and pumiceous muddy siltstone from one foot above the base of the unit of Cañon del Leon at Castle Rock (Sample CR-93-1-XR, McIntosh and Chamberlin, this volume). Tuffaceous sandstone may represent hyperconcentrated-flow deposit; muddy siltstone is slack water deposit.

159.1 Crest of hill. Snuffys steakhouse, saloon, tackle shop and gas pump on left. **0.1**

159.2 Road descends through cuts in Fence Lake Formation conglomerates and sandstones of paleocanyon fill, then crosses unnamed south-flowing tributary to Largo Creek. Paleocanyon wall is locally exposed 0.15 mi up this drainage. Here the upper Miocene canyon wall shows a 30-ft-high step as it rises northward onto the canyon rim, which is cut in lower Cañon del Leon beds. North of the paleocanyon rim the Fence Lake Formation is locally about 30 ft thick. Road crosses projected (buried) trace of Spur Lake fault near here. **0.1**

159.3 Water wells on right intersected 20 ft of alluvium, 80 ft of Fence Lake conglomerate (local aquifer) and 10 ft of light gray Oligocene sandstone (Buz Easterling, oral commun., 1993). Correlation of the Oligocene sandstone is uncertain, but local field relationships suggest that it is down-faulted sandstone of Escondido Mountain. As much as 7 mi of water lines have been installed to service the Quemado Lake Estates from these wells (Fig. 1-51). Nearly all of the lower 80 ft of Fence Lake Formation is saturated with water here. One of these wells is a stand by, the other is reported to produce approximately 100 gallons per minute with a submersible pump. (Buz Easterling, oral commun., 1993). **0.1**

159.4 Fence Lake Formation above road level on left is approximately 120 ft thick. This exposed thickness plus 80 ft intercepted in the water wells below the valley floor sum to a total of about 200 ft of fill along the axis of the paleocanyon. Fence Lake conglomerate is well exposed in the south wall of the modern valley at 4:00. **0.1**

159.5 Cattle guard. Enter Apache National Forest. **0.2**

159.7 Enter Quemado Lake Recreation Area. **0.3**

160.0 Parking lot (also spillway) on north side of Quemado Lake Dam. Well-imbricated boulder conglomerate of Fence Lake paleocanyon fill is exposed in cuts on left (Fig. 1.52). Construction of this earthen dam in 1970-1971 is summarized in the following minipaper. As stated on the official sign near the dam, Quemado Lake and the surrounding recreation area are managed by the U.S. Forest Service in cooperation with the New Mexico Department of Game and Fish. The lake has a surface area of approximately 131 acres. **0.1**

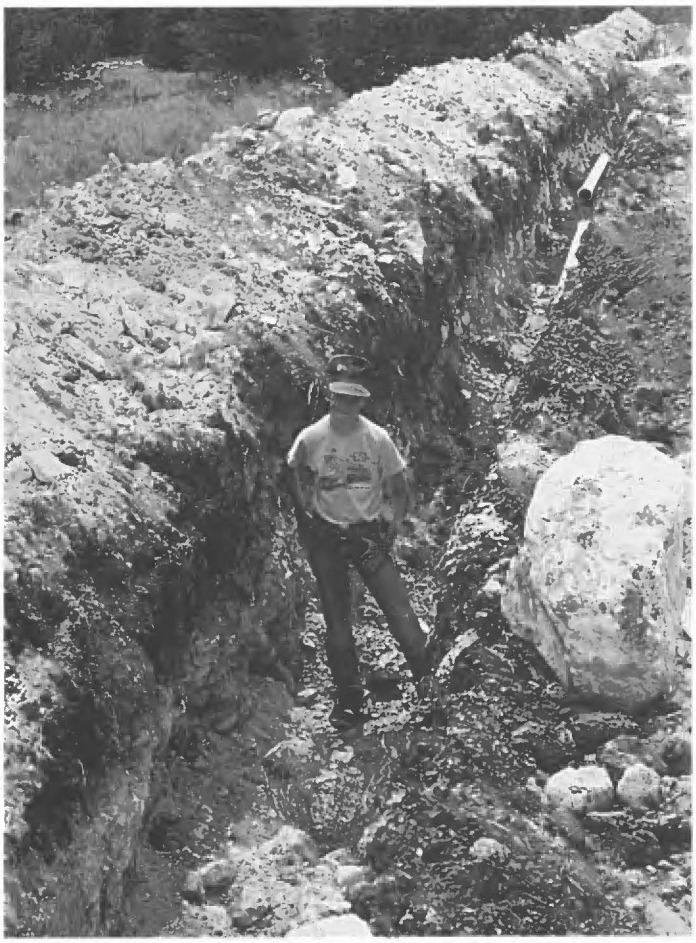


FIGURE 1.51. Trench in Fence Lake Formation at Quemado Lake Estates during development of a local water system, June 1992. Field assistant C. G. Chamberlin is only slightly larger than local maximum grain size of Fence Lake Formation (~5 ft).

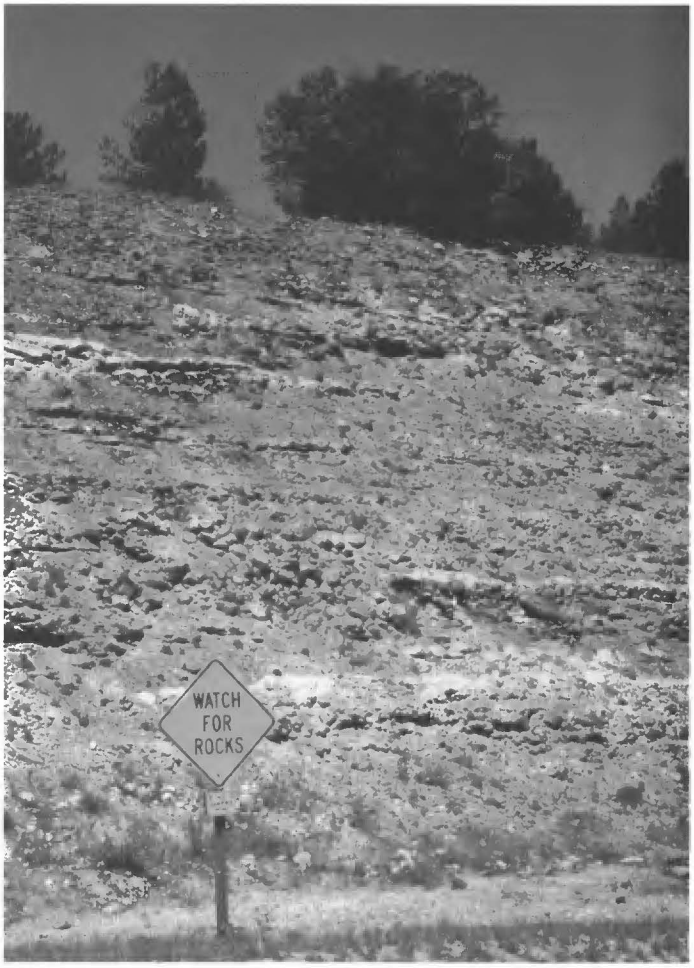


FIGURE 1.52. Roadcut in proximal Fence Lake Formation on NE side of Quemado Lake dam. Imbricated boulders indicate right to left (NW) paleoflow in this paleocanyon-fill deposit.

QUEMADO LAKE DAM

William C. Haneberg

New Mexico Bureau of Mines and Mineral Resources, Socorro, NM 87801

Quemado Lake Dam is an earthen embankment along Largo Creek, a tributary of the Little Colorado River, and lies within the Apache-Sitgreaves National Forest. Completed in 1971 and intended to promote recreation, the dam was constructed by the New Mexico Game and Fish Department under a special use permit from the US Forest Service. To this end, parking and camping are permitted in the spillway. Before receiving its present name, Quemado Lake Dam was referred to as Largo Creek Dam.

The dam is 924 ft long, 73 ft high, and 20 ft wide at its crest. It is zoned, with an impervious core flanked by semi-pervious transitional zones and pervious outer zones (Fig. 1.53). Up- and down-stream slopes are both 2.25:1 (horizontal to vertical) and covered with large riprap. Foundation materials are basaltic gravels and conglomerates of the middle to late Miocene Fence Lake Fm., which locally occurs as a 200-ft-thick paleo-valley fill into which are inset Quaternary alluvial deposits (R. M. Chamberlin, personal commun., 1993). Seepage problems were encountered during construction of the cutoff trench, which was quickly filled with muck. When the trench was cleaned, foundation materials were found to consist of volcanic boulder conglomerate with a poorly- to well-cemented clayey sand matrix. Maximum boulder diameter was 3 ft. Inspectors reported an absence of porous zones that might be conducive to piping, although gravelly stringers issuing groundwater were described near the top of the conglomerate. In addition, an abrupt change from a boulder conglomerate to a pebble conglomerate was observed in the cutoff trench near the right abutment. A State Engineer Office technical report dated 1958 includes logs of 10 shallow borings and cross-sections inferring a buried reverse fault along the axis of the Largo Creek valley. The fault was believed to be inactive, and the report further stated that a thick alluvial blanket beneath the dam would inhibit seepage along the fault. Cross-sections included on the plans for the current dam, however, do not include a fault and it is not known whether any seismic slope stability analyses were performed. The dam has performed well to date, with only minor problems such as rodent burrowing and plant growth along the embankment.

Outlet works at the Quemado Lake Dam consist of a 24-in. diameter concrete pipe with a capacity of 60 cfs, and the service spillway, which controls the reservoir elevation at 7628 ft, and has a capacity of 33,000 cfs. The emergency spillway (crest elevation 7634 ft) consists of a box weir drop inlet structure leading to a 5-ft-diameter concrete pipe, which in turn discharges into an open concrete channel and stilling basin along the right abutment. The emergency spillway was designed to pass in conjunction with the service spillway the 6 hr probable maximum precipitation (PMP) without overtopping the dam.

Drainage area of the Quemado Lake Dam is 62 mi^2. Quemado Lake normally stores 2000 acre-ft of water, with a maximum storage capacity of 2550 acre-ft. During design, evapotranspiration and seepage losses were anticipated to be on the order of 440 acre-ft per year. Enlargement of the reservoir was contemplated during the mid-1970s. The proposed increase in reservoir elevation would have decreased emergency storage (i.e., the amount of storage available between operating and emergency spillway elevations) from 860 acre-ft to an unacceptably low 152 acre-ft. Although a catastrophic failure would release some 152,000 cfs, the Quemado Lake Dam is classified as a low-hazard structure because of its remote location. Flood routing calculations predict that a catastrophic failure would increase water levels only a foot or so where Largo Creek crosses US-60 some 18 mi downstream from the dam.

Information for this note came primarily from reports and construction documents on file at the New Mexico State Engineer Office (SEO file 3026). The assistance provided by David Quintana and Larry Ferns of the SEO is greatly appreciated.

160.1 Road makes loop to right around small bay at north end of Quemado Lake. **0.2**

160.3 Road crosses northeastern paleocanyon margin; unconformity at base of Fence Lake Formation is poorly exposed in roadcut on left. **0.1**

160.4 High-angle, cross-bedded sandstone of Escondido Mountain is well exposed in roadcut on left (Fig. 1.54). Steepest cross bedding dips 30°E. **0.2**

160.6 Unconformity at base of Fence Lake Formation is well exposed about 30 ft above road on left. Variably cross-bedded sandstone of Escondido Mountain in lower third of cut. **0.1**

160.7 Road to new campground (under construction in summer of 1993) on right. **Continue straight ahead,** to old campground in valley floor at southeast end of lake. Sandstone of Escondido Mountain moderately well exposed on left for next 0.2 mi. **0.2**

160.9 Cross unconformity onto Fence Lake Formation. **0.1**

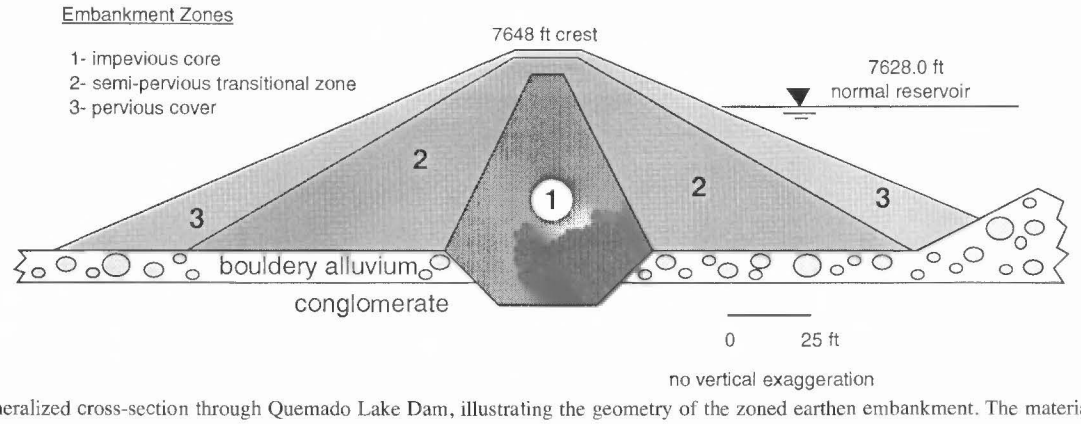


FIGURE 1.53. Generalized cross-section through Quemado Lake Dam, illustrating the geometry of the zoned earthen embankment. The material identified as bouldery alluvium in exploratory borings corresponds to Quarternary alluvium, and the conglomerate corresponds to the Fence Lake Formation.



FIGURE 1.54. High-angle cross bedding in the Oligocene sandstone of Escondido Mountain. Cross beds in this eolian sandstone dip predominantly to the east and imply prevailing westerly winds in Oligocene time.



FIGURE 1.55. El Caso Peak, which stands well above adjacent mesas capped by inset deposits of the Miocene Fence Lake Formation. Old Quemado Lake campground is located in valley floor to left of El Caso Peak.

161.0 Road crests above Quemado Lake; Agua Fria Mountain on skyline above lake at 4:00. **0.1**

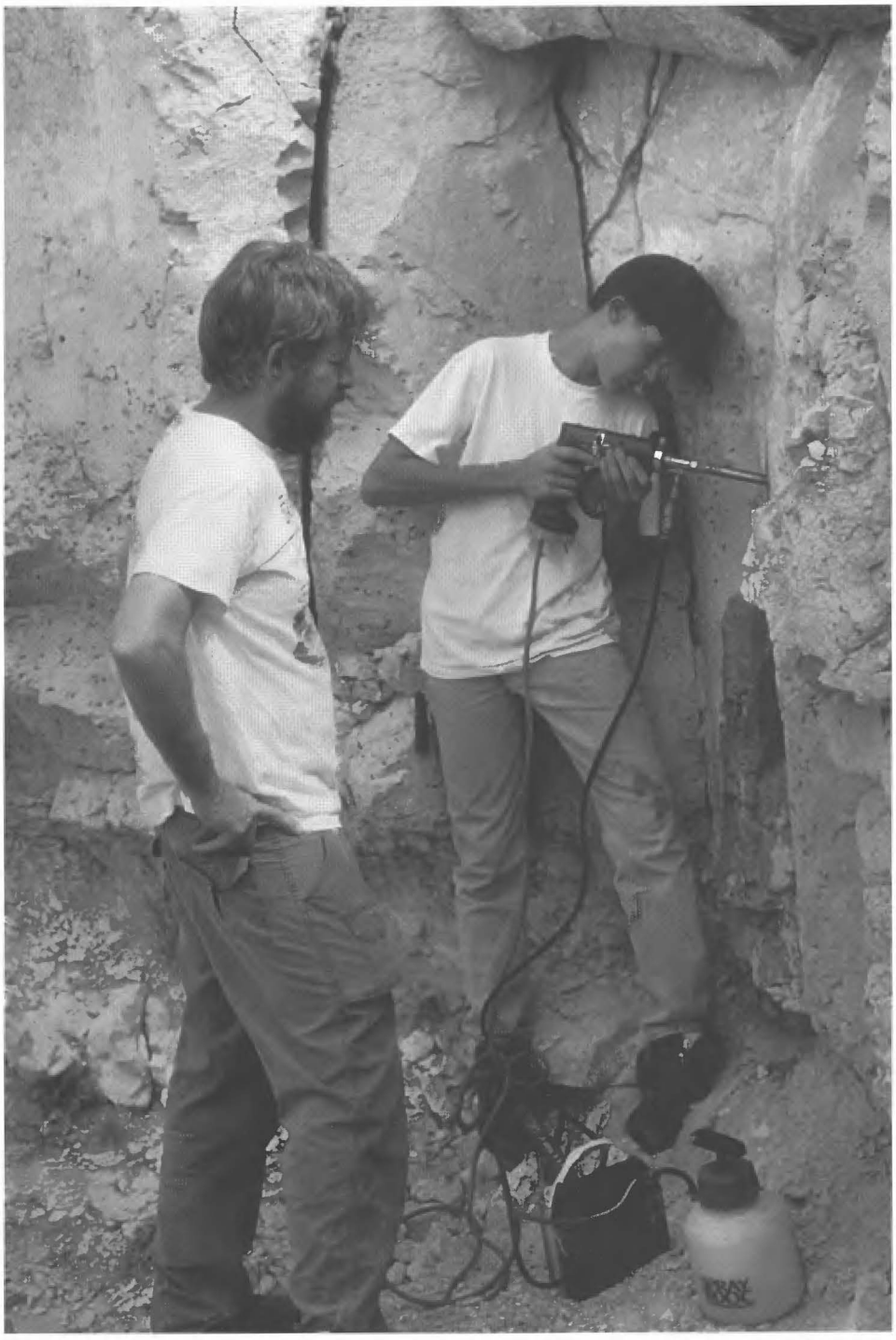
161.1 Road to new campground on left. El Caso Peak at 1:00 (Fig. 1.55) is capped by Oligocene Squirrel Springs Canyon Andesite overlying sandstone of Escondido Mountain. The latter is largely covered by colluvium that is not mapped on regional reconnaissance maps. **0.2**

161.3 Road cut on left exposes bouldery conglomerate overlying pedogenic(?) carbonate zone over cobble conglomerate, all in Fence Lake Formation. **0.1**

161.4 Fence Lake Formation unconformably overlies sandstone of Escondido Mountain in cut on left. **0.2**

161.6 First entrance to the older Quemado Lake campground on left. Additional entrances to campground on right for next mile. Find a campsite you like, park, set up camp and then enjoy catered BBQ in the pines.

End of first day road log.



William C. McIntosh (left) instructs Robert M. Chamberlin (right) on the technique of collecting oriented core samples for paleomagnetic analysis. Paleomagnetic analysis and $^{40}Ar/^{39}Ar$ geochronology confirm that this light gray crystal-poor ignimbrite at Saulsberry Ranch is the Rock House Canyon Tuff. Sample NM 1096, collected July 14, 1993.